

**Drug-conjugated biopolymers as osteosarcoma and rheumatoid arthritis
therapeutics**

Ethan Dickson Perkins

Submitted in accordance with the requirements for the degree of
Doctor of Philosophy

The University of Leeds
Faculty of Medicine and Health
School of Dentistry

September 2020

The candidate confirms that the work submitted is his own and that appropriate credit has been given where reference has been made to the work of others.

This copy has been supplied on the understanding that it is copyright material and that no quotation from the thesis may be published without proper acknowledgement.

The right of Ethan Dickson Perkins to be identified as Author of this work has been asserted by him in accordance with the Copyright, Designs and Patents Act 1988.

Acknowledgements

I would like to start by thanking the Leeds Alumnus, Clive Summerhayes for funding the PhD project. The generosity and kindness Clive has shown in making the PhD project a reality, is very much appreciated and will never be forgotten by myself. As well as Clive, I would also like to give thanks to my supervisor team, led by Professor David Wood, alongside Dr Giuseppe Tronci and Professor Stephen Russell. They have shown crucial support throughout the project and enabled me to develop my scientific knowledge and understanding of an area I wasn't familiar with at the beginning of the project, Biomaterials.

To my MSc lead supervisor at the University of Bradford, UK, Professor Rob Falconer I give great thanks. Your desire to assist my scientific development in the 5 years that I have known you, is extremely appreciated, particularly because for the majority of those years I haven't been a member of the same university as you. The willingness of yourself and Professor Paul Loadman to work alongside my current supervisory team in order to carry out the PhD project: allowing me to use your laboratory equipment whenever needed, allowing the use of the drug sequence you helped develop and the many out of hours emails, answering any questions I may have had, go well beyond the expectations of previous supervisors and for that I am extremely grateful to you both.

I would like to give thanks to my family and friends. My parents, for their hospitality during the research project as well as listening to my practice presentations, despite not understanding a word that I was saying. My family have always encouraged me to strive to achieve the best that I possibly can and I am thankful for that. My PhD friends, Ziyu, Ben, Amy, Alice and Sandeep, thank you for making the time we spent in the labs so enjoyable, even in times of unexpected experimental results, we still had a good time.

Finally, special thanks go to these individuals. Dr Robert Bedford, a former University of Leeds, PhD student whose endless advice and encouragement when writing my thesis proved invaluable. My best friends, Neil Massey and Lea Adkins for keeping my spirits high at the times when the project became increasingly stressful, thank you. Camilla – although we met part way through my project, I am thankful for your endless support throughout my write up year, which kept me going, even when it seemed impossible to complete.

Abstract

Complex diseases including osteosarcoma (OS) and rheumatoid arthritis (RA) require careful disease management. There is a need to update therapeutic treatments for these diseases, accommodating a more targeted and structurally supportive therapy. The risk of off-target toxicity could be reduced through the use of a hydrogel to deliver and anchor a selective peptide-conjugated prodrug (PCP), cleavable by an overexpressed protease at the disease site.

This study investigates the development of novel Hydrogel-PCP systems, aiming to selectively release naproxen (NAP) from the PCP component, through selective cleavage by matrix metalloproteinase 14 (MMP14), a proteolytic enzyme overexpressed within osteosarcoma and rheumatoid arthritis. Collagen-based hydrogels were initially functionalised with the photo-active monomer 4-vinylbenzyl chloride, prior to drug conjugation and photo-crosslinking under UV light. In light of no network formation by various photo-crosslinking methods a change in the crosslinking strategy was made. Chemical crosslinking using (4-(4,6-dimethoxy-1,3,5-triazin-2-yl)-4-methyl-morpholinium chloride) (DMTMM), successfully formed a gelatin based hydrogel-NAPPCP system (gel-NAPPCP). The release of NAP from gel-NAPPCP was analysed using LCMS after a 72-hour MMP14 recombinant enzyme assay was carried out. Cleavage by MMP14 at the Hof-Gly peptide bond in NAPPCP, a recognised cleavage site, did not occur, however the release of a NAP metabolite was detected at increased concentrations in more acidic conditions, providing an alternative for future drug release.

The DMTMM-induced crosslinking reaction takes place under physiological temperatures, allowing the exploration of an injectable *in situ* network forming gel-NAPPCP system, which was explored in synthetic bone cavities. Initial investigations demonstrate successful gel-NAPPCP hydrogel formation in these cavities, a promising step towards a more clinically desirable device compared to surgical implantation.

To conclude, this study provides a proof of concept for future investigations to improve MMP14 selective cleavage of NAPPCP in a hydrogel system to selectively target osteosarcoma and rheumatoid arthritis, using a clinically relevant delivery strategy.

Table of Contents

Acknowledgements	i
Abstract.....	ii
Table of Contents.....	iii
List of Tables.....	vi
List of Figures	vii
Abbreviations	xi
1.0 Introduction	2
1.1 Project Aims and Objectives	5
1.1.1 Project objectives.....	5
2.0 Literature review.....	8
2.1 Peptide-drug conjugates	8
2.1.1 Using peptide-drug conjugates to reduce unwanted toxicity	9
2.1.2 Self-assembling peptide-drug conjugates.....	11
2.2 Hydrogel systems and their use as drug delivery vehicles	13
2.2.1 Thermosensitive hydrogels.....	17
2.2.2 Magnetic hydrogels	19
2.2.3 Photopolymerisation hydrogels	20
2.2.4 Overcoming solubility complications.....	22
2.3 Targeted diseases and Hydrogel-PCP system component selection	24
2.3.1 Osteosarcoma – overview of cancer	25
2.3.2 Osteosarcoma – the disease.....	29
2.3.3 Rheumatoid arthritis	33
2.3.4 Biomaterial selection for hydrogel network formation.....	35
2.3.5 Proteolytic enzyme targeting for drug release.....	39
2.3.6 Selection of an active drug to release from a Hydrogel-PCP system	43
2.4 Hydrogel-PCP design and clinical application	46
2.4.1 Study design	46
2.4.2 Clinical significance.....	47
3.0 Photo-activated biopolymer hydrogels.....	50
3.1 Introduction.....	50
3.2 Materials.....	53
3.3 Methods.....	57

3.3.1 Functionalisation of biopolymer's lysine amine groups with 4-vinylbenzyl chloride	57
3.3.2 Determination of free amino groups occupied after functionalisation	58
3.3.2.1 Trinitrobenzenesulfonic acid assay.....	58
3.3.2.2 Ninhydrin assay.....	59
3.3.3 Drug conjugation via 1-(3-dimethylaminopropyl)-3-ethylcarbodiimide hydrochloride/N-hydroxysuccinimide reaction	60
3.3.4 Synthesis of UV-cured biopolymer networks	63
3.3.5 Synthesis of peptide-conjugated naproxen prodrug.....	63
3.3.6 LCMS confirmation of peptide-conjugated prodrug synthesis.....	64
3.3.7 MMP14 recombinant enzyme assay.....	65
3.3.8 HPLC drug release analysis	65
3.4 Results and Discussion.....	66
3.4.1 Functionalised biopolymers synthesis and UV inducible network formation concept	66
3.4.2 Confirmation of peptide-conjugated prodrug synthesis	71
3.4.3 Synthesis and UV network formation of NAPPCP conjugated col-4VBC25	73
3.4.4 UV crosslinking photo-active biopolymers to encapsulate drug-conjugated biopolymers	75
3.4.5 MMP14 selective recombinant enzyme assay	77
3.5 Conclusions.....	80
4.0 Chemically crosslinked biopolymer hydrogels	82
4.1 Introduction.....	82
4.1.1 Delivery route – implantation versus injection.....	84
4.2 Materials.....	87
4.3 Methods.....	87
4.3.1 Synthesis and confirmation of naproxen peptide-conjugated prodrug....	87
4.3.2 Drug conjugation to native biopolymer material	87
4.3.3 Confirmation of drug conjugation to gelatin biopolymers	87
4.3.4 Chemically-induced gelatin network formation and gelation kinetics.....	88

4.3.5 Quantification of swelling ratio and gel content.....	89
4.3.6 Rheological assessments.....	89
4.3.7 MMP14-Selective Recombinant Enzyme Assay	90
4.3.8 Initial Investigations of Injectable Device and In Situ Gel Formation	90
4.4 Results and Discussion.....	91
4.4.1 Confirmation of drug conjugation to native biopolymer material.....	91
4.4.2 Chemically-induced gelatin network formation.....	93
4.4.3 Assessment of gel content, swelling ratio and rheological properties	99
4.4.4 MMP14 selective recombinant enzyme assay	105
4.4.5 Investigating the clinical delivery route – injectability	116
4.5 Conclusions	121
5.0 Final Discussions	123
6.0 Conclusions.....	129
7.0 Future works	132
5.3.1 Peptide-conjugated prodrug functionalised gelatin hydrogels	132
5.3.2 Acidic release investigation	134
5.3.3 Clinical device developmental investigations.....	134
5.3.4 Peptide-conjugated photo-crosslinked hydrogels	135
6.0 References.....	i

List of Tables

Table 2.1. Examples of the variety of hydrogel materials, cross-linking methods and applications present in current literature.	16
Table 3.1. Materials and reagents used.	53
Table 3.2. Equipment information.....	56
Table 3.3. Methodology of gradient changes throughout LCMS and HPLC cycles.	64
Table 3.4. Functionalisation of gelatin with 4-vinylbenzyl chloride. Degree of functionalisation (F) measured in the 4VBC-reacted gelatin product via TNBS assay (n=3). Gelatin was reacted with 4-vinylbenzyl chloride (4VBC) at a range of molar excesses.	66
Table 3.5. Degree of functionalisation in atelocollagen. Quantification of amino group molar content and degree of functionalisation (F) in atelocollagen products (n=3) following either 4VBC, SSZ or NAPPCCP coupling. Degree of Functionalisation was calculated using an overall molar amino content of $3.03 \times 10^{-4} \text{ mol}\cdot\text{g}^{-1}$ in native AC, demonstrated by TNBS and Ninhydrin assays.	69
Table 3.6. Naproxen Peptide-Conjugated Prodrug Fragments. Fragmentation of Naproxen Peptide-Conjugated Prodrug (NAPPCCP), single, double and triple charged ions, as observed by mass spectrometry.....	72
Table 4.7. Functionalisation of gelatin with naproxen and NAPPCCP. Naproxen peptide-conjugated prodrugs (n=3) at varying concentrations, confirmed by ninhydrin assays, quantifying the unreacted amino groups of gelatin biopolymers.....	92

List of Figures

Figure 1.1. Commonly used clinical delivery routes. Delivery strategies versus proposed Hydrogel-PCP delivery strategies. The proposed Hydrogel-PCP consists of an active drug (naproxen) conjugated to peptide sequence, selective to matrix metalloproteinase 14 (MMP14) cleavage at the Hof-Gly peptide bond. The PCP is further conjugated to a collagen-based biopolymer, prior to network formation through either UV or chemical crosslinking.....	4
Figure 2.1. Hallmarks of cancer. The majority of cancers acquire the same set of functional capabilities during development through a range of mechanical strategies.	25
Figure 2.2. Structural similarities between methotrexate and folic acid. Methotrexate (left) and folic acid (right).....	31
Figure 2.3. Structure of hyaluronic acid. Repeating chains of D-glucuronic acid and <i>N</i> -acetyl-D-glucosamine containing free carboxylic groups (-COOH), hydroxyl groups (-OH) and acetyl (-CH ₃ CO) groups.	36
Figure 2.4. Degradation of the collagen triple helix structure to form gelatin strands which when chilled are capable of reforming the triple helical structure through non-covalent crosslinking.	38
Figure 2.5. Expression of MMP mRNA in human cell lines. Modified from the 2010 study by Atkinson <i>et al.</i> MT-MMPs are elevated in human preclinical tumour models. Expression of MMP mRNA in human cell lines grown in vitro (A) and as xenografts in vivo (B) as measured by quantitative RT-PCR. Expression values after normalization to 18S-rRNA and are gene specific. Classification of expression levels was determined from the C _T of each gene as either very high (C _T ≤ 25), high (C _T = 26-30), moderate (C _T = 31-35), low (C _T = 36-39), or not detected (CT = 40); see key for colour scheme. (C) Immunoblot of MT1-MMP protein expression in HT1080 and MCF7 tumour models [89].	41
Figure 2.6. Chemical structure of naproxen, ibuprofen and aspirin. Possible non-steroidal anti-inflammatory drugs (NSAIDs) to use as the drug warhead in the peptide-conjugated prodrug design, due to the single carboxylic acid group each possess.....	44
Figure 2.7. The hydrogel-naproxen PCP system. Designed to be selectively cleaved, at the Hof-Gly peptide bond, by MMP14 to trigger the release of naproxen from the	

PCP component. Naproxen-PCP (NAPPCP), conjugated to free amino lysine groups of a collagen-based biopolymer is crosslinked to form a Hydrogel-NAPPCP.....	47
Figure 3.1. Ninhydrin calibration curve. Isolated linear region of a ninhydrin assay calibration curve, demonstrating the region at which the quantity of free amino groups can be accurately determined with in a biopolymer.	60
Figure 3.2. Structural differences between study drugs. Sulfasalazine (red), naproxen (blue) and the naproxen peptide-conjugated prodrug (NAPPCP).	61
Figure 3.3. EDC/NHS-induced drug coupling to biopolymers. Coupling of naproxen (blue) or sulfasalazine (red) to a collagen-based biopolymer via EDC/NHS reactions to activate drug carboxylic groups before mixing with the biopolymer solution to readily react with free amino lysine groups.	62
Figure 3.4. Confirmation of network formation of col4VBC25 hydrogel. UV irradiation A) Dry hydrogel for storage and B) wet, swollen hydrogel.	70
Figure 3.5. Molecular structure of the Naproxen Peptide-Conjugated Prodrug.	71
Figure 3.6. LCMS confirmation of naproxen-peptide conjugated prodrug. Identification of NAPPCP - photo diode array absorbance spectrum at 330 nm (top); mass Spectrometry for peak at 7.46 mins, showing a doubly charged species of MW 644.89 consistent with the desired product (bottom). Purity in excess of 80% as shown by the lack peaks (other than NAPPCP), large enough to display a peak area.	72
Figure 3.7. UV-induced Crosslinking of collagen-based biopolymers. Following 4VBC functionalisation collagen-based biopolymers were crosslinked in the presence of I2959 photoinitiator.....	74
Figure 3.8. Confirmation of successful network formation of encapsulated hydrogels. Hydrogel network of col4VBC25 encapsulating either colSSZ or colNAPPCP A-B) colSSZ and C-D) colNAPPCP. Left side of figure depicts the encapsulated hydrogels in their dry state, whereas the right side shows the swollen state of the hydrogels.	76
Figure 3.9. HPLC spectra (absorbance chromatograms at 330 nm) of reaction buffer for MMP14 recombinant assay. Assessment of the release of naproxen metabolites from a col4VBC25encap-NAPPCP hydrogel network: pink: naproxen drug control, cyan: col4VBC25encap-NAPPCP gel, green: col4VBC25 control, blue: col4VBC25encap-NAPPCP gel repeat, and black: reaction buffer negative control.	78

Figure 3.10. HPLC analysis of acid degradation assay (absorbance chromatograms at 330 nm). Green: naproxen drug control, blue: col4VBCencap-NAPPCP and black: col4VBC25 control. 79

Figure 4.1. Injection delivery strategy. Gel-NAPPCP system, injected between the rheumatic joints, at the site of cartilage degradation, where *in situ* chemical crosslinking occurs to form a gel-NAPPCP hydrogel with a cartilage-like consistency. Structural support is provided by the hydrogel, whilst selectively releasing the anti-inflammatory drug, naproxen, through the cleavage of the peptide-conjugated sequence by MMP14..... 86

Figure 4.2. Chemical crosslinking of gelatin using DMTMM crosslinker. DMTMM activation of gelatin carboxylic groups, before reaction with free amino lysine groups of other gelatin strands, resulting in the formation of a hydrogel network..... 88

Figure 4.3. Hydrogel network formation by DMTMM-induced chemical crosslinking. Gelatin-control A) dry B) wet and gelatin-NAPPCP C) dry and D) wet..... 94

Figure 4.4. Gelation kinetics of chemically crosslinking gel-CT. Mixed with phosphate buffer saline and DMTMM crosslinker at A) 5 minutes B) 10 minutes C) 15 minutes D) 20 minutes and E) 25 minutes after. 97

Figure 4.5. Gelation kinetics of chemically crosslinking gel-NAPPCP. Mixed with phosphate buffer saline and DMTMM crosslinker at A) 5 minutes B) 10 minutes C) 15 minutes and D) 20 minutes after..... 98

Figure 4.6. Gel content (GC) chemically crosslinked hydrogels. Gel-CT (96.18 ± 1.55 %) and gel-NAPPCP (91.11 ± 1.05 %) hydrogels (n=4). A statistical difference ($p < 0.05$) between gel-CT and gel-NAPPCP gel contents was observed using a T-test analysis..... 99

Figure 4.7. Swelling Ratio of chemically crosslinked hydrogels. Gel-CT (950.98 ± 43.02 %) and gel-NAPPCP (914.19 ± 33.06 %) hydrogels (n=4), using DMTMM as a crosslinking activator. No statistical difference was observed ($p > 0.05$) from a T-test statistical analysis, comparing gel-CT and gel-NAPPCP. 100

Figure 4.8. Amplitude sweep showing the loss modulus G'' LVE region. A) gel-CT and B) gel-NAPPCP, under constant frequencies of 1 rad·s⁻¹. 102

Figure 4.9. Frequency sweep showing storage (G') and loss modulus (G''). A) gel-CT and B) gel-NAPPCP, under a constant shear strain of 10%, a value within the linear viscoelastic region of both gel types. 104

Figure 4.10. Photographic depiction of hydrogels after MMP14 assay. The deposits and sunken appearance of the A) gel-NAPPCP hydrogel after 72 hours in the presence of recombinant MMP14, compared to the structurally intact B) gel-CT hydrogel. 106

Figure 4.11. LCMS analysis of MMP14 recombinant assay. Tracking the release of naproxen peptide-conjugated prodrug metabolites A) NAPPCP control B) gel-CT control gel and C) gel-NAPPCP gel. Confirmation of key peaks confirmed by Mass Spectrometry D) 7.43 MS of NAPPCP peak shown by MH^{2+} charged mass and E) 17.28 MS of NAPPCP metabolite peak of MH charged mass of NAP-Arg metabolite (384 m/z). 108

Figure 4.12. Structural differences between A) ICT2588 and B) NAPPCP. Demonstrating the active drug components (blue) are coupled to alternative ends of the peptide conjugate with azademethylcolchicine coupled to the C-terminus and naproxen coupled to the N-terminus. The N-terminus of ICT2588 is occupied by the FITC endcap (red). 110

Figure 4.13. Acid degradation analysis using LCMS. A) gel-NAPPCP B) gel-CT and C) using MS to identify the peak located at 17.34 minutes in gel-NAPPCP, identified as NAP-Arg. 111

Figure 4.14. Gel content carried out on gel-CT and gel-NAPPCP hydrogels. A) after 3-day MMP14 recombinant enzyme assay and B) table exhibiting percentage values of gel content before and after the assay. Statistical analysis between gel-CT and gel-NAPPCP hydrogels before and after were compared using a T-test. No significant difference was observed between the gel-CT hydrogels, however a statistical difference in gel-NAPPCP was observed, between before and after samples. 115

Figure 4.15. Gelation of gelatin-control hydrogels in polyurethane synthetic bone. Crosslinked with DMTMM under physiological conditions A) horizontal image of cavities prior to network forming mixture injection B) horizontal image of cavities 25 minutes post network forming mixture injection and C) vertical image of cavities 25 minutes post network forming mixture injection. Polyurethane synthetic bone (40PCF). 118

Figure 4.16. Hydrogel gelation through polyurethane synthetic bone tunnel cavity. Gelatin-control A) front-facing B) side profile and gelatin-NAPPCP C) back-facing and D) side profile. 120

Abbreviations

4VBC	4-Vinylbenzyl Chloride
4VBC25	4-Vinylbenzyl Chloride (25 molar excess)
4VBC40	4-Vinylbenzyl Chloride (25 molar excess)
-COOH	Carboxylic Acid Acid Group
AC	Atelocollagen
AMF	Alternating Magnetic Field
Arg	Arginine
Bcl-2	B-Cell Lymphoma 2
BME	2-Mercaptoethanol
BGP	Bone Gla Protein
CaCl ₂	Calcium Chloride
CDDP	Cisplatin
Col-NAPPCP	Collagen-Naproxen Peptide-Conjugated Prodrug
Col4VBC	Collagen-4-Vinylbenzyl Chloride
Col4VBC25	Collagen-4-Vinylbenzyl Chloride (25 molar excess)
Col4VBC25encap-NAPPCP	Collagen-4-Vinylbenzyl Chloride (25 molar excess) encapsulating col-NAPPCP
Col4VBC25-NAPPCP	Collagen-4-Vinylbenzyl Chloride (25 molar excess) – Naproxen Peptide-Conjugated Prodrug
Col4VBC-SSZ	Collagen-4-Vinylbenzyl Chloride (25 molar excess) - Sulfasalazine
Col4VBC40	Collagen-4-Vinylbenzyl Chloride (40 molar excess)
COX	Cyclooxygenase
COX-2	Cyclooxygenase-2
CT	Computed Tomography
DCM	Dichloromethane

DHFR	Dihydrofolate Reductase
DIPEA	N,N-Diisopropylethylamine
DLBCL	Diffuse Large B-Cell Lymphoma
DMARD	Disease-Modifying Anti-Rheumatic Drugs
DMF	Dimethylformanamide
DMSO	Dimethyl Sulfoxide
DMTMM	4-(4,6-dimethoxy-1,3,5-triazin-2-yl)-4-methyl-morpholinium chloride
DOX	Doxorubicin
E2F	E2 Transcription Factor
ECM	Extracellular Matrix
EDC	1-(3-Dimethylaminopropyl)-3-ethylcarbodiimide hydrochloride
EMT	Epithelial-Mesenchymal Transition
ETS	E-Twenty-Six
FDA	Food and Drug Administration
FITC	Fluorescein Isothiocyanate
FLS	Fibroblast-Like Synoviocytes
G'	Storage Modulus
G''	Loss Modulus
GC	Gel Content
GelatinCOOH	Gelatin Carboxylic End Chain
Gel-CT	Gelatin-Control
Gel-NAPPCP	Gelatin-Naproxen Peptide-Conjugated Prodrug
Gel4VBC25-NAPPCP	Gelatin-4-Vinylbenzyl Chloride (25 molar excess) – Naproxen Peptide-Conjugated Prodrug
Gel4VBC25-SSZ	Gelatin-4-Vinylbenzyl Chloride (25 molar excess) – Sulfasalazine

GEM	Gemcitabine
GF	Growth Factors
Gly	Glycine
HA	Hyaluronic Acid
HCl	Hydrochloric Acid
HCTU	2-(6-Chloro-1-H-Benzotriazole-1-yl)-1,1,3,3-Tetramethylaminium Hexafluorophosphate
HER4	Human Epidermal Growth Factor Receptor 4
HLA-DR	Human Leukocyte Antigen-DR Isotype
Hof	Homophenylalanine
HPLC	High-Performance Liquid Chromatography
Hydrogel-PCP	Hydrogel-Peptide-Conjugated Prodrug
I2959	4-(2-Hydroxyethoxy) Phenyl-(2-Hydroxy-2-Propyl) Ketone (Iragcure 2959)
IL	Interleukin
KDa	Kilodaltons
LDH	Lactate Dehydrogenase
LCMS	Liquid Chromatography Mass Spectrometry
LCST	Low Critical Solution Temperature
Leu	Leucine
LVE	Linear Viscoelastic
MA	Methacrylate
MDP	Multidomain Peptide
MION	Magnetic Iron Oxide Nanoparticle
MMP Reaction Buffer	50mM Tris HCl (pH 7.5), 150mM NaCl, 5mM CaCl ₂ and 0.025% Brij-35 Buffer Solution
MMP14	Matrix Metalloproteinase 14

MS	Mass Spectrometry
MT-MMP	Membrane Type-Matrix Metalloproteinase
MT1-MMP	Membrane Type-Matrix Metalloproteinase 1
MPGA	Methacrylated PGA
MRI	Magnetic Resonance Imaging
MTD	Maximum Tolerated Dose
MTT	3-(4,5-Dimethylthiazol-2-Yl)-2,5-Diphenyltetrazolium Bromide
MTX	Methotrexate
MW	Molecular Weight
NaCl	Sodium Chloride
NaHCO ₃	Sodium Carbonate
NaOH	Sodium Hydroxide
NAP	Naproxen
NAPPCP	Naproxen Peptide-Conjugated Prodrug
NHS	N-Hydroxysuccinimide
NMP	N-Methyl-2-pyrrolidone
NSAID	Non-Steroidal Anti-Inflammatory Drugs
OPF	Oligo (Poly(Ethylene Glycol) Fumarate)
OS	Osteosarcoma
Oxali-Pt-Y-1	Oxaliplatinum Based Platinum (IV) Prodrug
p21	Protein 21
p53	Protein 53
PCP	Peptide-Conjugated Prodrug
PDC	Peptide-Drug Conjugate

PECT	(PECT, poly (ϵ -caprolactone-co-1,4,8-trioxo [4.6]spiro-9-undecanone)-poly(ethylene glycol)-poly (ϵ -caprolactone-co-1,4,8-trioxo [4.6]spiro-9-undecanone))
PEG	Polyethylene Glycol
PLGA	Poly(D,L-Lactic-Co-Glycolic Acid)
pRb	Retinoblastoma Protein
RA	Rheumatoid Arthritis
RACK1	Receptor of Activated Protein Kinase C 1
Ser	Serine
SMA	Sodium Methacrylate
SNAI1	Snail Family Transcriptional Repressor 1
SR	Swelling Ratio
SSZ	Sulfasalazine
TERT	Telomerase Reverse Transcriptase
TFA	Trifluoroacetic Acid
TIMP	Tissue Inhibitors of Metalloproteinases
TNBS	Trinitrobenzenesulfonic Acid
TNF	Tumour Necrosis Factor
Tyr	Tyrosine
UV	Ultraviolet
vWf	Von Willebrand's Factor
VEGF	Vascular Endothelial Growth Factor
WHO	World Health Organisation
wt.	Weight
γ -PGA	Poly-Gamma-Glutamic Acid

Chapter 1

Introduction

1.0 Introduction

Rheumatoid arthritis and osteosarcoma are complex diseases, often affecting the bone around a joint, particularly the knee in osteosarcoma [1] and the wrist in rheumatoid arthritis [2]. Whilst rheumatoid arthritis is a disease most commonly affecting adults, osteosarcoma occurs most frequently during childhood and adolescence. Osteosarcoma (OS) often requires surgery and powerful chemotherapy as a treatment, which is known to cause significant side-effects and unwanted toxicity to healthy tissues. In contrast rheumatoid arthritis (RA) is an autoimmune disease which is often treated by the use of disease-modifying antirheumatic drugs, immunosuppressors, for which off-target toxicity can also be detrimental [3]. For the treatment of both diseases, improved drug delivery could be significantly beneficial in reducing off-target toxicity. Treatment development for both diseases, particularly osteosarcoma, has seen very few advances in therapeutic treatments for many years. There is a clinical need for new interventions for both OS and RA:

- to reduce unwanted toxicity in healthy tissues
- improve efficiency of treatment delivery
- provide structural support to tissues
- maintain the therapeutic effect of treatments.

A major objective of drug delivery in disease therapeutics is the transportation of sufficient drug to the disease site, whilst reducing drug exposure to unaffected, healthy tissue [4]. By minimising the damage to healthy tissue caused by off-target drug toxicity, the therapeutic index is increased [5], allowing for the administration of a higher concentration of therapeutic agent (add another supporting reference) [6]. There are a wide variety of highly toxic therapeutic drugs, such as several chemotherapies, that could be utilised to better target other, less life-threatening diseases. An example of a chemotherapeutic drug which is currently used to treat another non-cancerous disease is methotrexate. Methotrexate is a highly effective cytotoxic drug used to treat several autoimmune diseases including rheumatoid arthritis [7] and Crohn's disease [8], although the mechanism by which methotrexate causes a therapeutic effect in cancer and rheumatoid arthritis is thought to be different [9]. Nevertheless, from a toxicological perspective it is crucial to deliver any therapeutic agent, particularly non-selective cytotoxic agents, to a disease site in a local fashion to reduce the risk of off-target toxicity. Delivery of a drug to the desired disease site is achieved through two main strategies, which aim to alter the

pharmacokinetic capabilities of the particular drug: The first of these methods involves the use of a drug delivery vehicle, such as nanoparticles or hydrogel conjugation of the drug to the gel, which release drugs through their own physiochemical properties, for example in response to temperature change [10, 11].

The second method involves covalent modification of the drug, temporarily inhibiting the drug's bioactivity (creating a so-called 'prodrug') in order to safely deliver it to the disease site [12].

The prodrug strategy offers several key advantages over the use of a drug delivery vehicle, particularly the reduced amount of inert materials left behind after drug metabolism and the minimised risk of premature drug release. Both of these advantages reduce the metabolic stress on the patient, further increasing the therapeutic index of the particular drug administered [13]. Due to the advantages prodrugs appear to have over the use of delivery vehicles, it is feasibly unsurprising that many more prodrugs have been developed and approved by the US Food and Drug Administration (FDA) compared to the delivery vehicle method. A recent example is the antibody-drug conjugate polatuzumab vedotin, which in June 2019 was granted accelerated approval by the FDA for the treatment of adults with relapsed/refractory diffuse large B-cell lymphoma (DLBCL) [14].

This project explores the possibility of combining *both* drug delivery methods to produce a novel, clinically relevant therapeutic treatment. Many complex diseases such as cancer or rheumatoid arthritis could benefit significantly from a prodrug, loaded onto a drug delivery vehicle, reducing the risk of off-target activation, leading to unwanted toxicity. Peptide-drug conjugates (also known as peptide-conjugated prodrugs) offer a selective drug release strategy through the exploitation of an overexpressed proteolytic enzyme within the disease site and have demonstrated increased drug therapeutic index. Peptide-conjugated prodrugs (PCPs) are generally delivered intravenously (as they would be degraded in stomach acid if administered orally), with little control surrounding how they reach the target site. Conjugating a PCP to a hydrogel network, before either implanting or injecting the hydrogel to act as a delivery vehicle would anchor the selective prodrug in place at the disease site, further limiting the risk of unwanted toxicity. Hydrogels are 3-dimensional polymer matrices with unique properties, one of which is the similar consistency to connective tissue, allowing them to act as tissue scaffolds, to promote processes including bone regeneration [15], as well as many being biodegradable [16, 17].

A novel system such as the one described here, is clinically desirable, for the treatment of rheumatoid arthritis, as it provides a selective and localised drug delivery system, through a completely biodegradable tissue support network. There are two possible delivery routes applicable to the gel system proposed: implantation and delivery by injection (*Figure 1.1.*)

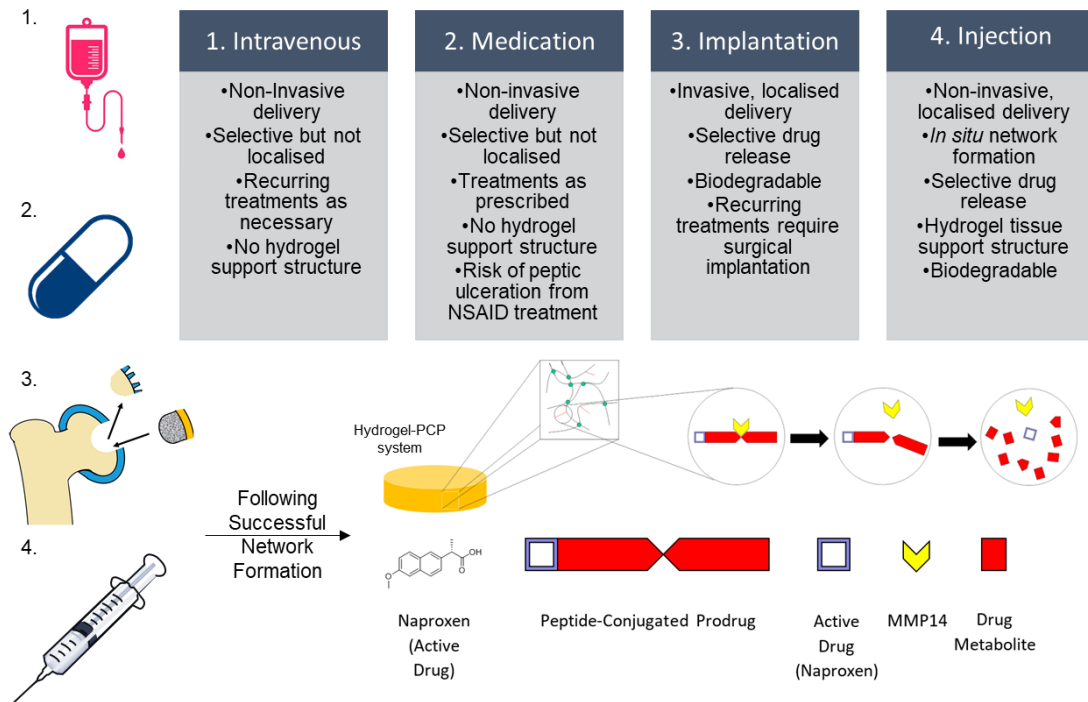


Figure 1.1. Commonly used clinical delivery routes. Delivery strategies versus proposed Hydrogel-PCP delivery strategies. The proposed Hydrogel-PCP consists of an active drug (naproxen) conjugated to peptide sequence, selective to matrix metalloproteinase 14 (MMP14) cleavage at the Hof-Gly peptide bond. The PCP is further conjugated to a collagen-based biopolymer, prior to network formation through either UV or chemical crosslinking.

1.1 Project Aims and Objectives

Therapeutic treatments, displaying reduced off-target toxicity are sought after for the treatment of complex diseases such as rheumatoid arthritis and osteosarcoma. The aim of this proof of concept study is to address the clinical requirement of a more targeted therapy to treat osteosarcoma and rheumatoid arthritis.

Naproxen, a non-steroidal anti-inflammatory drug well-known for its' anti-tumour effects and treatment of rheumatoid arthritis, will be conjugated to a peptide sequence, selective towards the active site of MMP14 to form a naproxen-PCP which will be coupled to a collagen-based biopolymer. The hydrogel-system will then be assessed for its' relevance in targeting the diseases: osteosarcoma and rheumatoid arthritis as well as to outline a possible clinical delivery route for the proposed drug delivery system.

The combination of medicinal chemistry and biomaterials outlined here aims to pave a path for new knowledge and direction in the selective toxicology research field. This will be achieved by providing a concept for a new, selective device to replace the somewhat stagnant therapeutic methods in the treatment of rheumatoid arthritis and osteosarcoma, which have seen little advances in therapies in the last decade. A series of objectives outlined below, shed light upon the path in which the research will follow to achieve the aim of the study.

1.1.1 Project objectives

1. *Synthesise a Hydrogel-PCP system from a collagen-based biopolymer, using UV irradiation of a photo-active molecule to induce network formation.*

There are two methods to achieve this objective: a) Following conjugation of the photo-active molecule to free amino groups of the biopolymer, further coupling of the selected drug compound will be carried out, prior to UV-induced network formation and b) encapsulation of a drug-conjugated biopolymer sample within a separate, photo-activate, functionalised biopolymer sample. To determine the most suitable degree of functionalisation with the selected photo-active molecule, a series of reactions will take place at varying molar excesses, following which the determination of remaining available amino groups (for drug conjugation and photopolymerisation to occur) will take place, before conjugating the desired therapeutic drug.

2. *Using a chemical crosslinker, synthesis a collagen-based Hydrogel-PCP system.*

The use of direct chemical crosslinking removes the need for a photo-active molecule and provides an alternative method of forming a hydrogel network, as well as providing an alternative delivery route option, i.e. via injection *in situ*. Varying molar excesses of chemical crosslinker will be reacted to assess the changes in gelation times to provide insight into a suitable gelation time to support the injectable delivery route. The use of DMTMM as a chemical crosslinker, as opposed to the traditionally used EDC/NHS will also be explored.

3. *Carry out a recombinant enzyme assay to assess initial drug release.*

Necessary to confirm the selective release by MMP14 from the drug-conjugated hydrogel system. The release profile may require modifications to the selected sequence to optimise the release by MMP14. An area to consider is the affect the hydrogel may have upon the release profile as MMP14 is a known collagen and gelatinase proteolytic enzyme and therefore may favourably cleave sites away from the peptide drug-conjugate cleavage site.

4. *Perform acid degradation assays on Hydrogel-PCP systems to assess the initial drug release.*

Acid degradation studies allow for the confirmation of drug presence within the Hydrogel-PCP system, should no selective drug release be observed. This would inform which further investigations or modifications to the Hydrogel-PCP system may be carried out to attempt to optimise the device.

5. *Investigate a possible delivery route of the Hydrogel-PCP system.*

The synthesis of a new therapeutic device requires a clinically viable delivery route. Therefore, the investigation into the most suitable delivery route for the relevant Hydrogel-PCP, is a necessary objective within this proof of concept study. If no viable delivery route can be developed, the Hydrogel-PCP concept must be adapted or be proven inadequate to continue investigating. A therapeutic agent is not viable if it cannot be safely or efficiently delivered.

Chapter 2
Literature Review

2.0 Literature review

This chapter outlines the key aspects of the thesis and reviews the literature related to the design of a novel Hydrogel-PCP system. It first discusses peptide-drug conjugates and their recent developments within a therapeutic setting. The use of hydrogel networks as drug delivery vehicles, to provide localised and controlled drug release, are then reviewed. The target diseases, osteosarcoma and rheumatoid arthritis are discussed before considering the most suitable attributes for the Hydrogel-PCP such as:

- *The biomaterial to form the hydrogel network from*
- *The proteolytic enzyme for drug release*
- *The active drug to be selectively released from the system.*

The finalised design of the Hydrogel-PCP system and its clinical significance are the reviewed.

2.1 Peptide-drug conjugates

Peptide-drug conjugates (PDCs) are an evolving class of prodrugs, formed by the covalent coupling of a specific peptide sequence (often recognised and cleaved by a target enzyme) to a drug, possibly via an additional cleavable linker and are often used to selectively target tumour cells [18]. The amino acid sequence can be adapted to control the physiochemical properties of the drug conjugate as well as to accelerate or decelerate the active targeting of a particular receptor or proteolytic enzyme present at the tumour site. Therefore, the utilisation of peptides to form a prodrug incorporates a substantial degree of functionality into PDCs. The short peptide chain length of approximately 8-12 amino acids often seen in PDCs (the typical optimal length for enzyme recognition) compliments the method further by being readily biodegradable and rarely eliciting any undesirable immunogenic response [19]. The variety in amino acid combinations allows for an easily achievable preparation of many different PDCs, as well as the manipulation of the sequence providing control over conjugate properties such as ionisation and hydrophobicity, which influence the bioavailability of PDCs *in vitro* and *in vivo* [20]. Peptide-conjugated prodrugs generally have a low molecular weight, allowing simple purification via High-Performance Liquid Chromatography (HPLC) techniques. The control of PDC molecular weight and purity is crucial when optimising the pharmacokinetics of PDCs. Previous work has demonstrated the importance of the

peptide sequence: minor modifications, for example a single amino acid change to the peptide sequence of a PDC can cause significant changes to the way the peptide conjugate is recognised and metabolised by the target proteolytic enzyme [21]. This significant alteration to a PDC's performance in drug delivery, is not only affected by a change in the amino acid sequence but also the drug and linker molecule used. Two key areas of PDC research with regards to drug delivery involve 1) The reduction of off-target toxicity and 2) self-assembling PDCs.

2.1.1 Using peptide-drug conjugates to reduce unwanted toxicity

An identified trait amongst more traditional anticancer drugs is their non-selective nature, often leading to the failure of chemotherapy treatment due to dose-limiting toxicity, for which the cardiovascular system is a common site for unwanted toxicity [22]. The use of PDCs is known to reduce off-target toxicity amongst highly toxic chemotherapies whilst also being able to overcome another common issue, drug insolubility in water. The conjugation of an anticancer drug to a hydrophilic peptide conjugate can increase the solubility of the insoluble drug, allowing for greater functionality and safer delivery of the drug itself [20]. In this section a commonly used peptide-type, integrin-targeting, is outlined due to the enhancement of drug delivery observed.

Integrin targeted peptide-drug conjugates address the goal of delivering anticancer therapeutics to a disease site whilst limiting or avoiding the fallout of off-target toxicity in healthy tissues. In any treatment, particularly in cancer, the first step of interaction between a therapeutic agent and the cell occurs at the cell's exterior surface; this mechanism is an area to be exploited, because of the differences in the expression of receptors and/or enzymes on or around tumour cell surfaces compared to that of normal tissues. The vast array of overexpressed receptors and enzymes found in tumour masses allows for a greater diversity in PDC design, providing a more specific and selective targeting platform, tailored to a particular cell type. Integrins are a type of regularly targeted and identified receptors, as they are critical for physiological development, maintenance and repair of tissues, making them ideal receptors for cancerous tissues to overexpress, where they have been associated with enhancing cell metastasis and angiogenesis through the cooperation of serine proteases and metalloproteases [23, 24].

In 2016, Cox *et al* developed cysteine-knot mini-proteins (knottins) peptide-drug conjugates, using a variety of drug-linker strategies to highlight an optimal conjugate as an effective inhibitor of tumour growth in a series of malignant cell lines, by delivering the drug, gemcitabine (GEM) [25]. The group provided evidence showing integrin-binding was crucial for potency, the mechanism for cellular internalisation is mediated by the integrin ($\alpha_v\beta_6$) and the GEM payload was successfully released intracellularly. This was demonstrated across a wide variety of malignant cell lines including U87MG and D270 glioblastoma cell lines, breast MB-468, ovarian A2780 and pancreatic cell lines BxPC3 and PANC-1 [25].

The $\alpha_v\beta_6$ integrin is a receptor involved in cell adhesion and commonly found to be overexpressed in cancerous cells compared to healthy cells. Conibear *et al* (2017), synthesised β_6 targeting compounds, through solid-phase protein synthesis, consisting of integrin-targeting peptides, cytotoxic platinum (IV) prodrugs and fluorescent or affinity probes joined with flexible linkers [26].

Although several other drug conjugate strategies such as antibody-drug conjugates have proven promising for targeted drug delivery, peptide-drug conjugates are more readily optimised and modified to improve the targeting properties towards cancer cells and other diseased cell types, to develop cleavable linkers for the conjugation of therapeutic drugs [27, 28]. Optimisation of the peptide-drug conjugate allows for control over the targeting, making it more or less selective, depending on the balance between therapeutic effect and unwanted toxicity. Conibear *et al* (2017) demonstrated the flexibility of using a PDC design for integrin-targeted drug delivery using the “Y” structure to form the PDC, oxali-Pt-Y-1 (oxaliplatin based platinum (IV) prodrug with Y shaped branch scaffold), with a versatility allowing each module of the structure to be interchangeable for more suitable components depending on the target. An example of this would be the adaptation of the peptide conjugate to target alternative integrins other than β_6 , or even other receptor types overexpressed in the targeted disease [26]. The Y shaped module design synthesised by Conibear *et al* (2017) distinguished itself from previously discussed antibody-drug conjugates and peptide-drug conjugates [25] due to the two targeting peptides incorporated into the PEG₂₇ linkers. The selective uptake of oxali-Pt from the oxali-Pt-Y-1 structure from cells was confirmed, as was the retention of the cytotoxic activity [26].

The study by Conibear *et al* (2017) serves as one example of a new selective approach using PDCs to safely deliver a therapeutic agent to a disease site whilst

limiting the amount of off-target toxicity by selecting a target release trigger overexpressed in the disease site and not in the healthy tissue. This improves the therapeutic index of the selected drug, allowing a higher drug dose to be administered before the maximum tolerated dose (MTD) is achieved.

2.1.2 Self-assembling peptide-drug conjugates

Peptide-drug conjugates were initially designed to improve solubility and provide functional diversity by taking advantage of short hydrophilic peptides. Through research, a tendency for peptide segments to undergo self-aggregation has been identified, capitalising on the combination of low molecular weight hydrophobic drugs and hydrophilic peptide segments. The use of self-assembling peptides has expanded in recent years with regards to drug delivery. Here, the examination of self-assembling peptides and their use in drug delivery is discussed.

An important class of drug carriers relies on the use of hydrogels, an area of biomaterials with significant drug release capabilities [29-31]. Hydrogels in recent years have drawn much interest in their use as drug delivery vehicles, and in their early days, the research field focussed on the use of polymer-based hydrogels [32]. The research field has now branched out into supramolecular hydrogels too, due to the formation of aqueous assemblies of low molecular weight gelators through interactions [31, 33]. Supramolecular hydrogels, particularly, peptide-based, possess unique characteristics including, biocompatibility, low-toxicity and biodegradability. The formation of peptide-based hydrogels can also be initiated due to stimuli changes, such as temperature or pH, suggesting a promising alternative to polymeric hydrogels. Peptide-based hydrogels have demonstrated significant success in drug delivery, an example of which involved the use of self-assembling *N*-fluorenylmethoxycarbonyl diphenylalanine to react with positively charged poly-L-lysine by electrostatic interactions. The self-assembled nanofibers formed helical structures similar to fimbrial antigens and showed antigenic activities, serving as a vaccine to trigger strong antitumour immune responses without any antigen and adjuvant [34]. Activated T cell responses were demonstrated without the addition of antigens, leading to the suppression of tumour growth [34]. Furthermore, the injectability of the self-assembling peptide-based hydrogels, provides a clinical advantage when compared with many polymeric, implantable hydrogel devices, due to the less invasive nature of delivery, as well as a reduction in the risk of infection and therefore unwanted toxicity.

Altunbas and colleagues demonstrated a sustained release of curcumin, an anti-inflammatory and anti-tumorigenic compound extracted from turmeric root (*Curcuma longa*), from self-assembling peptides in a non-invasive injectable system [35]. One of the more significant areas of the research by Altunbas *et al* (2011) is the insolubility of curcumin in aqueous solutions which often limits the therapeutic uses, however encapsulation of curcumin and self-assembling peptide gelation that occurs in aqueous, physiological conditions, appears to overcome the curcumin insolubility complications. Research carried out has demonstrated curcumin is capable of inducing apoptosis in a variety of cancer cell lines, including MCF-7 and MDA-MB cell lines in a time and dose-dependent manner [36]. A 2009 review of curcumin and the effects it has upon cancer cell lines describes how it can selectively kill tumour cells and not the healthy cells, through the regulation of several cell signalling pathways, including but not limited to: cell survival pathway (Bcl-2), tumour suppressor pathways (p53 and p21) and the cell-proliferation pathway (c-myc) [37]. In relation to the use of self-assembling peptides, Altunbas and colleagues demonstrated growth of the human medulloblastoma cell line, DAOY on hydrogels not loaded with curcumin, however hydrogels loaded with curcumin inhibited DAOY cell growth. Further investigations showed that curcumin, released from the MAX8 hydrogels was functional, however in hydrogels containing a greater peptide concentration there was evidence of decreased cell death, thought to be due to the peptide inhibiting curcumin from freely moving through the hydrogel network due to hydrophobic interactions resulting in a slowed drug release in higher peptide concentrations [35]. These findings demonstrate an area where drug release is not only possible using self-assembling peptides as delivery vehicles, but also controllable by altering the peptide concentration versus the drug concentration to suit the delivery strategy.

Self-assembling peptides have proven to be strong candidates for drug delivery, as the rate of drug release can be controlled. The self-assembling peptide hydrogels themselves demonstrate versatility through the variety of applications they can be used for including drug delivery [38], tissue engineering [39] and wound healing [40]. The advantages of self-assembling peptides when compared to polymeric hydrogels appear superior, however the selection of the hydrogel type relies heavily upon the specific end-use application. Several polymeric hydrogels provide properties similar and, in some cases, superior to those of self-assembling peptides, including thermosetting properties, enhanced biodegradability and superior mechanical properties.

2.2 Hydrogel systems and their use as drug delivery vehicles

Recently, hydrogels have become an area of focus for delivering anticancer treatments due to their wide tunability and cross-linking properties. Hydrogels consist of 3-dimensional networks, made up of hydrophilic polymers, cross-linked either by physical intra-/inter- molecular attractions or through covalent bonds. Their ability to readily absorb water and biological fluids is very much desired in applications such as wound healing [41], due to their similar consistency to the extracellular matrix. The hydrophilic properties of hydrogels are largely due to the presence of hydrophilic moieties, for example carboxyl, amide, amino and hydroxyl groups within the polymeric backbone chains [42-44] as well as the presence of crosslinks among polymer chains, which prevents the dissolution of the polymer in water. Hydrogels were originally used for contact lenses after Wichterle *et al* developed a poly(2-hydroxyethyl methacrylate)-based hydrogel over 50 years ago [45]. Research within the hydrogel field has progressed considerably since the work of Wichterle *et al*, particularly within the last 20 years. As the field of research has expanded, the variety of biomedical applications associated with hydrogels has broadened and now includes, but is not limited to, wound healing [46], tissue engineering and drug delivery as well as controlled drug release [47]. There are now several types of hydrogel, widely used to address these applications; three popular types are homopolymer, copolymer and the previously discussed self-assembling peptide systems. Both, homo and copolymer hydrogels originate from either synthetic-based or biopolymer-based materials, of which the biopolymer-based materials will form the basis of this research project. Each of these hydrogel types have advantages and disadvantages depending on the type of application desired, for example the self-assembling peptide-based hydrogels lack covalent bonding [48] and as a result are generally mechanically weaker than a crosslinked homo- or copolymer.

Due to their tissue-like consistency and tuneable characteristics through functionalisation of the backbone polymer, hydrogels have become extremely popular as tissue engineering scaffolds or drug release devices. As well as their tuneable characteristics, a wide range of polymeric biomaterials, from both natural and synthetic sources can be used as a starting material. The extensive variety allows a hydrogel to have unique properties, such as being magnetic, thermosensitive and photo-active, each of which has recently demonstrated a use as a delivery vehicle for localised drug delivery. Similarly, to the type of hydrogel material, the unique properties required of the hydrogel system depend upon the type of application, the delivery of the device and if used for drug delivery desired rate of

drug release. Table X indicates some examples of hydrogels used within a variety of applications.

Type of Hydrogel	Monomer	Functionalised with molecule	Cross-linker	Specific reaction conditions	References	Applications
Homopolymer	Oligo PEG fumarate ²	Sodium methacrylate	I2959	Free-radical photopolymerisation	[49-55]	Drug delivery, wound healing, Tissue engineering
	Collagen ¹	4VBC				
	Gelatin ¹					
	Agarose ¹	Poly(vinyl alcohol)	<i>N,N'</i> -Methylene bisacrylamide			
	Chitosan ¹	N/A	N/A - Thermosensitive	1% lactic acid solution and 1.5 ml glycerol in distilled water		
Copolymer	PLGA-PEG-PLGA ²	N/A	N/A- Thermosensitive	Tuneable temperature of solution-gel transition based on concentration	[56-60]	Drug delivery, wound dressing
	Hyaluronic acid and Chitosan ¹	N/A	N/A	24 mg/ml carboxymethyl chitosan mixed with 60 mg/ml aldehyde HA using a traditional double syringe		

	Alginate and PEG-diamines ²	N/A	Chemical	EDC/NHS solution		
	Cellulose and poly(N-vinyl pyrrolidone) ¹	N/A	Cobalt-60	Radioactive polymerisation		
Self-assembling peptide systems	Heparin ³	N/A	Chemical	EDC/sulfo-NHS solution and low temperature	[61-63]	Tissue regeneration, drug delivery
	Multidomain peptide chains ³	N/A	Presence of negatively charged phosphate ions	Dissolved in deionised water containing 298 mM sucrose at 20 mg/ml		
	D-peptides (peptide chains containing D-amino acids) ³	N/A	N/A- Thermosensitive	Self-assembly upon cooling to room temperature after boiling		

Table 2.1. Examples of the variety of hydrogel materials, cross-linking methods and applications present in current literature.

¹ Denotes biopolymer-based hydrogels

² Denotes synthetic-based hydrogels

³ Denotes self-assembling peptide systems

Using hydrogels as delivery vehicles for therapeutic drugs, enables greater therapeutic doses to be administered, as well as a reduced risk of off-target toxicity which, as discussed earlier, is a major clinical drawback within disease treatments, particularly anticancer treatments. In this section, three key varieties of hydrogels will be discussed alongside current literature, to aid in the selection of a suitable hydrogel material and type for the design of a novel Hydrogel-PCP system in Chapter 2.3.4.

2.2.1 Thermosensitive hydrogels

The use of thermosensitive hydrogels as drug delivery vehicles has become increasingly popular, particularly the lower critical solution temperature (LCST) gels. This is due to their ability to appear in a liquid polymer form at room temperatures, however upon being implanted or exposed to physiological temperatures they stiffen to become more gel-like, forming a hydrogel network [64]. Their liquid state at room temperature allows drugs to be mixed with them, which are loaded onto the hydrogels in response to temperature increase. An advantage of using a thermosensitive hydrogel is the removal of a chemical stimuli which is usually required to trigger the release of a drug from its vehicle. Drug diffusion from thermosensitive gels can play a crucial role in drug release [65]. The process of liquid to gel is also reversible which allows thermosensitive hydrogels to be easily implanted and removed from the target site [66, 67]. An example of a thermosensitive hydrogel used in drug delivery is the triblock copolymer composed of poly(D,L-lactic-co-glycolic acid) (PLGA) and polyethylene glycol (PEG) also known as PLGA-PEG-PLGA. Some advantages of this copolymer are its simplistic design, which does not require organic solvents for either its synthesis or purification, and that the polymer is also biodegradable and biocompatible. From a drug delivery perspective, the PLGA-PEG-PLGA hydrogel can deliver both hydrophilic and hydrophobic drugs, has little systemic toxicity, and has been widely used as a cancer drug delivery vehicle [68]. In 2001, Zentner *et al* used PLGA-PEG-PLGA to deliver paclitaxel to tumour sites - controlling the release for up to 50 days, whilst demonstrating minimal drug release in healthy tissue [60]. More recently this gel has been used in a co-delivery study of 3 commonly used anticancer drugs, doxorubicin (DOX), cisplatin (CDDP) and methotrexate (MTX) for the treatment of osteosarcoma. As with many other cancer therapeutic drugs, DOX, CDDP and MTX are non-selective and highly cytotoxic agents which are linked to off

target toxicity [69-71]. Therefore, the need to safely deliver these drugs is key and has been demonstrated by Ma *et al* [59].

Ma *et al*, using a 20 wt.% PLGA-PEG-PLGA hydrogel, due to its appropriate sol-gel transition temperature and gelation time, loaded DOX, CDDP and MTX and assessed the *in vitro* drug release [59]. MTX and DOX demonstrated an initial fast release for 2 days after administration, before a sustained release over 10 days. CDDP however, exhibited 70% release in the first 2 days, thought to be due to its enhanced solubility and reduced substitution of Cl⁻ ion activity [72].

The group's *in vitro* study indicated the hydrogel demonstrated cytocompatibility in both the osteosarcoma cell lines (Saos-2 and MG-63) as well as the normal tissue cell line (L929). Cytotoxicity was assessed using an MTT assay, which exhibited enhanced cytotoxicity on Saos-2 and MG-63 cell lines when the hydrogels were co-loaded with all three drugs. *In vivo*, it was shown by Ma and colleagues that drug-loaded PLGA-PEG-PLGA hydrogels demonstrated increased tumour inhibition efficacies for up to 16 days, compared to treatments with free drugs. It must also be noted that in this study, co-loaded hydrogels exhibited greater antitumour effects than hydrogels loaded with a single drug [59].

In terms of reducing off-target toxicity, which as previously stated is a key objective in selective methods of treatment, Ma *et al* also assessed systemic toxicity effects. During the *in vivo* study, body weight checks were carried out, which indicated low systemic toxicity was associated with this method of localised treatment due to no significant weight loss shown in the mice [59].

To further assess the off-target toxicity, H&E stains were also carried out on the organs of sacrificed mice including, liver, heart, kidney and spleen. No obvious abnormalities were shown by the H&E staining, suggesting no off-target toxicity during the study, due to the localised methods of treatment [59].

The study by Ma *et al* serves as a key example of enhanced delivery and sustained antitumour effects which can be achieved using thermosensitive hydrogels as delivery vehicles for anticancer drugs. Of course, there are various other thermosensitive hydrogels which could be used, for example the PECT based hydrogels [73] and anticancer drugs such as paclitaxel and docetaxel [74, 75].

2.2.2 Magnetic hydrogels

Magnetic hydrogels are another variation of hydrogels used for several applications, including drug delivery. A common nanoparticle used to give the hydrogels their magnetic characteristics is a magnetic iron oxide nanoparticle (MION). Due to their unique properties, small size, low toxicity, availability as well as their detection and separation techniques, to mention a few, MIONs make ideal compounds to be used in the production of nanoparticles. Another reason as to why MIONs are commonly used is that they can be coated in a wide range of materials [76] such as polymers, for example PEG, which can form hydrogels through surface initiated photopolymerisation. The release of therapeutic drugs coupled to these magnetic hydrogels can be carried out by passing alternating magnetic fields (AMF) through them. The AMF causes an increase in temperature of the hydrogel, leading to an increased rate of diffusion of the drug. A 2012 study by Meenach *et al* demonstrated the efficacy of paclitaxel, that was delivered by PEG-iron oxide hydrogel nanocomposites, was increased when temperatures reached hyperthermic levels (41-45°C) in A549 lung carcinoma cells [77].

A key advantage of using MIONs to deliver therapeutic drugs is by pulsating the hydrogels using AMF, which provides controlled bursts of drug release to the target area. There are several ways in which research groups have used MIONs to benefit their drug delivery hydrogel vehicles either by using the technique alone or combining it with another type of hydrogel such as a thermosensitive hydrogel [78].

A recent paper has demonstrated the use of magnetic and pH responsive K-carrageenan/chitosan complexes for the controlled release of methotrexate (MTX) [79]. It was shown that a greater quantity of MTX could be loaded onto the hydrogels with a higher magnetic content, thought to be due to the high surface area of the nanoparticles, as well as methotrexate's favourable interactions with hydroxyl groups of magnetite [80]. In terms of the magnetic hydrogels, drug release at different pHs was identified. It was found that MTX at a pH level of 5.3 released approximately 50% of the total MTX within the first 4hrs after administration, with the rest being released at a sustained rate over the next 48hrs. However, at a pH of 7.4, approximately 68% of the administered MTX was released over the initial 4hrs, and the majority of the remaining released over the next 7hrs [79].

This study provided the concept for the delivery of MTX, and potentially other therapeutic drugs, using magnetic and pH responsive hydrogels which could be applied to other types of hydrogel in the future. The Mahdavinia *et al* study also

compliments research carried out by other groups such as that by Davaran *et al* in 2014 who used poly(NIPAAm-MAA-VP) magnetic (Fe_3O_4) hydrogel nanocomposites as an effective carrier for targeting in drug delivery systems as an anticancer treatment method [81]. Similarly to the work of Meenach *et al* (2012), Davaran and colleagues observed increased drug release at 40°C in acidic conditions compared to 37°C, however drug release was assessed in basic conditions at 37°C which may have also affected the drug release [81].

All in all, the use of magnetic hydrogels and the varying degree of drug release at different pHs have displayed impressive results in their use as anticancer drug delivery vehicles.

2.2.3 Photopolymerisation hydrogels

The increasingly popular use of photo-active molecules to functionalise the desired biomaterial can provide control over the network architecture as well as the mechanical and swelling properties. The photo-crosslinking strategies have been applied to the formation of synthetic polymer systems where their tunability and biocompatibility have been reported in detail [82-84]. Photo-activated hydrogels have been used for a variety of applications including the generation of on-demand H_2O_2 in cell culture [85], tissue engineering [86] and localised drug delivery [87]. However, the use of solely photo-activated hydrogels in drug delivery as opposed to a hybrid-type hydrogel is relatively new, particularly where the use of harmful UV light to form the hydrogel is avoided [88].

In 2012, Bakó and colleagues synthesised a methacrylated PGA (MPGA) based hydrogel via free radical polymerisation in a photoinitiator-supplemented PBS solution containing 30% w/w of MPGA. Metronidazole, was loaded as a drug onto the hydrogel, and the release rate was assessed by immersing the MPGA loaded gels in PBS and HPLC of the supernatant at regular time intervals[87].

The release measurements were carried out in five parallel experiments to ensure reliable data. Bakó *et al* (2012) found that drug release was primarily ruled by the hydrogel swelling behaviour due to the rapid increase of swelling in the first two hours, which prompted the initial burst effect. After 2 hours, the rate of drug released remained at a sustained level for the next 6 hours. It must be noted that release profiles were carried out by Bakó *et al* in *in vitro* conditions only, where mixing speeds and the amount on medium was increased [87]. Therefore, drug release would likely be slower when tested in *in vivo* or *ex vivo* environments.

During the toxicological assessment, when compared with PGA, the MPGA polymer exhibited no notable differences in either an MTT or LDH assay. For both polymers, the cytotoxicity did not exceed 4%, and was therefore deemed non-toxic. The MPGA hydrogels were also analysed and again were shown to be non-toxic. In the hydrogel form, the LDH assay demonstrated cytotoxicity levels of 3.82% and the MTT assay results were 104.2%, indicating no cell toxicity [87].

These results provide strong evidence for the use of MPGA and the potential for other solely photo-activated hydrogels in drug delivery due to their non-toxic nature. Another key point that must be noted, is the use of blue dental light, as opposed to UV light to induce hydrogel network formation, which has become a greater sought-after method of forming hydrogels due to the unwanted radiation associated with UV light, combine with the ability to induce network formation *in situ*, for example in the mouth during dental procedures.

There is a limited amount of research involving the use of photo-crosslinked hydrogels for the delivery of anticancer drugs. In 2010, Dadsetan *et al* synthesised oligo (poly(ethylene glycol) fumarate) (OPF) hydrogels modified with sodium methacrylate (SMA), through photopolymerisation under UV light [51]. The group loaded DOX onto hydrogels by incubating the gel discs in 1 ml of aqueous DOX at varying concentrations at 37°C. It was demonstrated that non-SMA modified OPF hydrogels showed greater initial burst release of DOX as well as an overall amount released during the 15-day assay. The higher the SMA content the lower the release seen over 15 days; however, release could have continued for a greater period of time, which was not assessed in this study. Over the 15 days, in non-SMA modified OPF hydrogels, 100% of the loaded DOX was released whereas the HG-SMA50 exhibited 57% DOX release and the HG-SMA300 (high density charged hydrogels), just 20% [51]. This sustained release, may be more advantageous when targeting certain cancers, as recent studies have shown a lower, more sustained release can provide greater control over the cancer growth, prolonging the tumour progression time [89].

In terms of cell toxicity however, Dadsetan and colleagues demonstrated that although the release of DOX was lower, the cell toxicity was significant in the osteosarcoma cell line MG63, with the maximum killing effect at DOX concentrations greater than 1 µg/ml. The group also showed the toxicity between hydrogels loaded with DOX versus hydrogels without DOX loading. As expected in hydrogels lacking DOX, the MG63 cells maintained their viability, indicating the non-toxic nature of the

hydrogels, whereas the DOX loaded hydrogels exhibited significant toxicity with minimal cell survival over three days [51].

2.2.4 Overcoming solubility complications

Another challenge that many anticancer drugs, such as paclitaxel, face is the insolubility in aqueous environments [90]. Insolubility poses real obstacles in terms of the delivery of a therapeutic agent, not only in cancer but all forms of therapeutic treatments [91]. This is because if a drug is insoluble then it cannot be readily administered by intravenous methods or dissolved to couple to a vehicle. The use of hydrogels has shown significant progress in recent times for the delivery of hydrophobic, insoluble drugs [92-94]. Various techniques have been applied towards overcoming the insolubility of anticancer drugs using hydrogels, from peptide nanofibers [94] to the complete encapsulation of the therapeutic agents in micelles [95]. In 2016 Li *et al* designed and synthesised injectable multidomain peptide (MDP) hydrogels, which contain a hydrophobic binding pocket. The MDP consists of a peptide made of alternating hydrophilic and hydrophobic amino acids with charged residues at both termini. In aqueous solutions, this design allows hydrophobic side-chains to aggregate, forming a peptide dimer. Several peptide dimers form a further sequester of hydrophobic residues from contact with the surrounding aqueous solutions [94]. Interestingly, Li and colleagues were able to alter the release profile of the loaded drugs, by increasing the amount of drug encapsulated within the formed nanofibers. It was demonstrated, that the greater the encapsulation of the anticancer drug SN-38, the slower the release profile, showing 60% total drug release over 8 days in the most encapsulated hydrogel ($K_2(SL)_3SA(SL)_2K_2$). The other two loaded hydrogels tested by Li *et al* demonstrated more than 90% release of SN-38 in the initial 24 hours [94]. Another anticancer drug which was assessed, daunorubicin, exhibited short term drug release (95% release over the initial 4 hours) from the hydrogels, irrespective of the encapsulation. The group also demonstrated the drug release of anti-inflammatory (diflunisal and etodolac) and antibiotic drugs (levofloxacin and norfloxacin), which could be used as combinational therapies when treating certain diseases [94].

The work reported by Li *et al* is just one example of the use of hydrogels to overcome the inconvenience of delivering insoluble therapeutic drugs in an ever-growing field of research [95-97]. By using hydrogels to deliver both soluble and insoluble drugs, unlike liquid-based drug carriers, hydrogels can remain within the

disease site, which enables the localised targeting of a drug, reducing the amount of off-target toxicity [98, 99].

To summarise, hydrogels are useful vehicles for the delivery of drugs to a target site requiring therapeutic treatment, as their tuneable properties allow for a wide variety of applicable characteristics to suit a range of environments, whilst reducing the risk of unwanted off-target toxicity. The unique tailoring of hydrogel characteristics, result in finely tuned properties, selected to be specific towards the end use requirements of the material.

2.3 Targeted diseases and Hydrogel-PCP system component selection

Peptide drug conjugates, also known as peptide-conjugated prodrugs (PCP), are a sequence of peptides, covalently coupled to a drug with a view of delivering the conjugated drug to a target site for release in a localised area to improve the drug efficiency or reduce unwanted off-target toxicity [20]. There are several means of achieving drug release from a PCP, two methods involve 1) a localised, passive release from the natural break down of the biodegradable PCP and 2) a selective release, targeting an overexpressed enzyme in the disease, or condition the drug is aimed at treating. The latter of these methods requires a protecting endcap to avoid any unwanted metabolism of the peptide chain, whilst the middle section of the chain being selective to an active site of an overexpressed proteolytic enzyme [100]. Many diseases require pathological changes to promote symptoms, of which, enzymes often play a key role, whether that involves an up or down regulation of enzyme expression. Overexpression of these enzymes makes them ideal targets to exploit when using PCPs to target the disease [101]. Peptide-conjugated prodrugs also begin to address the complication of delivery of insoluble drugs, which particularly in diseases such as cancer, appear to be the more successful therapeutic treatments [102]. However, PCPs are not the only way to overcome insolubility, or deliver a drug for a localised treatment, as previously discussed, hydrogels are also useful delivery vehicles. The careful selection of the base material used for the hydrogel, could allow PCPs to be conjugated to the polymer, enhancing the localised delivery of a drug, particularly if the PCP was used as a selective release mechanism by targeting an overexpressed proteolytic enzyme to cleave and release the therapeutic drug in the disease tissue whilst reducing the release to normal tissue [103, 104]. Selection of a suitable hydrogel base material is necessary depending upon the intended delivery site. For example, where a disease occurs in a site under mechanical pressures such as within a joint, the hydrogel base material would also be required to withstand similar levels of mechanical stress, although the selected material cannot be too rigid, as between a joint the gel would need to be fluid and move, as cartilage, the connective tissue between joints does. Using hydrogels to deliver a selective PCP could provide a tissue support network whilst administering a therapeutic agent to the affected area.

For the purposes of this study two different diseases were selected as possible treatment targets; these were osteosarcoma and rheumatoid arthritis, which both require clinical interventions to provide a more targeted therapeutic strategy.

2.3.1 Osteosarcoma – overview of cancer

Collectively, cancer is a leading cause of death worldwide and was responsible for approximately 9.6 million deaths during 2018 according to the World Health Organisation. Cancer occurs as the result of a mutation which causes the rapid division of abnormal cells, able to grow beyond their usual boundaries by evading apoptosis and acquiring limitless replicative potential. Evading apoptosis is one of 6 hallmarks of cancer published by Hanahan and Weinberg in 2000 [105], describing 6 common traits that oversees the transformation from healthy cell to cancerous (malignant) cell (*Figure 2.1.*).

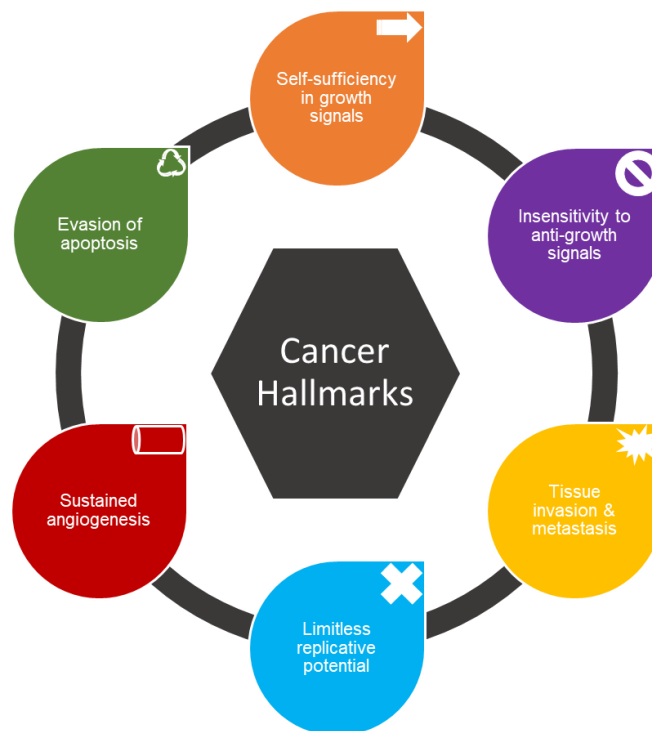


Figure 2.1. Hallmarks of cancer. The majority of cancers acquire the same set of functional capabilities during development through a range of mechanical strategies.

Cancer Hallmark – Growth signal self-sufficiency: The ability of cancer cells to generate their own growth signals reduces the dependence on stimulation from their healthy tissue microenvironment. In normal cells, the majority of soluble mitogenic growth factors (GF) are produced by one cell type, which in turn stimulates the proliferation of another, however cancer cells acquire the ability to synthesise their own GFs which they are responsive to, allowing the establishment of a positive feedback cycle, often referred to as autocrine stimulation [105]. As well as producing

their own GFs, certain types of cancer cells overexpress growth factor cell surface receptors, usually tyrosine kinase [106]. The overexpression of GF receptors may lead to hypersensitive responses to moderate levels of GF which would not normally trigger proliferation. For example, the human epidermal growth factor receptor 4 (HER4) is overexpressed in osteosarcoma and promotes cell survival and chemoresistance [107].

Cancer Hallmark – antigrowth signal insensitivity: Whilst becoming self-sufficient in the production of their own growth factors, cancer cells also become unresponsive towards antigrowth signals. Antigrowth signals work through two mechanisms, 1) forcing cells out of an active proliferative state and into a quiescent (G_0) state or 2) by permanently relinquishing their proliferation potential by being induced into postmitotic states [105]. For cancer cells to thrive, antiproliferative signals must be evaded, often through the disruption of the retinoblastoma protein (pRb) pathway. When in a hypophosphorylated state, pRb prevents cell proliferation by sequestering and altering the function of E2 Transcription Factors (E2F), controlling the expression of genes required for progression from G1 to S phase during the cell cycle [108]. Cancer cells disrupt the pRb pathway, leading to the liberation of E2F, allowing cell proliferation to occur irrespectively of antigrowth factor signals which would ordinarily prevent advancement through the G1 phase of the cell cycle.

Cancer Hallmark – Evading apoptosis: The rate of cell proliferation is not the only factor governing the expansion of tumour cell populations, the rate of cell attrition which is mostly represented by programmed cell death, apoptosis also plays a part. Apoptosis is monitored by stimuli indicating whether a cell should live or die and is usually triggered by the mitochondria in response to proapoptotic signals, releasing cytochrome C [109]. The Bcl-2 family of proteins regulate mitochondrial cell death signalling through several proapoptotic (Bax, Bak, Bid, Bim) and antiapoptotic (Bcl-2, Bcl-XL and Bcl-W) proteins, as well as the p53 tumour suppressor gene which induces apoptosis in response to DNA damage, leading to the upregulation of Bax expression to stimulate the release of cytochrome C from mitochondria. Evading apoptosis is a crucial trait for cancer cells to acquire in order to form a tumour mass. Evidence to support this consensus can be seen in a paper by Liu *et al* (2018), where RACK1 (receptor of activated protein kinase C 1) was overexpressed, leading to the facilitation of Bcl-2 expression and the restraint of Bim expression, in turn causing increased chemoresistance towards cisplatin [110], a chemotherapeutic drug

interfering with DNA replication within the cell leading to apoptosis induction [111], causing the prevention of apoptosis.

Cancer Hallmark – limitless replicative potential: The three previously described hallmarks, all involve the uncoupling of a healthy cell's natural growth program from signals within the environment. Although cells can provide themselves with growth signals and evade apoptosis, studies have indicated that this is not always sufficient enough to ensure expansive tumour growth. Cells managing to evade apoptosis still require the ability of limitless replicative potential, allowing them to continually divide above the usual 60-70 doublings seen in various normal human cell types. In healthy cells chromosomal telomeres, comprised of some thousands of repeats of 6 base pairs (bp) sequence elements become 50-100bp shorter upon each cell division, thus allowing the counting of cell generations to be possible. The loss of telomeric DNA from the ends of the chromosome at each cell cycle replication is due to the inability of DNA polymerases to fully replicate the 3' ends of chromosomal DNA during the S phase of the cell cycle [112]. Over the course of successive replication cycles, the erosion of telomeres ultimately causes them to lose their ability to protect the ends of the chromosomal DNA. Once unprotected, chromosomal ends fuse leading to karyotypic disarray associated with crisis, resulting in the death of the affected cell [112, 113]. Telomere maintenance is observed in many malignant cells [114], the majority of which do so through the upregulation of the telomerase enzyme, lengthening the telomeric DNA [115]. Mechanisms causing the upregulation of telomerase often revolve around a mutation within the core promotor region of the telomerase reverse transcriptase (TERT), which is an essential molecule for the catalytic activity of telomerase [116]. These mutations increase TERT transcriptional activity by creating de novo consensus binding motifs for E-twenty-six (ETS) transcription factors [117], leading to limitless replicative potential.

Cancer Hallmark – Sustained angiogenesis: The nutrients supplied to a tissue region are vital to cellular function and survival. Once a tissue is developed, the growth of new blood vessels – angiogenesis – is carefully regulated as cells lack the intrinsic ability to promote blood vessel growth. In order for a cell mass to progress to a larger size, to provide the essential oxygen and nutrients it requires, neoplasia's must develop angiogenic capabilities [118, 119].

The ability to induce and sustain angiogenesis is discretely acquired during tumour development by an "angiogenic switch" from vascular quiescence. Hanahan

and Folkman showed three transgenic mouse models acquired angiogenic capabilities, activated in mid-stage lesions, before the appearance of full-blown tumours [118]. The switch is activated by changing the balance of angiogenesis inducers and inhibitors. A common strategy involves altering gene transcription. Many tumours are shown to have increased vascular endothelial growth factor (VEGF) compared to normal tissue [118, 120, 121]. Another is the downregulation of endogenous inhibitors such as thrombospondin-1, which can be caused by a loss of p53 function [122], commonly seen in many tumours. Proteolytic enzymes such as MMP14 (matrix metalloproteinase-14) are also shown to promote angiogenesis and inhibit apoptosis by mediating VEGF in a variety of cornea [123] and breast carcinomas [124].

Cancer Hallmark – Tissue invasion and metastasis: The complex processes of invasion and metastasis enables cancer cells to escape the primary tumour site and colonise a new site within the body where, space and nutrients do not initially limit the metastasised tumour growth. Extracellular proteins play crucial roles in tumour metastasis, degrading the extracellular matrix (ECM) allowing migration and invasion to occur. Matrix metalloproteinases (MMPs) are a well-researched family of proteins for their roles in tumour metastasis and the acquisition of other cancer hallmarks. In oral squamous cell carcinoma, the transcription factor, Snail (SNAI1) upregulates MMP2 and MMP9, initiating epithelial-mesenchymal transition (EMT) [125]. Epithelial-mesenchymal transition is the process by which epithelial cells lose their cell polarity and cell-cell adhesion, achieving cell invasive and migratory characteristics. A widely observed cell-to-environment change in cancer involves E-cadherin, a homotypic cell-to-cell interaction molecule expressed in epithelial cells. Coupling between cells via E-cadherin bridges allows the transmission of antigrowth signals [126]. Function of E-cadherin is lost in many epithelial cancers by mechanisms including the mutational inactivation of E-cadherin genes, transcriptional repression or proteolysis of the extracellular cadherin domain [126].

2.3.2 Osteosarcoma – the disease

Osteosarcoma (OS) is the most common type of bone cancer and commonly arises in children and adolescence. The 5-year survival rate of localised osteosarcoma is approximately 80%, however those with metastatic osteosarcoma have a significantly lower survival rate. Survival rates in the decade leading to 2009 have shown little increase, suggesting a need for new treatment options [127, 128]. The disease itself is a malignant, abnormal growth of osteoblasts usually originating from the metaphysis of long bones and are known to metastasise early on in their progression, of which a usual metastatic site is the lungs (pulmonary metastases). Lung metastases osteosarcoma patients have poor prognosis, and a 5-year survival rate of approximately 30% according to the 2019 study by Huang *et al* [129] despite having surgery and chemotherapy treatments.

The exact cause of osteosarcoma remains unknown, however defects in pRb and p53 genes play key roles in the development of OS. Mutations in pRb gene are observed in a high percentage of osteosarcoma and small cell lung carcinomas. In patients carrying germline Rb mutations, osteosarcoma is the second most common cancer type, with greater than 70% of cases demonstrating a molecular change or mutation at the Rb locus [130, 131]. Similarly, p53 plays a variety of different roles within the development of OS as p53 regulates the cell cycle, apoptosis and cell differentiation [132]. In human patients with Li-Fraumeni syndrome, an autosomal dominant hereditary disorder linked to germline mutations of the p53 tumour suppressor gene, OS is reported to occur more frequently [133, 134]. It is unsurprising that mutations in p53 lead to cellular acquisition of several key cancer hallmarks in osteosarcoma, of which mesenchymal stem cells and preosteoblasts have been identified as the cellular origin of OS [135, 136].

The diagnosis of OS involves radiological investigations including but not limited to: x-ray, CT scans and MRI scans. Radiological investigations suggest 91% appear in the metaphyseal areas of long bone, of which almost 50% of osteosarcomas occur around the knee [137]. After complete history, clinical examinations and imaging have been carried out, a biopsy is used to confirm the diagnosis and reveal the specific type and grade of the tumour [137]. Open incisional biopsies are performed through small incisions and have a major advantage of providing adequate quantities of tissue for histopathology, immunohistochemistry and genetic studies. However, open biopsies require more time and risk contamination of normal tissues during the surgical procedure. Closed method

biopsies, particularly percutaneous core needle biopsies have advanced significantly to become a safe and accurate method for diagnosing bone tumours. A Jamshidi needle is used to take multiple cores from a representative region of the tumour and is a less extensive and less time-consuming outpatient procedure, carried out under local anaesthesia with minimal soft tissue trauma and less contamination of normal tissue by tumour cells [137, 138]. Several research groups support core needle biopsies as it provides sufficient sample for diagnosis with minimal complications [139-141]. As suggested by the American Joint Committee on Cancer, a 4 grade system is used for osteosarcoma, with grades 1 and 2 considered as “low-grade” and grades 3 and 4 “high-grade” [142]. This is supported by the World Health Organisation which groups the grades into a two tier system (low and high-grade) [143]. Low-grade osteosarcoma is considered to be non-metastatic, whereas high-grade is of a higher risk of metastasis, where chemotherapy tends to be mandatory in patients with a high grade diagnosis [144].

Current treatments for osteosarcoma include neoadjuvant chemotherapy, followed by surgery to remove the primary tumour and any evident metastatic disease, followed by further chemotherapy after surgery [145]. The most accepted chemotherapeutic for osteosarcoma is methotrexate (at very high doses), a DNA synthesis disrupting agent which irreversibly competitively inhibits dihydrofolate reductase (DHFR) which catalyses the oxidation of folates (*Figure 2.2.*). DHFR inhibition prevents the production of thymidylate in DNA synthesis, leading to cell proliferation arrest and eventually apoptosis or autophagy [146]. Methotrexate is administered with a leucovorin rescue which is an antidote to methotrexate and replenishes depleted tetrahydrofolate stores, a mainstay treatment of OS chemotherapy [146]. Combinational chemotherapy between MTX and other drugs such as doxorubicin are used to improve survival rates compared to MTX alone [147-149]. Other treatments of OS include non-steroidal anti-inflammatory drugs which are widely used to reduce pain and inflammation, but are also toxic to certain cancers [150]. Several sarcomas, including osteosarcoma express cyclooxygenase-2 (COX-2) [151, 152]. Non-steroidal anti-inflammatory drugs significantly inhibit COX-2 at a therapeutic dose, making them possible treatments for OS [153].

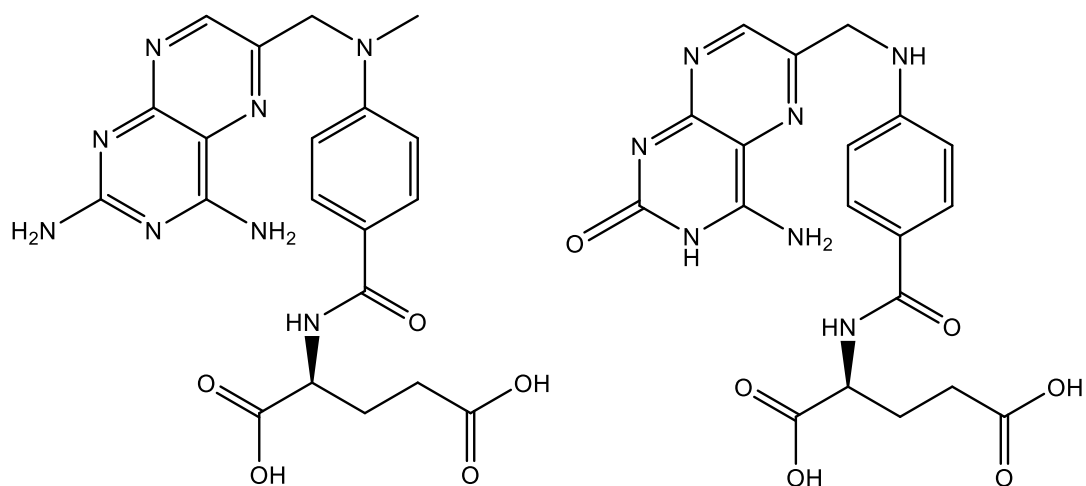


Figure 2.2. Structural similarities between methotrexate and folic acid. Methotrexate (left) and folic acid (right).

There is a crucial need for clinical intervention with regards to osteosarcoma treatments. The current medical therapy for this disease has seen little change for the last 50 years and still relies heavily on the aforementioned chemotherapy-surgery-chemotherapy strategy [154]. Ignoring the non-selective and invasive nature of the current treatment, the need for improved treatment deliveries are required to improve patient welfare. Chemotherapy is plagued with side-effects including but not limited to: hair loss, nausea, fatigue and anaemia, all of which can contribute to an already unpleasant illness. New, more selective means of targeting OS are required and in recent years there have been several promising developments such as the study carried out by Shan *et al* (2020) which locally delivered methotrexate and alendronate in a controlled manner, using an injectable thermosensitive hydrogel as a delivery vehicle [155]. Shan *et al* observed inhibited tumour growth, as well as a reduction in bone destruction and lung metastasis caused by OS using the injectable delivery device [155]. The use of a hydrogel to deliver a novel therapeutic treatment is advantageous in complex disease such as osteosarcoma and rheumatoid arthritis where the drugs commonly required for treatment are often capable of causing severe off-target toxicity. By selectively releasing the therapeutic agent in a localised manner, the off-target toxicity can be reduced, limiting the side effects of chemotherapy as well as damage to healthy tissues around the disease site.

As described, cancers require a set of characteristics in order to achieve immortality, evade apoptosis and invade tissues and therefore the up or down regulation of particular cellular components must occur, for example enzyme

expressions. Often a tumour overexpresses the matrix metalloproteinase (MMP) family of enzymes, to achieve tissue invasion due to their ability to degrade the extracellular matrix and involvement in angiogenesis [156-158]. The exploitation of overexpressed proteolytic enzymes could pave the way for a new, selective therapeutic osteosarcoma treatment using a PCP delivery strategy. The use of a PCP, particularly if a chemotherapeutic agent were to be conjugated, would allow for a safer delivery route to the tumour site, minimising the risk of off-target toxicity and damage to healthy tissues. As previously described in Section 2.2, hydrogels are another suitable delivery strategy to target osteosarcoma and could be implanted at the time of surgery or injected for *in situ* network formation to administer therapeutic drugs to the tumour site. The advantages of a selective and localised administration of a chemotherapeutic drug such as MTX improves the therapeutic index of the particular drug, allowing for a higher dose, or prolonged drug administration to be administered whilst maintaining the same or lower toxicity to healthy tissues.

2.3.3 Rheumatoid arthritis

Rheumatoid arthritis (RA) is a long-term disease affecting joints, caused by an autoimmune disorder, however the exact cause remains unclear. Approximately 80% of patients carry the epitope of the HLA-DRB1*04 cluster [159]. Rheumatoid arthritis usually arises during productive years of adulthood (between 20-40 years of age). According to the World Health Organisation, prevalence varies between 0.3 and 1% and is more common in women and developed countries, and within 10 years of onset over 50% of patients are unable to carry out full-time work [160]. Warm, swollen and painful joints are amongst the most common symptoms of RA, as well as stiffness in joints, particularly after periods of rest. These symptoms are a result of inflammation around the joint and over time this inflammation leads to the erosion and damaging of the joint surface, for example cartilage degradation [161]. Inflammation occurs within the synovial membrane, the innermost part of the joint, which is normally a thin layer, a few cells thick [162].

Various immune modulators (cytokines and effector cells) as well as signalling pathways are involved in the pathophysiology of RA [163]. Pro-inflammatory cytokines such as IL-6 and TNF- α are involved in RA pathogenesis, playing dominant roles including, B and T cell proliferation, increased MMP and cytokine release [164] as well as osteoporosis [165] and cardiovascular disease promotion [166]. Tissue degradation is associated with the accumulation of several cell populations within the synovial membrane and the formation of a proliferating pannus. These cell populations include, macrophages, both T and B lymphocytes and dendritic cells [167]. The space where cartilage and pannus meet is occupied predominantly by macrophages and fibroblast-like synoviocytes (FLS) which have the potential to secrete proteolytic enzymes of which matrix metalloproteinases and cathepsin mRNA are expressed from the earliest stages of RA [168]. The FLSs synthesis of MMPs triggers the disassembly of type-II collagen (cartilage) networks, leading to the alteration of glycosaminoglycan content and water retention directly causing biomechanical dysfunction [169]. Endogenous enzyme inhibitors, such as tissue inhibitors of metalloproteinases (TIMPs) have failed to reverse the destructive cascade and articular cartilage has limited regenerative potential. These ultimately lead to the destruction of surface cartilage and the appearance of joint-space narrowing [159, 169].

Treatment of RA commonly involves the use of disease-modifying anti-rheumatic drugs (DMARDs) or non-steroidal anti-inflammatory drugs (NSAIDs) either

separately or in combination with each other. Of the disease-modifying anti-rheumatic drugs, methotrexate is the first choice due to its ability to overcome the immune cells attacking joints. The prodrug, sulfasalazine is another common choice of DMARD used to treat RA. Routine choices of NSAID to be prescribed to treat rheumatoid arthritis include ibuprofen and naproxen. Oral medication or injections are the most common forms of treatment for RA; however, these are non-selective and potentially expose healthy tissue to off-target toxicity, particularly where methotrexate is used.

Rheumatoid arthritis, like osteosarcoma, requires an updated therapeutic strategy, to enhance the targeted delivery of treatments. The novel Hydrogel-PCP described here, addresses the clinically relevant needs of RA with regards to treatment, through the suggestion of a novel system to selectively deliver therapeutic treatments in a localised manner to reduce off-target toxicity. Various hydrogel therapies for rheumatoid arthritis have been researched [170], particularly hyaluronic acid (HA) based hydrogels [171]. Hyaluronic acid is major component of synovial fluid and cartilage and has been used to deliver therapeutic treatments, whilst protecting cells and anatomical structures against mechanical stress. Kim *et al* (2011), synthesised tyramine modified HA, injectable hydrogels which during crosslinking encapsulated the anti-inflammatory drug, dexamethasone [172]. Sustained release of dexamethasone was accomplished up to a month after delivery in *in vitro* and *in vivo* assessments.

More selective release methods could be applied to treat RA such as the exploitation of the overexpressed proteolytic enzymes within the synovial membrane to actively release a therapeutic drug from a peptide conjugate. This differs from the approaches by researches such as Kim *et al*, as drug release is dependent upon a proteolytic enzyme overexpressed within the disease site and lower levels in healthy tissue, limiting the risk of off-target drug release. Similarly, the hydrogel system proposed here, could serve structural support network, to alleviate pain caused by mechanical stresses within the joint. The selection of a hydrogel base material with a similar consistency to cartilage, for example HA or type I collagen with implantable delivery applications could be implanted at the site of cartilage degradation to provide a supporting structure around the joint to relieve bone erosion [173]. Furthermore, the implanted hydrogel may be subject to degradation by cartilage degrading enzymes more favourably over cartilage, leading to the indirect protection of remaining cartilage within the affected areas.

2.3.4 Biomaterial selection for hydrogel network formation

The selection of a hydrogel base material is reliant on the intended use of the hydrogel itself. In terms of OS and RA, a suitable selection would be a hydrogel material which mimics the consistency and appearance of connective tissue, given that RA treatment is required at the site of cartilage degradation and most osteosarcoma tumours occur along the edge of a long bone. Examples of hydrogel types, previously discussed (*Table 2.1.*), demonstrate a selection of hydrogels which may be suitable for the creation of the Hydrogel-PCP system. Previous work by colleagues within the research group have outlined the use of type I atelocollagen and its tuneable characteristics when functionalised with the photo-active molecule 4-vinylbenzyl chloride (4VBC), making a collagen-based material a suitable candidate for the selected biomaterial [52, 174]. Other biomaterials include Polyethylene Glycol (PEG) and Hyaluronic Acid (HA), both of which are well researched. PEG is an artificial polymer and is thought to be the 'gold standard' of artificial matrices [175]. An advantage of artificial biopolymers over natural networks is the bioactive functionalities, including cell adhesive sequences and growth factors which can be implemented into precise densities whilst controlling substrate mechanical properties independently [176]. Properties of PEG that make it a desirable polymer, for example its intrinsic low-protein adsorption properties, reduced inflammatory profile and safe in *in vivo* conditions, not to mention the variety of different crosslinking strategies including both chemical and covalent crosslinking [175]. The controllable properties as well as the use of PEG as a drug delivery gel by research groups such as Ashley *et al* (2013) [177] would make PEG a strong selection as the biomaterial for the Hydrogel-PCP system, if not for one crucial disadvantage, the non-biodegradable nature of PEG [178]. For the design of the Hydrogel-PCP system, a biodegradable polymer is required to produce an as minimally invasive clinical delivery strategy as possible, if a non-biodegradable polymer was used, further surgery to remove the implanted polymer after treatment would be required, providing another invasive procedure and an increased risk of infection.

The role of HA and collagen-derived biopolymers in bone regeneration and connective tissue, particularly in RA and Osteosarcoma, as well as their naturally biodegradable nature makes them ideal candidates as the building block to use in the Hydrogel-PCP system.

Hyaluronic acid is a biopolymer, synthesised by a class of integral membrane proteins called hyaluronan synthases which lengthen HA by adding D-glucuronic acid and *N*-acetyl-D-glucosamine to the polysaccharide backbone [179]. The naturally occurring HA is a crucial component of articular cartilage and has been reported to have beneficial effects on inflammatory arthritis, although this is biphasic. Roth *et al* (2005) found that HA therapies had anti-inflammatory effects and showed inhibition of cartilage degradation in early chronic phases, however in late chronic disease stages, HA promoted cartilage damage and joint swelling [180]. This could be overlooked depending on the type of drug delivered by the Hydrogel-PCP system, however HA also lacks free amino groups, instead containing only free carboxylic groups, hydroxyl groups and acetyl groups (*Figure 2.3*).

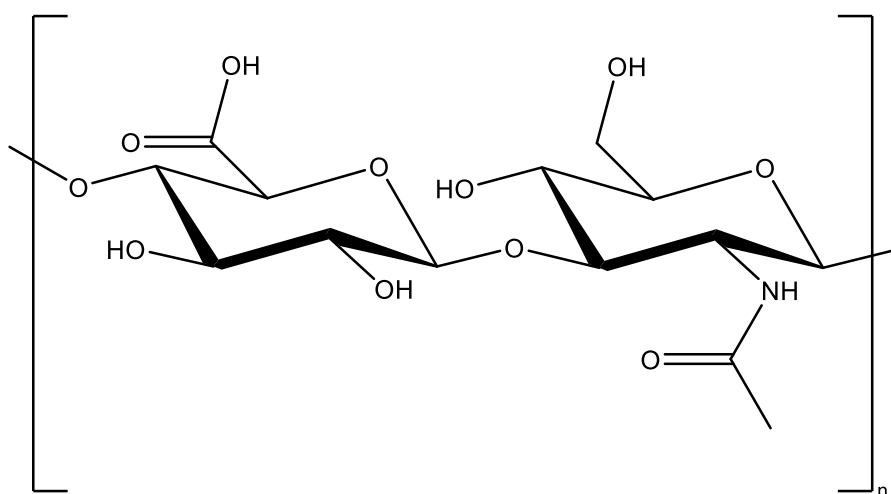


Figure 2.3. Structure of hyaluronic acid. Repeating chains of D-glucuronic acid and *N*-acetyl-D-glucosamine containing free carboxylic groups (-COOH), hydroxyl groups (-OH) and acetyl (-CH₃CO) groups.

Due to the nature of the peptide-conjugated prodrug synthesised here, the C-terminal is free to react with a free amino group on the selected biopolymer backbone. In HA a linker would be required to conjugate the PCP, which could significantly alter the rate of drug cleavage by the chosen proteolytic target enzyme. For this reason, combine with the biphasic treatment of HA in inflammatory arthritis, HA was deemed unsuitable for use as the backbone biomaterial in the Hydrogel-PCP system.

Collagen is one of the most abundant proteins within the human body and due to the unique molecular organisation, it is a commonly used material for

regenerative medicine [181] and wound healing [182]. The collagen superfamily contains 28 members and have a common structural feature, a triple helix which ranges from most of the structure (approximately 96% in type I collagen) to less than 10% of the structure (collagen XII) [183]. The triple helix consists of three polypeptide chains, known as α chains which can be identical to form homotrimers (collagen II – $[\alpha 1(\text{II})]_3$) or different to form heterotrimers (collagen IX – $[\alpha 1(\text{IX}), \alpha 2(\text{IX}), \alpha 3(\text{IX})]$). Sequences of the triple helices are comprised of Gly-X-Y repeats, X and Y frequently being proline and 4-hydroxyproline, respectively. The most abundant collagens are the fibrillar types (I, II, III, V and XI) and their extensive cross-linking capabilities provide mechanical strength that is needed for high stress tissue such as cartilage, bone and skin [184]. The mechanical properties of fibril-forming collagens are dependent on their cross-linking which can include 1) disulphide bonds (type III for example); 2) the $\text{N}^\epsilon(\gamma\text{-glutamyl})$ lysine isopeptide [185]; 3) reducible, mature cross-links by the lysyl oxidase pathway and 4) advanced glycation end products [183, 186]. Lysyl-mediated crosslinking takes place at the intra- and intermolecular levels between collagen molecules and involves lysine, hydroxylysine and histidine residues belonging to either the same or different types of collagens [187]. Crosslinking of collagen is tissue-specific as opposed to type-specific, however collagen can be functionalised or crosslinked artificially to form a hydrogel with unique characteristics.

Aside from being able to absorb large amounts of water and exudate as well as resist mechanical pressures, collagen hydrogels are enzymatically degradable by MMP activity, a family of enzymes overexpressed in OS and RA. The partially hydrolysed form of collagen, gelatin also makes a suitable selection for use as a hydrogel base material, of which photo-activated gelatin methacryloyl hydrogels have been used in the tissue engineering of cartilage constructs [188]. Due to being degraded collagen, gelatin can vary in molecular size significantly, characterised by the “bloom”. Generally, a high bloom gelatin is between 225-300g (molecular mass ranging between 50,000 and 100,000 Da), and consists of longer polypeptide chains, most similar to collagen. Gelatin is also capable of reforming the triple helix structure of collagen in a reversible manner when chilled or heated (above 37°C), allowing the gelatin biopolymer to auto-crosslink at room temperature through non-covalent bonding (*Figure 2.4.*).

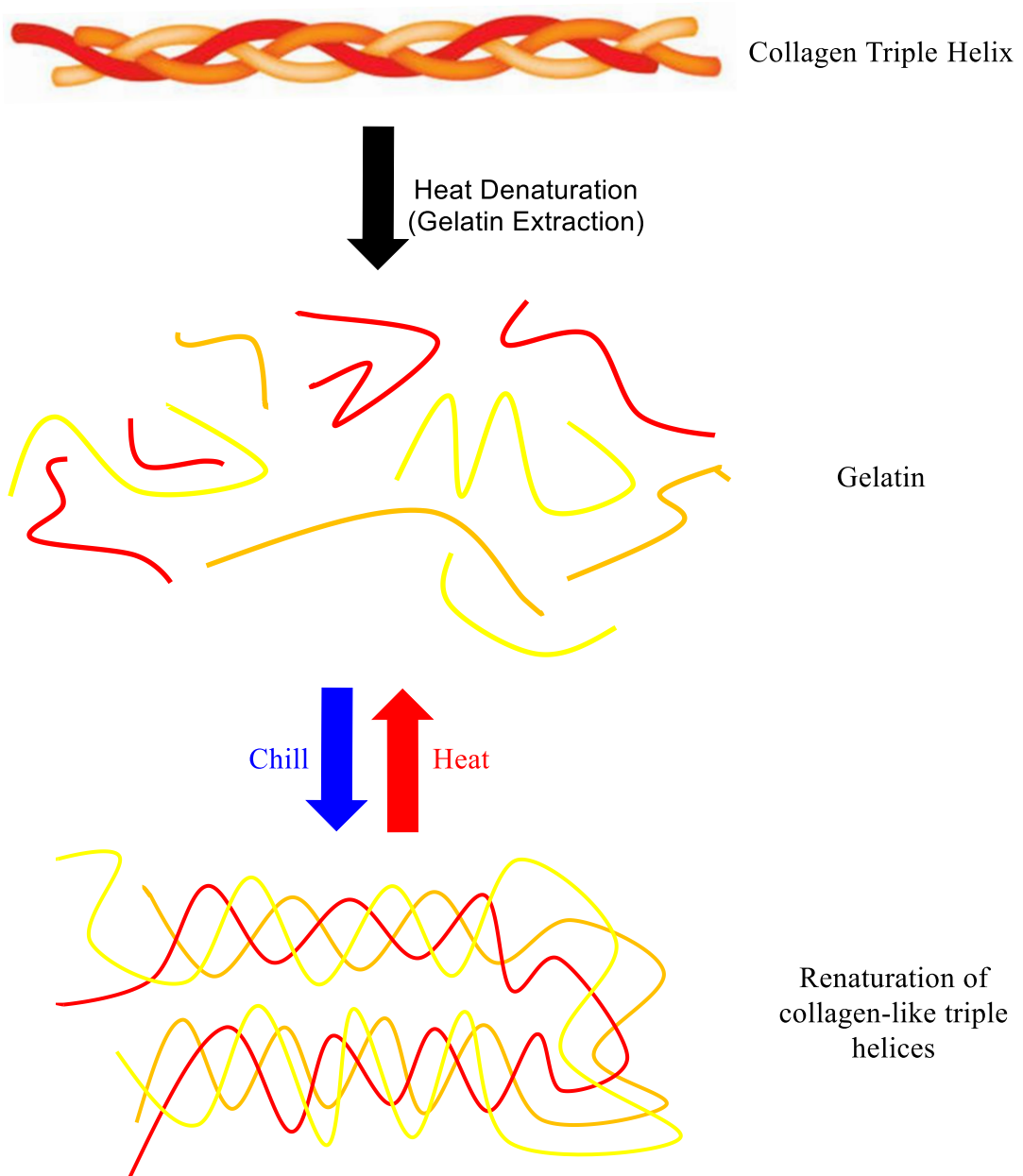


Figure 2.4. Degradation of the collagen triple helix structure to form gelatin strands which when chilled are capable of reforming the triple helical structure through non-covalent crosslinking.

The delicate nature of the novel study proposed here, requires a thorough understanding of the selected base material, which the research group has expertise in , e.g. with respect to the design of collagen and collagen-derived materials, holding the patent for collagen-derived 4VBC functionalised biopolymers [189]. This expertise will prove invaluable in the hypothesis that both collagen and high bloom gelatin would be ideal materials to use as a hydrogel base layer in OS and RA targeting, due to the degree of tuning and versatility through a variety of applications

[53, 190, 191] as well as the biodegradability due to enzymatic breakdown [192]. The PCP coupling to collagen or gelatin is also made simple by the repeating chains of amino acids within the biomaterials, particularly free amino lysine groups [193, 194]. The free amino lysine groups make ideal targets for peptide conjugation to the tail end of the PCP due to a free carboxylic group which can be activated using a carbodiimide reaction.

The readily available nature of gelatin and the similarities it shares with collagen, makes both collagen and gelatin suitable choices to be used initially, with one to be excluded, should it become no longer viable as a hydrogel material for the Hydrogel-PCP system.

2.3.5 Proteolytic enzyme targeting for drug release

Many disease pathologies require changes in the regulation of inter and extracellular contributors such as cytokines and proteolytic enzymes, in order to drive the disease forward [195, 196]. Enzymes play major roles in several biological processes, in particular cell multiplication, collagen synthesis and turnover, wound repair and the removal of dead tissue debris following inflammation and digestion [197-199]. A family of proteins, known as proteolytic enzymes, lyse chains of proteins to carry out a range of functions. The super family can be further divided into exopeptidases, which target protein termini and endopeptidases which target sites within a protein [200]. For the nature of this study exopeptidases cannot be targeted due to each end of the peptide-conjugate being occupied, either by drug or hydrogel biomaterial, endopeptidases however, can be targeted for drug release. Endopeptidases account for various catalytic mechanisms, and within this group are endopeptidases such as: cysteine proteases, serine proteases, metalloproteases and more [201-203]. Each group of proteolytic enzymes contribute to a range of biological processes. In order for the Hydrogel-PCP system to be fully biodegradable the hydrogel itself, made of collagen or gelatin, must be accessible to collagenase and gelatinase proteolytic enzymes and as a result targeting one of these enzymes for drug release would be a suitable selection, if they are overexpressed in the target diseases. Of these proteolytic enzymes there are two families, metalloproteinases [204] and selected papain-like cysteine proteases [205], which are able to cleave the triple helical region of fibril-forming collagen, causing the unwinding and degradation of the collagen structure. Of these cysteine proteases cathepsins K and L are known to attack the triple helix of fibril-forming collagen [206]. Both Cathepsin K and L are

overexpressed in RA [207], where cathepsin K is linked to radiological destruction [208] and is overexpressed in some saos-2 osteosarcoma cells [209].

Peptide-conjugated prodrugs can release the active drugs through non-selective degradation by several proteolytic enzymes, or through selective cleavage by one specific enzyme. The selective method of drug release involves the protected end of the peptide chain through the use of an endcap, whilst the middle section of the peptide chain is a specific and recognisable sequence to the particular target enzyme for cleavage and the initiation of drug release. In order to begin tailoring a peptide sequence specific to the recognition site of the targeted proteolytic enzyme, the enzyme must be selected. Overexpressed proteolytic enzymes within the targeted disease serve as a significant starting point for the selection of the enzyme. Ideally it is most suitable that the intended target enzyme is overexpressed in disease tissue but not the healthy surrounding tissue. As outlined, MMPs appear to be overexpressed in both osteosarcoma and rheumatoid arthritis, as well as possessing collagenase and gelatinase activity, therefore MMPs would make an ideal family of enzymes to select the target enzyme from.

Matrix Metalloproteinases (MMPs) are a family of calcium-dependant zinc-containing endopeptidases and are involved in the degradation of extracellular matrix (ECM) proteins [210, 211]. Due to their wide range of activity across a vast range of biological processes including: angiogenesis [212], wound healing [211], collagen turnover in development [213] and innate immune responses [214], it is unsurprising they are overexpressed in many diseases, particularly cancers (*Figure 2.5*).

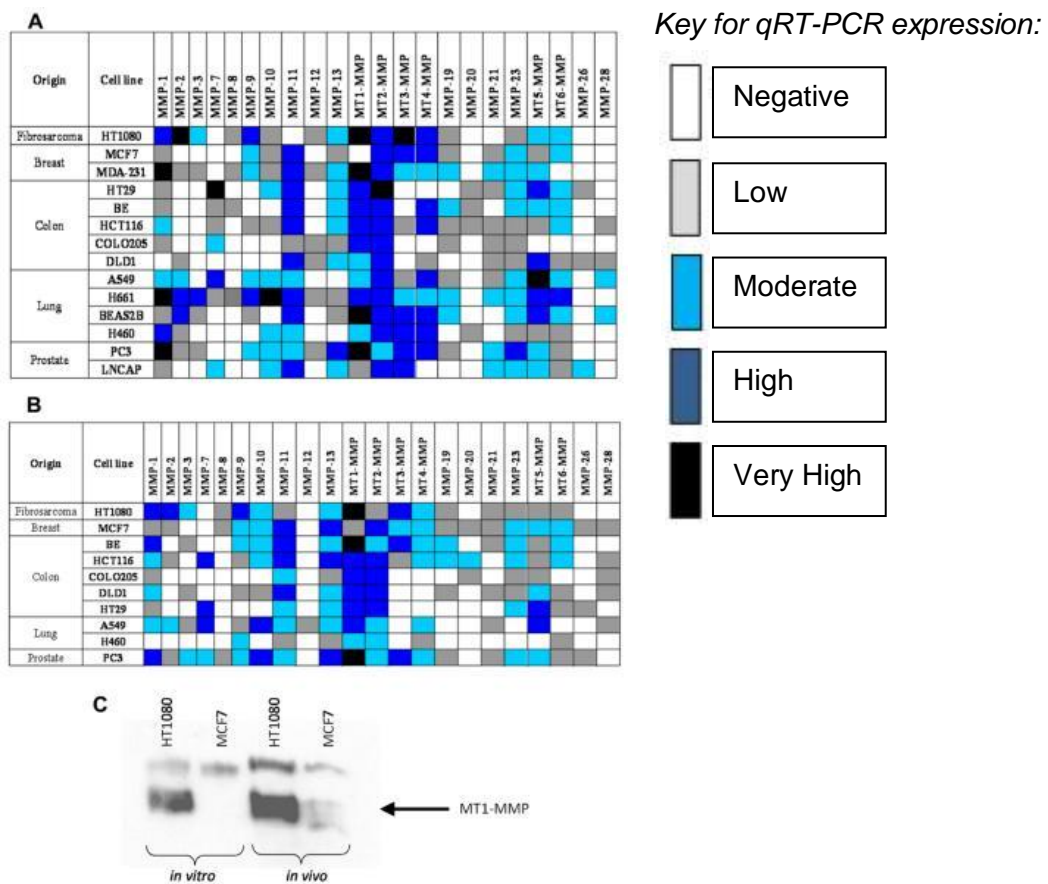


Figure 2.5. Expression of MMP mRNA in human cell lines. Modified from the 2010 study by Atkinson *et al.* MT-MMPs are elevated in human preclinical tumour models. Expression of MMP mRNA in human cell lines grown in vitro (A) and as xenografts in vivo (B) as measured by quantitative RT-PCR. Expression values after normalization to 18S-rRNA and are gene specific. Classification of expression levels was determined from the C_T of each gene as either very high ($C_T \leq 25$), high ($C_T = 26-30$), moderate ($C_T = 31-35$), low ($C_T = 36-39$), or not detected ($C_T = 40$); see key for colour scheme. (C) Immunoblot of MT1-MMP protein expression in HT1080 and MCF7 tumour models [103].

The MMP family can be further divided into two, secreted and membrane bound, however they are also often divided based on their substrate specificity and basic domain structure, for example collagenases, gelatinases and membrane type-MMPS (MT-MMPs). Many MMPs are activated from their pro- state allowing their proteolytic activity to proceed. The membrane type 1-MMP (MT1-MMP) also known as MMP14 is a key regulator of several crucial MMPs in collagen and gelatin turnover.

MMP14 is activated intracellularly by the Golgi apparatus and once activated at the cell surface, pro-MMP2 and pro-MMP13 are activated [215]. The MMPs which MMP14 activates, namely MMP2 and MMP13, have been demonstrated to play crucial roles in several diseases including cancer and rheumatoid arthritis [215-219]. Due to the crucial role played in activating key cancer and RA disease progression MMPs, MMP14 is an ideal target for the cleavage of the PCP peptide sequence. Furthermore, the expression and involvement of MMP14 within RA and OS makes it a key driver in the pathogenesis of both diseases, rather than solely an activator of disease-progressing enzymes [220-222]. In rheumatoid arthritis MMP14 has been identified as the key collagenolytic enzyme for invasion into the matrix from synovial cells [222] and is also linked to the degradation of other matrix components in cartilage such as aggrecan [223].

In osteosarcoma cell lines, Kajita *et al* (2001) demonstrated the promotion of cell migration regulated by MMP14 by cleaving CD44H and releasing it from the cell surface in MG-63 cells, triggering and enhancing cell motility. Expression of only MMP14 or CD44H on the cell surface demonstrated no improved cell motility, suggesting MMP14 increases cell migration through the processing of CD44H [224]. Another tumour promoting role that MMP14 is involved, is tumour angiogenesis. Down regulation of MMP14 has shown the inhibition of angiogenesis by interfering with $\alpha 2\beta 1$ receptor activity, negatively impacting osteosarcoma progression [225, 226]. Osteosarcoma tissues expressing high MMP14 levels are found interact with collagen alpha-2 (I) encoded by the COL1A2 gene [227]. Gene expression levels between osteosarcoma and normal bone tissue revealed MMP14 as one of the most significantly upregulated genes [228].

The involvement of MMP14 in both osteosarcoma and rheumatoid arthritis makes it a suitable target for sequencing a peptide-drug conjugate for the selective release of the chosen active drug. Involvement aside, the selection of a suitable proteolytic enzyme still requires a long and careful process to ensure the optimal targeting sequence is selected. As a result, MMP14 provides a further indication that it would make a suitable target enzyme, as we have previously targeted MMP14 for the release of the previously discussed chemotherapeutic drug, methotrexate [21], working alongside the research group behind the vascular disrupting agent PCP, ICT2588 [103, 229]. The process of honing a peptide sequence suitable to a target enzyme is a long process, of which the recognition can be significantly altered as a result of a minor change in the sequence. Therefore, due to the pivotal roles played

in both OS and RA, combined with the previous work, carried out with colleagues from the University of Bradford, UK, providing a starting sequence for our Hydrogel-PCP system, MMP14 makes an ideal enzyme to target for the selective and localised release of a chosen drug from a hydrogel support structure.

2.3.6 Selection of an active drug to release from a Hydrogel-PCP system

To treat a disease such as rheumatoid arthritis (RA) or osteosarcoma, a therapeutic agent is often required. There are a variety of drugs that could be selected to treat either of these diseases including, methotrexate (MTX) which is a well-known and researched drug for the treatment of both diseases. At first glance, MTX appears an ideal candidate for the selection of a therapeutic, particularly due to MTX containing, free, natural carboxylic acid groups (-COOH). The advantage of a free carboxylic group on a drug removes the need to use a linker compound when coupling the drug to a peptide-conjugate, which may cause unintended reductions in enzyme targeting and cleavage. Methotrexate however, contains two free carboxylic groups, which may cause complications when conjugating the MTX-prodrugs to a hydrogel, as the side-chain free carboxylic group in MTX's structure may conjugate rather than the desired alpha -COOH.

The nature of the novel system, proposed here relies on research from two scientific fields, which if successful opens up a new therapeutic direction for a variety of diseases. With this in mind, methotrexate, although a renowned first line treatment for both OS and RA, may not be the most suitable selection to prove such a delicate concept. Furthermore, the theory of using a peptide-conjugated prodrug delivery system is that, any disease overexpressing a proteolytic enzyme can be targeted to release the selected drug, once a selective sequence is established for the particular proteolytic enzyme. This can be achieved by adjusting the peptide-conjugate sequence to suit the binding site of the target enzyme. As a result, the selection of a drug, is not intended to be a drug specific to a particular disease (but should still show significant evidence for treatment of both OS and RA), rather, one that is applicable to several diseases, such as a non-steroidal anti-inflammatory drug (NSAIDs) for example naproxen (NAP) [230, 231]. Inflammation plays a key role in a wide range of diseases, of which both acute and chronic inflammation have been linked to many different diseases [232]. Therefore, the use of NSAIDs in the design of a peptide-conjugated prodrug hydrogel delivery system enables its' usage across a broad spectrum of diseases and conditions, that are not solely limited to RA and

osteosarcoma. Furthermore, from a toxicological perspective, the links between NSAIDs and the occurrence of peptic ulcers leave room for the alternative delivery of NSAIDs to reduce the risk of off-target toxicity [233, 234].

There is growing evidence for the use of NSAIDs in the treatment of several cancers [235-237]. The majority of NSAIDs work through the inhibition of cyclooxygenase (COX), a key biological mediator in processes such as inflammation and cancer progression [238] and research has shown the overexpression of COX-2 in the progression of RA and OS [239, 240]. There are several viable choices of NSAIDs to apply to the Hydrogel-PCP system such as ibuprofen, aspirin and naproxen, all of which possess a free -COOH group (Figure 2.6.). Naproxen, a commonly used NSAID for the treatment of RA is a longer acting drug than ibuprofen and aspirin and has been shown to have therapeutic effects for RA treatment when other NSAIDs have proven in-effective [241]. In terms of osteosarcoma, naproxen is proven by Correia *et al*, to have a dose-dependent therapeutic effect [242]. Correia and colleagues found naproxen blocked cell proliferation in MG-63 osteosarcoma cell lines as well as elevated levels of autophagosomes in cells treated with naproxen. An increase in apoptotic cells was also found suggesting the mechanism of action of the drug is through autophagy [242] which is in line with cells treated with another NSAID, meloxicam [243].

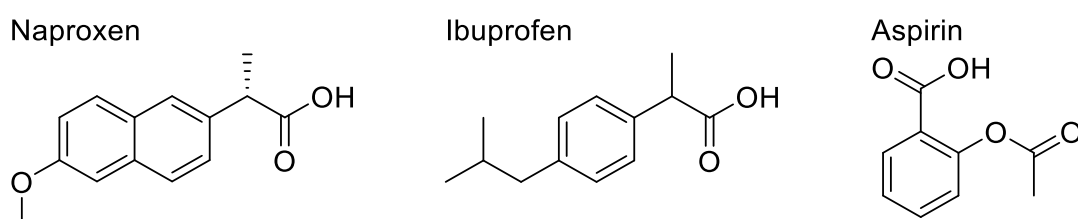


Figure 2.6. Chemical structure of naproxen, ibuprofen and aspirin. Possible non-steroidal anti-inflammatory drugs (NSAIDs) to use as the drug warhead in the peptide-conjugated prodrug design, due to the single carboxylic acid group each possess.

Due to the longer lasting effects and the therapeutic effects upon both RA and OS, naproxen was selected to be the active drug warhead for the Hydrogel-PCP system. The non-selective effect naproxen possesses makes it an ideal option to make more selective and reduce the risk of gastric ulcers by providing an alternative

delivery route and making the release selective to further reduce any unwanted toxicity. Furthermore, the suggested drug release strategy could be made applicable to several other diseases, making the selection of a NSAID an ideal choice due to the vast variety of diseases displaying inflammation.

2.4 Hydrogel-PCP design and clinical application

Therapeutic agents, particularly those with cytotoxic effects often require alterations to administer them more safely, whether this be through antibody drug conjugation [244], peptide drug conjugation [245] or the use of a delivery vehicle such as hydrogels [246] or micelles [247]. By combining two of these drug delivery methods the therapeutic index of the delivered agent could be further increased. The use of PCPs, coupled to hydrogels, forms a unique delivery system, which in a localised and selective manner releases a therapeutic drug, whilst providing structural support to a variety of tissues, depending on the hydrogel design. The release of the active drug from the anchored PCP, exploits the overexpression of the targeted proteolytic enzymes in the diseases selected to focus the design of the therapeutic system around, osteosarcoma and rheumatoid arthritis.

2.4.1 Study design

The proof of concept study centres around the design of a novel Hydrogel-PCP, of which each system component is tailored to the intended disease targets, RA and OS, whilst maintaining the applicability to other diseases exhibiting inflammatory symptoms. Outlined in this sub chapter, is the design of the carefully constructed Hydrogel-PCP therapeutic system.

The selected drug, naproxen is coupled to a peptide-conjugate, via its' free -COOH group to form a PCP. The peptide-conjugate is made up of a sequence of 8-12 amino acids with a glycine-homophenylalanine (Hof-Gly) bond towards the centre of the sequence which is the site cleavable by MMP14, as previously shown by Gill et al [229]. Each of the remaining 6-10 amino acids are carefully selected to either aid MMP14 recognition or to freely dissociate once cleavage of the peptide-conjugate occurs and the amino acid ends become deprotected. Ordinarily, the PCP would possess an endcap, however the conjugation of the conjugate-tail to the collagen or gelatin hydrogel backbone, enables the hydrogel itself to serve as an endcap to the PCP component. The tuneable hydrogel system component provides structural support within RA, with an implantable device to take on the consistency of cartilage and in OS, the ability to withstand mechanical stress from cancerous effects such as inflammation and increased tumour mass [248, 249]. Therefore, the Hydrogel-PCP system is made up of naproxen, conjugated to a peptide-conjugate selective towards MMP14, coupled to a biopolymer material (collagen or gelatin), prior to induced

network formation and crosslinking to synthesise a hydrogel-naproxen PCP (*Figure 2.7*).

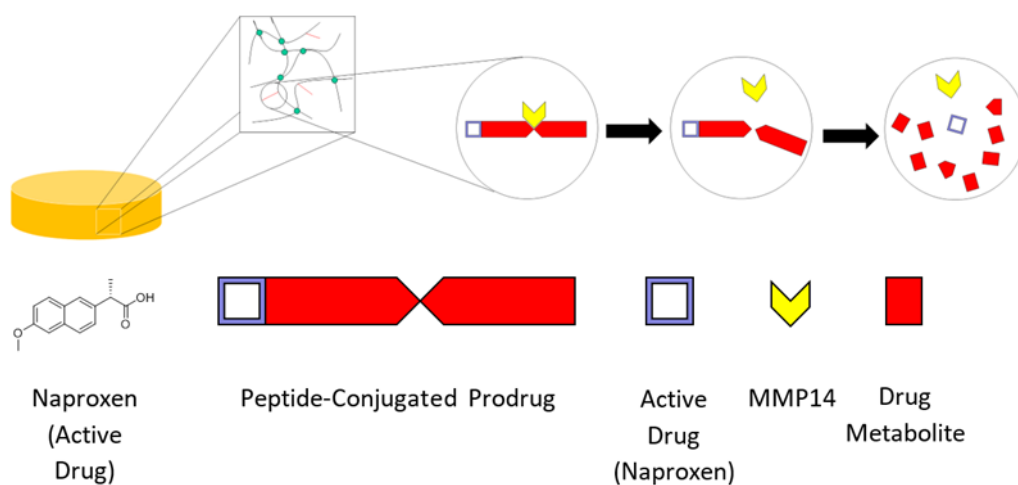


Figure 2.7. The hydrogel-naproxen PCP system. Designed to be selectively cleaved, at the Hof-Gly peptide bond, by MMP14 to trigger the release of naproxen from the PCP component. Naproxen-PCP (NAPPCP), conjugated to free amino lysine groups of a collagen-based biopolymer is crosslinked to form a Hydrogel-NAPPCP.

2.4.2 Clinical significance

The outlined proof of concept study, suggests the local and selective release of an active therapeutic drug from a tissue scaffold support network anchored at the disease site. The verdict of whether to use a localised drug delivery treatment should be based upon clinical findings and therapeutic responses recorded in literature [250]. However, a proof of concept study, lacks concrete therapeutic evidence that the delivery system is suitable for the clinical application and therefore must use related literature and assess whether the desired end product is considered to be a clinically more desirable delivery method than current clinical options.

Naproxen as a drug is widely shown to have therapeutic effects across a variety of diseases including RA and OS as previously discussed [251]. Considering the link between NSAIDs and peptic ulcers due to their inhibition of the COX-2 isoform [252, 253], of which naproxen is considered to be a higher risk NSAID for causing peptic ulceration [234]. The undesirable toxic side effect of naproxen could be avoided through the use of a naproxen-based PCP. The proposed MMP14

targeting PCP strategy has shown promising results, albeit using an alternative drug warhead, demonstrating no increase in von Willebrand's factor (vWf), a clinical marker of cardiotoxicity, compared to the selected drug alone, when using the PCP component [229]. As discussed in Chapter 2.2, drug-loaded hydrogels have exhibited low signs of off-target toxicity when targeting cancers. The loading of a drug to a hydrogel is less secure than the physical conjugation to the hydrogel itself, demonstrating a further safety measure employed in the Hydrogel-PCP system proposed here.

Naproxen is a strong candidate for the treatment due to the reduced risk of thromboembolic cardiovascular events in RA and anti-tumour effects in OS, on top of the anti-inflammatory properties naproxen is normally used for [242, 254, 255]. Containing a single -COOH group, allows for straightforward coupling of naproxen to a peptide conjugate, temporarily disabling naproxen, allowing safer delivery to a disease site. The use of a naproxen-based Hydrogel-PCP system to target RA and OS provides a novel therapeutic strategy that if successful, could be simply adapted to target any disease overexpressing MMP14, using any drug that could be substituted for naproxen, such as methotrexate or ibuprofen.

The alternative delivery route for naproxen combined with the reduced toxicity shown in the use of a PCP, as well as the structural support a hydrogel provides, suggests a strong argument for enhanced clinical relevance compared to current measures used. Delivery of the Hydrogel-PCP system relies upon one of two strategies to be investigated here: firstly, the surgical implantation of a readily formed Hydrogel-PCP system to administer therapeutic effects to the target disease and the surgical wound and secondly, an injectable system which undergoes *in situ* crosslinking to form a Hydrogel-PCP system within the disease area, bypassing the need for surgical implantation.

Chapter 3

Photo-activated biopolymer hydrogels

3.0 Photo-activated biopolymer hydrogels.

The purpose of this chapter is to investigate the formation of UV cured, collagen-based Hydrogel-PCP systems. Initial functionalisation of free amino lysine groups of collagen-based biopolymers with the photo-active molecule 4-vinylbenzyl chloride (4VBC) is carried out. Collagen-based materials, both native and functionalised undergo EDC/NHS-induced conjugation of a model drug, sulfasalazine (and later the synthesised naproxen peptide-conjugated prodrug). All functionalisation of biopolymers is assessed using a TNBS and/or a ninhydrin colorimetric assay.

Two UV-induced crosslinking strategies are carried out to form photopolymerised collagen-based drug-conjugated hydrogel networks:

- *Dual functionalised collagen-based materials with 4VBC and drug*
- *Encapsulation of a drug-conjugated collagen sample within a 4VBC-functionalised collagen sample.*

Analysis of drug release by MMP14 selective cleavage was carried out by High Performance Liquid Chromatography (HPLC).

3.1 Introduction

A wide variety of hydrogel materials and crosslinking methods are already well established and provide a broad range of unique characteristics, allowing them to be used for many different applications [47, 256, 257] whether that be magnetic hydrogels or releasing a substance in response to pH change, for instance. Ultraviolet free radical crosslinking is just one example of a well-established crosslinking strategy. Chemical crosslinking is another well-established strategy which can induce network formation in a variety of materials including gelatin biopolymers [258, 259].

Development of these hydrogel systems has begun to branch out into other scientific fields to produce selective drug delivery vehicles, whether that be in response to an external stimulus or through other means such as enzymatic activity. Examples of these hydrogel systems include, but are not limited to: hydrogel/micelles, so-called 'nanogels', thermo-responsive and magnetic hydrogels [260, 261]. The selectivity of these systems has demonstrated a reduction in associated drug-toxicity and has begun to overcome other complications associated with hydrogel-drug delivery facets, including solubility issues. Photo-crosslinking is a

thoroughly researched method enabling gel network formation, so that visible light can now be used to induce *in situ* gel formation, further improving the clinical relevance of this method in local applications [262]. The application of UV-cured gel networks for drug delivery has been extensively researched to provide a localised release of drugs from the network gels [263], limiting the need for alternative, potentially more toxic means of drug delivery. Highly selective release strategies have been investigated in UV-cured hydrogel systems, for example, the glucose-sensitive release of metronidazole by the widening of hydrogel pores to control drug release [264].

Previous research into the establishment of collagen and collagen-derived UV-cured hydrogel systems with the photo-active molecule 4-vinylbenzyl chloride (4VBC) [52, 174] has provided sufficient evidence to suggest it for the use as a selective and localised drug delivery vehicle. The programmable macroscopic properties, which can be obtained through 4VBC UV-crosslinking, have shown the formation of biocompatible collagen systems leading to a variety of unique hydrogel characteristics based on the degree of functionalisation of the collagen biopolymer [52, 265]. The strong platform of a tuneable, UV-curable hydrogel that is capable of taking on the consistency of connective tissue could be further strengthened by the addition of another novel unit, an MMP14 responsive peptide-conjugated prodrug, to accomplish localised, MMP responsive and highly selective drug release from the gel network in diseases such as rheumatoid arthritis and osteosarcoma. Peptide-conjugated prodrugs (PCPs) allow for a selective release in diseased tissues by the cleavage of the peptide-conjugate through the activity of a specific overexpressed proteolytic enzyme [229, 266].

Selectivity in drug release plays a key role in the reduction of off-target toxicity [267]. Cancer is an example of a disease where the reduction of off-target toxicity is vital. Chemotherapies are extremely effective in killing cancerous cells; however, the crucial drawback is that chemotherapies are also lethal to healthy tissue, causing a reduction in the amount of therapeutic drug which can be administered. Selective methods of delivering therapeutic alternatives to traditional chemotherapy, such as the peptide drug-conjugates, nanoparticles and immunotherapy have become focus points in recent years due to their ability to reduce off-target toxicity and increase the therapeutic index of a particular treatment [103, 268], allowing for a greater dose to be administered before unacceptable levels of off-target toxicity are reached. These selective methods still require the successful delivery and anchoring or containment

within a disease site, which can pose challenges. An example of this could be seen in osteosarcoma, a disease that often effects children and adolescents where collagen turnover is accelerated to keep up with the demand of bone development. In the study by Sartorio *et al*, the levels of bone Gla protein (BGP), a marker of osteoblast function, for healthy children were over 3 times that of healthy adults [269], demonstrating increased bone development. The selected target enzyme, Matrix metalloproteinase-14 plays a key role in collagen turnover and is overexpressed in healthy tissues during bone development [270-272] making it vital that the risk of off-target drug activation is minimised when using an MMP14 selective release strategy. Using a hydrogel drug delivery strategy as proposed here, could anchor the prodrug in place at the disease site allowing for overexpressed MMP14 within the disease site to release the therapeutic drug, minimising contact with healthy MMP14 expressing tissues, that would occur if the Naproxen Peptide-Conjugated Prodrug (NAPPCP) was administered intravenously. It is therefore crucial to synthesis a hydrogel network, capable of supporting drug coupling or loading for long enough to successfully implant or deliver the hydrogel at the disease site.

The work described in this chapter investigates the potential of synthesising a UV crosslinked 4VBC-functionalised collagen or gelatin biopolymer network, conjugated with a naproxen-PCP, as well as the assessment of the selective release capabilities by MMP14 cleavage. This novel approach aims to link two evolving scientific fields, which have the potential to vastly accelerate one another, to form highly selective, localised therapies with a delivery application that is of clinical relevance.

3.2 Materials

All materials used that would not commonly be found in laboratories are listed below (*Table 3.1.*) with supplier information. All specialist equipment used is also detailed with supplier information (*Table 3.2.*).

Table 3.1. Materials and reagents used.

Material / Reagent	Supplier	Product Number / Code	CAS Number	Additional Information
(H-Tyr(tBu)-2-CITrt) Resin	Novabiochem	856066	N/A	5g, sub at filling: 0.76 mmole/g
1-(3-Dimethylaminopropyl)-3-ethylcarbodiimide hydrochloride, EDC	Alfa Aesar	A10807	25952-53-8	25g
2-Hydroxy-4'-(2-hydroxyethoxy)-2-methylpropiophenone, I2959	Sigma Aldrich	1002444239	106797-53-9	50g
2-Mercaptoethanol, BME	Sigma Aldrich	101684197	60-24-2	100ml
4-vinylbenzyl chloride	Sigma Aldrich	101952539	1592-20-7	100ml
Acetic Acid	Fluka Analytical	45740	64-19-7	1l
Acetone	Fisher Chemical	A/0560117	67-64-1	2.5l
Birjj-35	Sigma Aldrich	1001606014	9002-92-0	100ml
Calcium Chloride	Alfa Aesar	12316	10043-52-4	1kg
Dichloromethane	Fisher Chemical	D/1850/17	75-09-2	2.5l
Diethyl Ether	Fisher Chemical	D/2400117	60-29-7	2.5l
Diethyl Ether	Sigma Aldrich	102050220	60-29-7	1l
Dimethyl Sulfoxide	Sigma Aldrich	101921134	67-68-5	500ml

Dimethylformamide	Fisher Chemical	D/3840/17	68-12-2	2.5l
DMTMM	Fluorochem	045163	3945-69-5	25g
Ethanol	VWR Chemicals	20821.365	64-17-5	5l
Fmoc-Arg(Pbf)-OH	Activotec	N/A	154445- 77-9	100g
Fmoc-Cit-OH	Fluorochem	N/A	133174- 15-9	25g
Fmoc-Gly-OH	Activotec	FLG-01	29022-11- 5	100g
Fmoc-Hof-OH	Fluorochem	N/A	132684- 59-4	10g
Fmoc-Leu-OH	Activotec	FLL-01	35661-60- 0	100g
Fmoc-Ser(tBu)-OH	Novabiochem	852019	71989-33- 8	25g
Fmoc-Tyr(tBu)-OH	Activotec	FLY-01	71989-38- 3	100g
Gelatin, Type A	MP Biomedicals	901771	9000-70-8	100g
Hydrochloric Acid 6mol/l	VWR Chemicals	2611.5000	7647-01-0	5l
Synthetic bone	Sawbone	1522-05	N/A	40PCF
Matrix Metalloproteinase 14	Biovision	8009-10	N/A	10µg
Methanol	Fisher Chemical	M/4056/17	67-56-1	2.5l
Methanol	VWR Chemicals	20846.361	67-56-1	5l
N,N-Diisopropyl Ethylamine	AGTC Bioproducts	AGBC7012	7087-68-5	1l
Naproxen	Sigma Aldrich	PHR104	22204-53- 1	500mg
N- Hydroxysuccinimide, NHS	Alfa Aesar	A10312	6066-82-6	100g

Ninhydrin	Alfa Aesar	A10409	485-47-2	25g
N-Methylpyrrolidone	AGTC Bioproducts	AGBC7006	872-50-4	2.5l
O-(1H-6-Chlorobenzotriazole-1-yl)-1,1,3,3-Tetramethyluronium Hexafluorophosphate	Activotec	N/A	330646-87-9	100g
Picrylsulfonic acid solution, TNBS	Sigma Aldrich	1002507883	2508-19-2	10ml
Piperidine	Sigma Aldrich	101085663	110-89-4	1l
Rhodamine B	Alfa Aesar	A13572	81-88-9	50g
Sodium Bicarbonate	Alfa Aesar	A170005	144-55-8	500g
Sodium Hydroxide	Alfa Aesar	B24414	1310-73-2	500g
Sulfasalazine	LKT Laboratories	S8247	599-79-1	50g
Triethylamine	Sigma Aldrich	101513370	121-44-8	1l
Trifluoroacetic Acid	Fluorochem	001271	76-05-1	2.5kg
Triisopropylsilane	Sigma Aldrich	101650254	6485-79-6	50g
Tris/HCl, 1M solution, pH 7.5	Affymetrix	22639 1 LT	N/A	1l Lot: 4217732
Tween20	VWR Chemicals	663684B	9005-64-5	500ml
Type I Atelocollagen	Collagen Solutions	FS22006	N/A	6mg/ml 1l

Table 3.2. Equipment information.

Equipment	Supplier	Model	Additional Information
Benchtop Centrifuge	Thermo Scientific	Heraeus Megafuge 16R	
Floor Standing Centrifuge	Beckman Coulter	Avanti J-26 XP	
		2695	Separation Module
Liquid Chromatography-Mass Spectrometer	Waters Alliance	996	PDA Detector
		Micromass ZQ	Mass Detector
		Z3818, 250 x 2.1 mm	Hichrom RPB microbore column, HICHROM-250AM
OD Plate Reader	Thermo Scientific	3001	Varioskan Flash
Peptide Synthesiser	Biotage	Syro I	Fully automated parallel peptide synthesiser
Rheometer	Anton Paar	MCR302	
Shaking Incubator	Thermo Scientific	MAXQ4450	
Spectrophotometer	Jenway	6305	
Unstirred Water Bath	Clifton	N/A	Heats up to 100°C
UV Lamp	Spectroline	CM-10	UVL-16 EL Series UV Lamp
Water Purification System	Elga	Purelab Option Q DV-25	

3.3 Methods

3.3.1 Functionalisation of biopolymer's lysine amine groups with 4-vinylbenzyl chloride

Gelatin – High strength gelatin (~250g BLOOM) was dissolved in 10% w/v PBS solution for 2 hours at 60°C. 1% v/v of Tween20 was added to the mixture, followed by triethylamine and finally 4-vinylbenzyl chloride at the desired molar excess and left to stir for 6-8 hours at 40°C. For example, to functionalise 10g gelatin with a 25 molar excess of 4VBC: 10g gelatin is dissolved in 100 ml PBS and left to stir at 60°C for 2 hours. Once full dissolved 1 ml (1% v/v) Tween20 is added to the solution, followed by 8.822 ml TEA and 8.914 ml 4VBC (calculated using the following equation, with a 25 molar excess) and left to stir at 40°C for 6-8 hours.

$$\text{Biopolymer}(g) \times \text{mol}(\text{Lys}) \times \text{MolarExcess} = \text{Coefficient}$$

$$\frac{(\text{Coefficient} \times \text{MW})}{\text{Density}} = \text{Volume Required (ml)}$$

where MW is the molecular weight.

The reaction solution was then precipitated in ethanol (up to 10-fold volume excess of the reaction mixture) for 5 hours, before being drained and placed in an incubator to dry.

Atelocollagen – Pepsin-extracted type I bovine atelocollagen (AC, 6 mg/ml) was diluted to 3 mg/ml with 10mM HCl, followed by neutralisation to a pH of 7.4. Tween20 (at 1% v/v), triethylamine and 4-vinylbenzyl chloride were added using the above equation as demonstrated in gelatin, and left to stir for 24 hours at room temperature. Following this, the reaction solution was precipitated by stirring in up to a 10-fold volume excess of ethanol for 24 hours before being centrifuged at 11,000 rpm for 45 minutes, after which the biopolymer was collected and dried at room temperature.

The dry substances were stored at room temperature prior to quantification of the degree of functionalisation of the reacted biopolymers.

3.3.2 Determination of free amino groups occupied after functionalisation

Two colorimetric assays, TNBS and ninhydrin [273, 274], commonly used for the determination of amino groups in proteins were employed to assess the degree of functionalisation of AC. Both TNBS and ninhydrin have recently both exhibited correlations with ¹H-NMR spectroscopy when carried out to assess the characterisation of reacted collagen-based [275]. Therefore, the selection of TNBS and ninhydrin assays was made to determine the molar content of free lysine groups in both native and reacted pepsin-solubilised AC samples, allowing the indirect quantification of F to be calculated.

3.3.2.1 Trinitrobenzenesulfonic acid assay

Determination of occupied free amino lysine groups (degree of functionalisation, F) of collagen or gelatin, after coupling of 4VBC was carried out using a Trinitrobenzenesulfonic (TNBS) colorimetric assay as per [273]. Briefly, 11 mg reaction sample was placed into vials before adding 1 ml 4% NaHCO₃ and 1 ml 0.5% of TNBS solution. Blank control vials initially contained 1 ml of 4% NaHCO₃ and 3 ml HCL (6M).

Samples were incubated at 40°C, under shaking for 4 hours, prior to 3 ml HCL being added to the reaction vials and 1 ml of 0.5% TNBS solution added to the blank control before shaking at 60°C for a further hour. All vials were then left to cool at room temperature before the addition of 5 ml water to each vial. Unreacted TNBS was removed with diethyl ether (3 x 20 ml washes). Next, 5 ml of aqueous phase was aliquoted out and heated for 15 minutes to remove any remaining diethyl ether. Finally, 15 ml water was added, before the absorbance was measured at 346nm, and the degree of functionalisation calculated.

$$\frac{\text{mol(Lys)}}{\text{g(collagen/gelatin)}} = \frac{2 \times A_{346} \times 0.02}{(1.46 \times 10^4) \times b \times x}$$

$$F = 1 - \frac{\text{mol(Lys)Funct. Collagen}}{\text{mol(Lys)Collagen}}$$

where A₃₄₆ is the absorbance at 346nm, 0.02 is the volume (in litres) of the final sample solution, 1.46x10⁻⁴ equates to the molar absorption coefficient for 2,4,6-trinitrophenol lysine (M⁻¹cm⁻¹), b is the path length (1 cm) and the sample weight (g) is defined as x.

3.3.2.2 Ninhydrin assay

Further confirmation of the number of functionalised free amino groups, and degree of functionalisation, was accomplished using a ninhydrin assay [274, 275], which was also used to assess the extent of drug conjugation, as the drug was expected to be coupled to the remaining free lysine groups after 4VBC functionalisation.

First, a calibration curve was established by preparing a molar range between 0 and $5 \times 10^{-6} \text{ mol} \cdot \text{g}^{-1}$, derived from a glycine stock solution, before being made up to 4 ml with water. An 8% w/v ninhydrin solution was prepared in DMSO and 1 ml of ninhydrin solution was added to each sample vial, giving a total of 5 ml per vial. Samples were reacted at 95 °C for 15 minutes, before being cooled on ice and 1 ml of ethanol added to halt the reaction. The addition of ethanol made a total dilution of 6-fold for each sample. The absorbance was measured at 570nm and plotted against the glycine molar content.

The linear region of the calibration curve (*Figure 3.1.*), ranging between 2.0×10^{-6} and $4.5 \times 10^{-6} \text{ mol} \cdot \text{g}^{-1}$ was used to accurately determine the occupation of free amino lysine groups, providing an accurate measurement within the linear region, as confirmed with the TNBS assay.

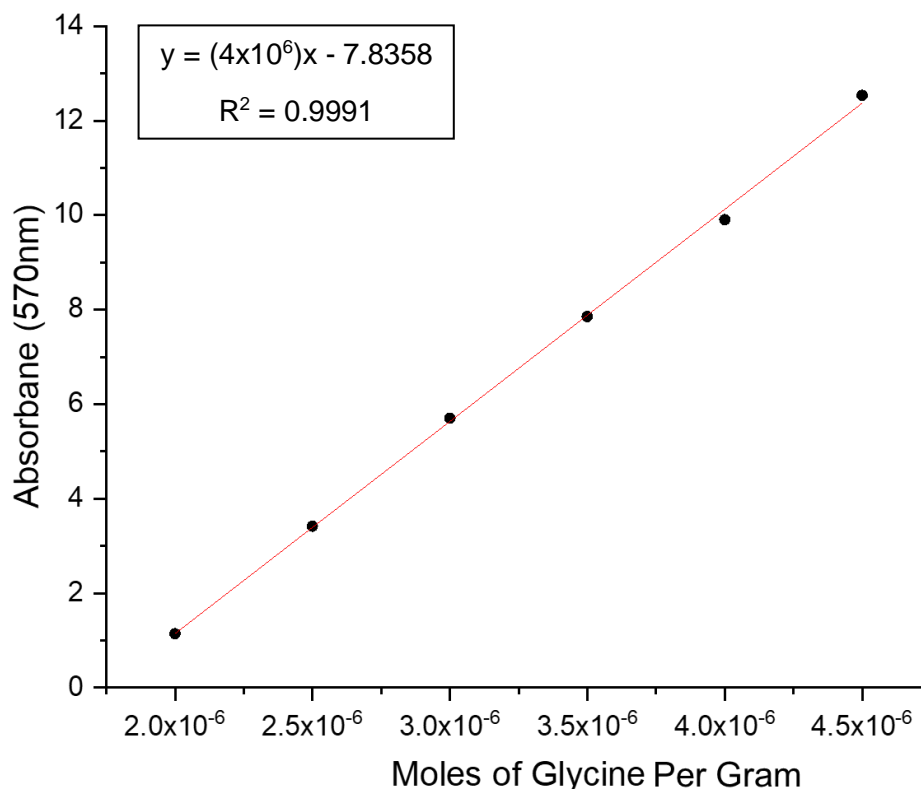


Figure 3.1. Ninhydrin calibration curve. Isolated linear region of a ninhydrin assay calibration curve, demonstrating the region at which the quantity of free amino groups can be accurately determined with in a biopolymer.

Functionalised samples were prepared as described; however, 10 mg of sample was weighed out and 4 ml water added prior to the addition of 1 ml ninhydrin solution, before following the protocol and plotting the absorbance onto the calibration curve to determine the degree of functionalisation between samples.

3.3.3 Drug conjugation via 1-(3-dimethylaminopropyl)-3-ethylcarbodiimide hydrochloride/N-hydroxysuccinimide reaction

The EDC/NHS activation of drug carboxylic groups was carried out with varying molar ratios with respect to the free lysine $\text{mol}\cdot\text{g}^{-1}$ of the biopolymer the drug was conjugated to, similar to the method of 4VBC functionalisation (Chapter 3.3.1). Initial conjugation reactions were carried out with sulfasalazine (SSZ), a readily available drug compound with a single carboxylic acid group, prior to the conjugation

with naproxen and naproxen peptide-conjugated prodrugs, which were less readily available (Figure 3.2.).

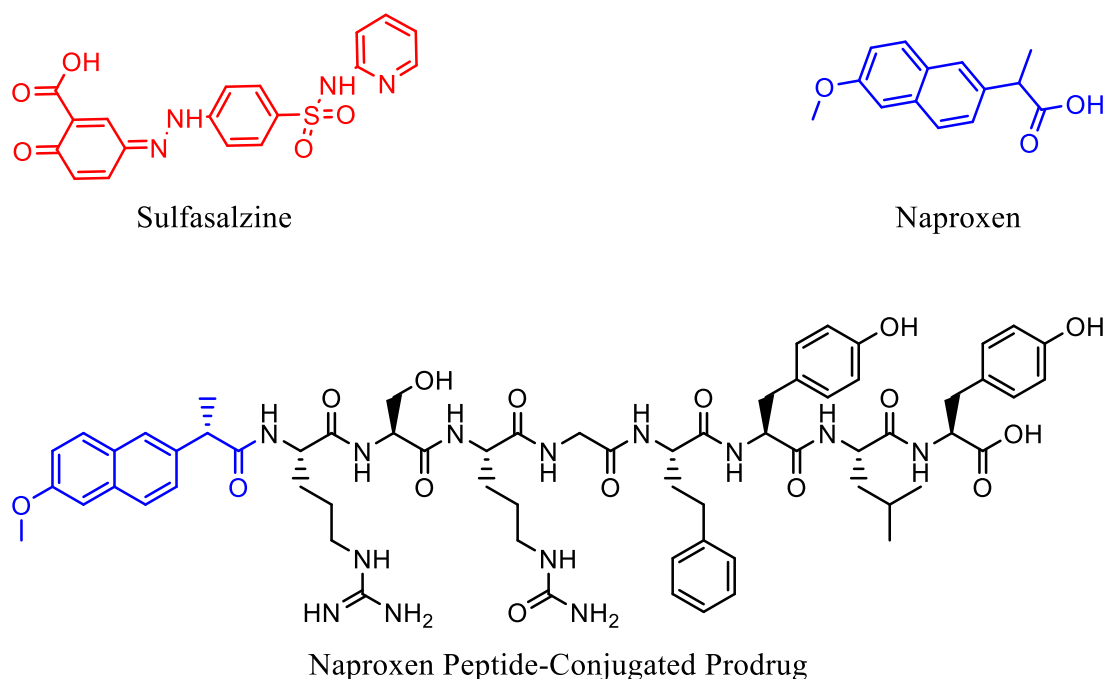


Figure 3.2. Structural differences between study drugs. Sulfasalazine (red), naproxen (blue) and the naproxen peptide-conjugated prodrug (NAPPCP).

Drugs were dissolved in minimal DMSO, before the addition of EDC and NHS to the solution, and left to react for 1 hour at room temperature (Figure 3.3.). The volume of DMSO required to dissolve the drug is not sufficient to significantly negatively impact the coupling reaction, after which the coupled biopolymer is dried and washed, removing the DMSO used to initially dissolve the drug. Following this reaction, 2-Mercaptoethanol (BME) was added and reacted for 15 minutes to quench any unreacted EDC, before adding the activated drug solution to a dissolved solution of biopolymer and left to react at the conditions required to dissolve the respective biopolymer. Once reacted, gelatin drug-conjugated biopolymers were precipitated for 5 hours in a 10-fold volume excess of ethanol, collected and then air dried. Atelocollagen drug-conjugated biopolymers were also placed in 10-fold volume excess of ethanol, however were stirred for 24 hours, prior to centrifugation at 11,000 rpm for 45 minutes and air drying.

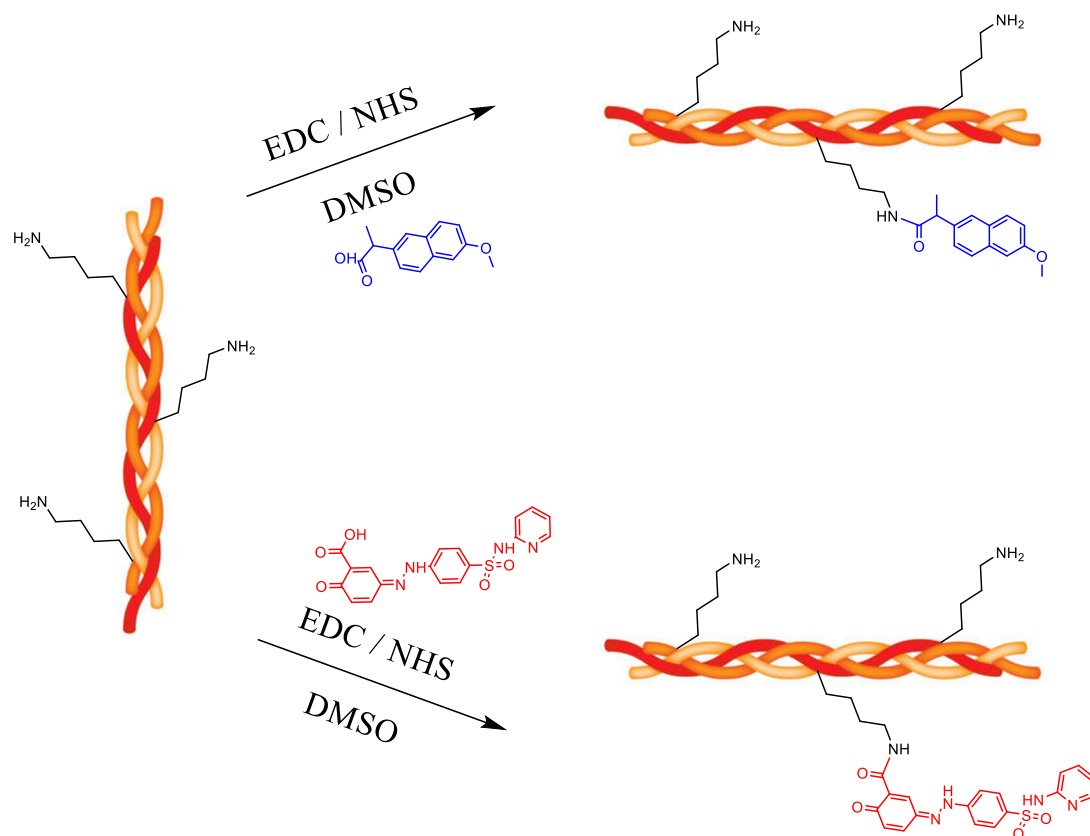


Figure 3.3. EDC/NHS-induced drug coupling to biopolymers. Coupling of naproxen (blue) or sulfasalazine (red) to a collagen-based biopolymer via EDC/NHS reactions to activate drug carboxylic groups before mixing with the biopolymer solution to readily react with free amino lysine groups.

3.3.4 Synthesis of UV-cured biopolymer networks

4VBC-Functionalised atelocollagen or gelatin products were dissolved at fixed concentrations of 0.8 wt.% and 10 wt.% respectively in 10mM HCl (pH 2.1), containing 1% I2959 photoinitiator. To prepare 1% I2959 solutions, I2959 was dissolved at 60°C for 3 hours. The dissolved polymer solutions were cast onto 24 well plates at known masses, and irradiated by UV light (346nm, 8mW cm⁻²) for 30 minutes on both the top and bottom sides. The UV-cured hydrogel networks were carefully removed from the well plates and washed with diH₂O, prior to washing in ascending ethanol concentrations and air drying before storing.

3.3.5 Synthesis of peptide-conjugated naproxen prodrug

The synthesis of peptide-conjugated naproxen prodrugs was carried out by automated means. Peptide conjugates were synthesised onto H-Tyr (tBu)-2-(ITrt) resin at a substitution value of 0.76 mmoles/g, prepared by swelling in DMF for 20 minutes. The resin was washed and shaken in 40% piperidine/DMF for 3 minutes to deprotect the Fmoc protecting group from the previous amino acid in the sequence. This step was repeated a further 2 times with drainage of the piperidine/DMF after each cycle. The calculated amino acids in the coupling sequence and HCTU mass (2.5 equivalents) were mixed and dissolved in the minimum amount of DMF (calculated by the synthesiser) and were loaded into the synthesiser with the calculated quantities added for each coupling cycle, of which 3 cycles occurred for each new amino acid addition. Alongside the amino acid and HCTU, DIPEA/NMP were added to improve coupling efficiency. Each amino acid coupling cycle was intermittently shaken for 15 minutes, before being drained and repeated until 3 cycles had occurred. After the third coupling reaction, the resin and sample vessel were washed 3 times with DMF. The deprotection and coupling stages were then repeated until all of the amino acids and naproxen were added, with the drug coupling step being manually input into the automated synthesiser.

Once naproxen was coupled, the resin was thoroughly washed initially in DMF, followed by methanol and finally dichloromethane, before being dried under vacuum overnight. Conventional cleavage was carried out next to remove the sidechain protecting groups and release the compound from the resin, by preparing a 2 ml cleavage 'cocktail' containing 95:2.5:2.5 TFA:triisopropylsilane:water. The cleavage cocktail was added to the peptide conjugate, which was left to stand for 4

hours with gentle agitation hourly (using a glass pipette to blow air over the solution to disturb the resin beads). The cocktail, containing peptide conjugate and resin was transferred into a sintered glass funnel and a minimal quantity of TFA was added to completely dissolve the compound in order to maximise the amount filtered. The filtrate was collected in a round bottomed flask and the solvent was evaporated in a rotary evaporator, to leave the peptide conjugate behind. The peptide was triturated with cold diethyl ether and washed a further 3 times in the glass sintered funnel. The peptide remained in the funnel, and was dissolved in 95% acetic acid before collection in another round bottomed flask. The flask was then rotated in a dewer bowl containing dry ice and acetone to form a frozen shell around the inside of the flask to increase surface area prior to overnight freeze drying.

3.3.6 LCMS confirmation of peptide-conjugated prodrug synthesis

Confirmation and analysis of successful peptide-conjugated prodrug synthesis was carried out using an LCMS method. A HICHROM RPB column 25cm x 2.1mm (HICHROM-250AM) was used. The flow rate used during each LCMS cycle was 0.30 ml/min, with a gradient method beginning with 90% mobile phase A (9:1 water:methanol, containing 0.1% formic acid) and 10% mobile phase B (1:9 water:methanol, containing 0.1% formic acid) and increasing linearly to 95% mobile phase B over 40 minutes (*Table 3.3*). The detection method used was the tracking of absorbance at 330 nm, a peak absorbance for naproxen (the drug used in the synthesis of the peptide-conjugated prodrug) [276].

Table 3.3. Methodology of gradient changes throughout LCMS and HPLC cycles.

Time (min)	Mobile Phase A (%)	Mobile Phase B (%)	Flow Rate (ml/min)
0.00	90.0	10.0	0.30
40.00	5.0	95.0	0.30
41.00	90.0	10.0	0.30
50.00	90.0	10.0	0.30

3.3.7 MMP14 recombinant enzyme assay

To confirm drug release from the hydrogel networks, an MMP14 recombinant enzyme assay was carried out. Briefly, an MMP reaction buffer consisting of: 50 mM Tris-HCl, pH 7.5, 150 mM NaCl, 5 mM CaCl₂ and 0.025% Brij-35 was prepared. Recombinant MMP14 was reconstituted in MMP reaction buffer and dry hydrogels were also swollen in MMP reaction buffer. In a 12 well plate well, containing a swollen hydrogel sample, a calculated quantity of enzyme was added (0.5 µg enzyme to 10 µM of drug on the gel) and made up to 3 ml with MMP reaction buffer. The reaction was incubated at 37°C for 3 days. At the end of the reaction, hydrogels were blotted and left to dry at room temperature and the remaining MMP reaction buffer solution was collected and centrifuged at 10,000 g for 5 minutes before removing the supernatant. The pellet was re-dissolved in a known volume of methanol prior to analysis by HPLC or LCMS.

Alongside the MMP14 recombinant assay, acid degradation of hydrogels was also performed. Briefly, hydrogel samples were left submerged in 3 ml of 6 M HCl at 37°C until the hydrogel had fully dissolved, at which point 6 M NaOH was added to neutralise the acidic conditions. Samples were spun down on a centrifuge at 10,000 g for 5 minutes before discarding the supernatant and collecting the pellet as described in the above.

3.3.8 HPLC drug release analysis

HPLC analysis of MMP reaction buffer was carried out, following the same methodology, as that used during the LCMS peptide-conjugated prodrug confirmation (*Table 3.3.*), using the same column, a HICHROM RPB column 25cm x 2.1mm (HICHROM-250AM), again with a 0.30 ml/min flow rate. Again, detection method used was the tracking of absorbance at 330nm.

3.4 Results and Discussion

3.4.1 Functionalised biopolymers synthesis and UV inducible network formation concept

Following reaction with 4VBC, the degree of functionalisation (F), representing the coupling of photo-active molecules to the AC backbone was determined. The reaction of AC with 4VBC monomers occurs through lysine-initiated nucleophilic substitution causing the consumption of free amino acid groups, as well as the coupling of 4-vinylbenzyl residues.

The overall content of primary lysine groups in native gelatin ($2.53 \cdot 10^{-4} \text{ mol} \cdot \text{g}^{-1}$) and atelocollagen ($3.03 \cdot 10^{-4} \text{ mol} \cdot \text{g}^{-1}$) was recorded via TNBS assay and results proved to be similar to values reported in literature (*Table 3.4.*) [275, 277]. In AC, both colorimetric methods demonstrated a comparable decrease in amino groups molar content for 4VBC, and drug conjugates (*Table 3.5.*). Coupling of 4VBC to atelocollagen biopolymers, exhibited in *Table 3.5.* are in line with previous reports [278], $^1\text{H-NMR}$ was not carried out due to sample complications in 4VBC-functionalised AC of overlapping AC species [275].

Table 3.4. Functionalisation of gelatin with 4-vinylbenzyl chloride. Degree of functionalisation (F) measured in the 4VBC-reacted gelatin product via TNBS assay (n=3). Gelatin was reacted with 4-vinylbenzyl chloride (4VBC) at a range of molar excesses.

Sample ID	Amine Groups / $\text{mol} \cdot \text{g}^{-1}$ ($\times 10^{-4}$)	F / %
Native	2.53 ± 0.07	N/A
Gel4VBC8	1.58 ± 0.08	37 ± 3
Gel4VBC10	1.34 ± 0.05	47 ± 2
Gel4VBC15	1.16 ± 0.07	54 ± 3
Gel4VBC25	0.83 ± 0.06	67 ± 2

The functionalisation of gelatin with 4VBC and drug conjugates were carried out prior to similar methods of functionalisation in AC due to the ready availability of gelatin and comparable chemical composition and molar content lysine. For conceptual purposes, a 25-molar excess of 4VBC was reacted with gelatin as the initial functionalisation, proceeded by a further coupling of 1 molar excess of sulfasalazine (SSZ) to the remaining free lysine groups. Functionalisation of gelatin-4VBC25 was confirmed via TNBS only (*Table 3.4.*), due to the limitations of the

ninhydrin assay being unable to measure the amount of free lysine groups accurately below $1.9 \cdot 10^{-4} \text{ mol} \cdot \text{g}^{-1}$ (i.e. below 25% functionalisation in gelatin and 37% functionalisation in AC). Although the ninhydrin assay is limited in accurately quantifying the full range of functionalisation, the ninhydrin assay allows for the quantification of coupling with compounds displaying similar peak absorbance to the one of TNBS (346 nm), e.g. naproxen [279]. The ninhydrin assay releases a chromophore with a peak absorbance wavelength of 570 nm, which is far away from the absorbance peak of TNBS (346 nm). Therefore, if the desired degree of functionalisation of the selected biopolymer with a particular compound is within the linear region of the ninhydrin calibration curve then an accurate quantification of free amino groups can be calculated and thus the functionalisation can be determined.

Further coupling of SSZ via an EDC/NHS reaction was carried out, resulting in a pale orange biopolymer colour, as opposed to the off-white appearance of gel4VBC. The orange colour remained after several washes, indicating the successful coupling of SSZ. The ninhydrin assay could not be used to confirm drug presence, due to the high degree of functionalisation of 4VBC and the SSZ peak absorbance of 359 nm [280] which overlaps with the TNBS peak absorbance. Therefore, the degradation of gel4VBC25 and gel4VBC-SSZ in acid was carried out and the absorbance measured at 359nm, the peak absorbance of SSZ. The results showed little absorbance in the degraded gel4VBC, however in gel4VBC-SSZ a significantly higher absorbance reading was recorded compared to the control, further suggesting the successful coupling of SSZ to gel4VBC25, as SSZ was the only alteration to gel4VBC. As the coupling of compounds to gelatin served as a concept only, the results of the successful coupling were not quantified or displayed, however the EDC/NHS coupling method was later confirmed by ninhydrin and acid degradation, indicating successful coupling of SSZ.

Crosslinking of gel4VBC under ultraviolet light in the presence of I2959, a method widely used in research [281-283], confirmed the formation of 3-dimensional insoluble polymer matrices. The network formation via UV crosslinking of gel4VBC-SSZ was not initially carried out, as the purpose of gel4VBC-SSZ was to confirm whether drug coupling to a 4VBC functionalised biopolymer was possible.

Following successful dual functionalisation of gelatin biopolymers, dual functionalisation of AC was attempted at varying molar excesses, (*Table 3.5*). All col4VBC samples were photo-crosslinked in I2959, with col4VBC10 forming a weak gel which upon handling breaks down, likely due to the lower degree of

functionalisation, resulting in less covalent bonding during crosslinking. Due to the fragile nature of handling col4VBC10 it was excluded from the study as it is unlikely the gel would withstand the mechanical pressures within an RA target environment (within the synovial membrane). Col4VBC25 yielded an approximate 17% functionalisation of free amino lysine groups, whereas col4VBC40 and col4VBC50 yielded around 30% 35% respectively, as demonstrated by TNBS. Due to the coupling of SSZ to col4VBC requiring a ninhydrin assay to confirm and quantify degree of drug functionalisation, col4VBC40 and col4VBC50 were removed from this study as the maximum degree of functionalisation that can be accurately determined using the ninhydrin assay in AC is 35%. Another justification for the exclusion of three of the col4VBC excesses is that col4VBC25 is widely characterised and col4VBC25 hydrogels provide sufficient enough structural support [52, 174], ignoring the potential added structural support provided by drug conjugation. Further functionalisation of col4VBC25 was carried out by conjugating the model drug SSZ to the remaining $2.51 \cdot 10^{-4} \text{ mol} \cdot \text{g}^{-1}$ lysine amino groups at a 1 molar excess. The retrieved product was analysed using the ninhydrin assay, whereby the results fell within the nonlinear region of the ninhydrin calibration curve (which in AC occurs above 35% functionalisation) and were therefore excluded. It can however be noted that a further 18% of the total AC free lysine groups were occupied after SSZ drug conjugation, proving a successful drug conjugation. A separate sample of AC was also reacted with a 1 molar excess of SSZ to estimate the approximate degree of functionalisation (*Table 3.5*).

Table 3.5. Degree of functionalisation in atelocollagen. Quantification of amino group molar content and degree of functionalisation (F) in atelocollagen products (n=3) following either 4VBC, SSZ or NAPPCP coupling. Degree of Functionalisation was calculated using an overall molar amino content of $3.03 \times 10^{-4} \text{ mol}\cdot\text{g}^{-1}$ in native AC, demonstrated by TNBS and Ninhydrin assays.

¹ Denotes F calculated using TNBS native free Lys figure.

² Denotes F calculated using Ninhydrin native free Lys figure.

Sample ID	Amine Groups / $\text{mol}\cdot\text{g}^{-1}$ ($\times 10^{-4}$)		F / %
	TNBS	Ninhydrin	
Native AC	3.03 ± 0.05	3.03 ± 0.02	N/A
Col4VBC10	2.69 ± 0.10	2.58 ± 0.19	12 ± 3 ¹
Col4VBC25	2.49 ± 0.02	2.51 ± 0.14	17 ± 1 ¹
Col4VBC40	2.11 ± 0.02	N/A	30 ± 1 ¹
Col4VBC50	1.99 ± 0.03	N/A	34 ± 1 ¹
ColSSZ1	N/A	1.96 ± 0.002	34 ± 0.1 ²
ColNAPPCP1	N/A	1.97 ± 0.001	35 ± 0.02 ²

The resulting col4VBC25-SSZ, as well as col4VBC25 were reacted separately at a collagen concentration of 0.8 wt.% in 1% I2959 solution made up with 10mM HCl as described in Chapter 3.3.4 in accordance with previous research [52, 275]. The 0.8 wt.% of AC was used compared to the 10 wt.% used in gelatin solutions [284] due to the larger molecular weight and lower solubility of AC with respect to gelatin. Network formation of col-4VBC25 occurred as expected (*Figure 3.5.*), however, unexpectedly no network formation was observed in the col4VBC25-SSZ samples, suggesting no crosslinking could take place after drug conjugation.

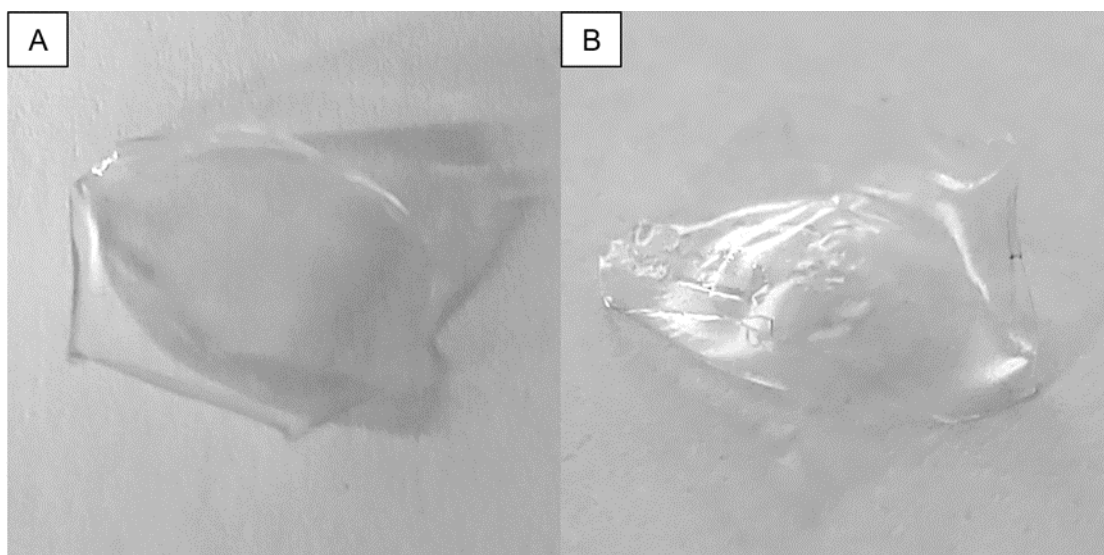


Figure 3.4. Confirmation of network formation of col4VBC25 hydrogel. UV irradiation A) Dry hydrogel for storage and B) wet, swollen hydrogel.

As a result, UV crosslinking was attempted in the previously synthesised gel4VBC25-SSZ, as well as the previously successful network forming gel4VBC as a control, following the 10 wt.% in 1% I2959 solution methods described previously. Similarly, to the col4VBC25-SSZ no network formation was observed in the drug conjugated sample, yet successful network formation resulted in the gel4VBC25 mixture. A theory for the absence of network formation by UV irradiation in drug conjugated-4VBC25 biopolymers, may be due to a shielding effect, often seen in peptide conjugation. An example of this would be the recent research by El-Sayed et al who conjugated dextran to arginine deiminase (ADI), causing a fortification effect, resulting in an increased resistance to proteolysis by proteinase K and trypsin at the ADI recognition sites [285]. This may have occurred when SSZ was coupled to the 4VBC25 biopolymers, shielding remaining lysine groups from photo-activated 4VBC, thus preventing UV-induced network formation.

To confirm whether the lack of network formation via UV crosslinking was due to SSZ alone, the focus drug, naproxen peptide-conjugated prodrug (NAPPCP), was synthesised to assess the possibility of dual functionalisation of a biopolymer with 4VBC and NAPPCP.

3.4.2 Confirmation of peptide-conjugated prodrug synthesis

Synthesis of naproxen peptide conjugated prodrug (*Figure 3.5.*) products produced consistent yields with purity in excess of 80% (*Figure 3.6.*), due to three cycles of peptide and drug coupling. A purity of over 80% was deemed acceptable for the proof of concept study carried out here, due to the detectable quantities which could be identified during the release phase of the study. The predicted molecular weight of NAPPCP was $1288.47 \text{ g}\cdot\text{mol}^{-1}$ ($\text{C}_{65}\text{H}_{85}\text{N}_{13}\text{O}_{15}$), The exact mass of the compound was $1287.63 \text{ g}\cdot\text{mol}^{-1}$. Fragmentation of NAPCP and the relevant mass per charge as seen through mass spectrometry (exact mass) were also calculated (*Table 3.6.*).

Previous works in peptide synthesis, involving two amino acid coupling cycles, required purification after synthesis of the PCP prodrugs, of similar sized sequence chains [21]. The decision to employ 3 coupling cycles per amino acid and drug was made to reduce the need for HPLC purification after synthesis. As mentioned for the proof of concept a purity of >80% was deemed to be acceptable. Many coupling reactions yield a higher rate of coupling, if a higher equivalents ratio is used. The addition of a third coupling reaction further increases the equivalents ratio, resulting in a higher percentage of successful couplings and therefore, a lower percentage of unsuccessful couplings which in turn may couple to the next amino acid in the sequence, leading to impurities in the final sample. This is a similar concept to the increased degree of functionalisation of a biopolymer observed after reactions at a higher molar excess of functionalising compound.

Prior to conjugating the newly synthesised NAPCP, LCMS was carried out to confirm the successful synthesis of the prodrug by identifying the doubly charged species of the compound (644.89 m/z) (*Figure 3.6.*).

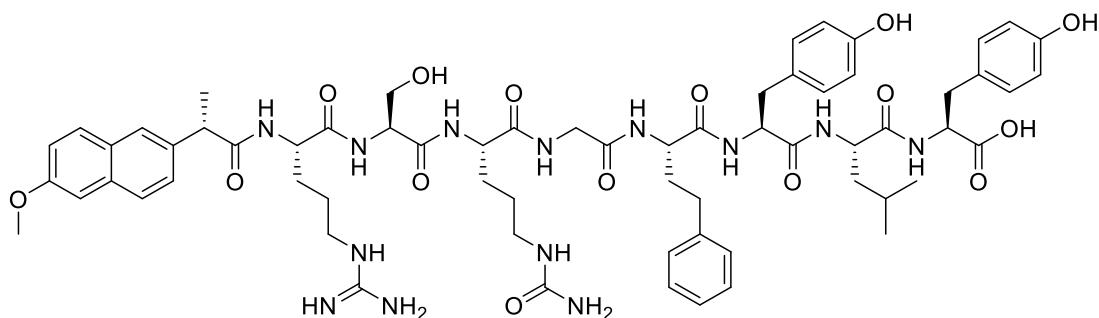


Figure 3.5. Molecular structure of the Naproxen Peptide-Conjugated Prodrug.

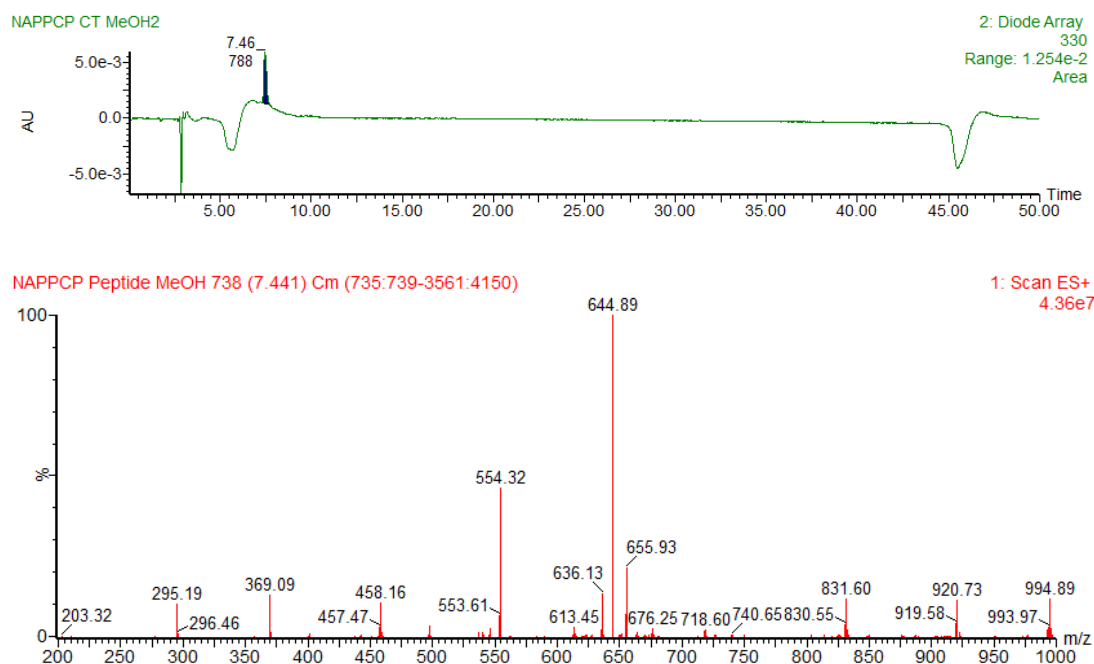


Figure 3.6. LCMS confirmation of naproxen-peptide conjugated prodrug. Identification of NAPPCP - photo diode array absorbance spectrum at 330 nm (top); mass Spectrometry for peak at 7.46 mins, showing a doubly charged species of MW 644.89 consistent with the desired product (bottom). Purity in excess of 80% as shown by the lack peaks (other than NAPPCP), large enough to display a peak area.

Table 3.6. Naproxen Peptide-Conjugated Prodrug Fragments. Fragmentation of Naproxen Peptide-Conjugated Prodrug (NAPPCP), single, double and triple charged ions, as observed by mass spectrometry.

NAPPCP Fragment Sequence	MH	MH ²⁺	MH ³⁺
NAP-Arg-Ser-Cit-Gly-Hof-Tyr-Leu-Tyr	1287.63	644.82	430.21
NAP-Arg-Ser-Cit-Gly-Hof-Tyr-Leu	1123.58	562.79	375.53
NAP-Arg-Ser-Cit-Gly-Hof-Tyr	1010.50	506.25	337.83
NAP-Arg-Ser-Cit-Gly-Hof	847.43	424.72	283.48
NAP-Arg-Ser-Cit-Gly	686.35	344.18	229.83
NAP-Arg-Ser-Cit	629.33	315.67	210.78
NAP-Arg-Ser	472.24	237.12	157.41
NAP-Arg	385.21	193.61	128.40
NAP	230.09	-	-

The peptide-conjugate sequence of NAPPCP which is modelled from another peptide-conjugated prodrug known in literature as ICT2588, a PCP for the vascular disrupting agent azademethylcolchicine, was developed by a research team at the University of Bradford, UK [103, 229]. The proteolytic cleavage site of the peptide-conjugate lies between homophenylalanine (Hof) and glycine (Gly) and is recognised by membrane-type matrix metalloproteinase 1 (MT-MMP1), or MMP14 [229]. Permission to use this particular peptide-conjugate sequence significantly increased the possibility of developing a selective and localised drug-conjugated biopolymer and proving the initial concept. This is due to the sensitivity surrounding the synthesis of a peptide-conjugated prodrug, the alteration of a single amino acid can vastly alter the rate of conjugate cleavage in the presence of MMP14 and increase potential for other proteases to cleave it in non-target tissues, therefore the ability to use an already recognised sequence provides a greater possibility of successful MMP14 cleavage, when the NAPPCP is conjugated to a biopolymer.

3.4.3 Synthesis and UV network formation of NAPPCP conjugated col-4VBC25

As the primary aim of this study was to conjugate a naproxen peptide-conjugated prodrug to a biopolymer, sulfasalazine was employed as a model drug to confirm initial conjugation was possible. Using sulfasalazine, conjugation to biopolymers, via an EDC/NHS reaction was confirmed, however UV initiated network formation subsequently failed. Therefore, using minimal quantities required, the conjugation of NAPPCP to col4VBC25 was carried out in an attempt to successfully UV crosslink a drug conjugated-4VBC25 biopolymer. The decision to trial NAPPCP conjugation in AC as opposed to gelatin, was made to significantly reduce the quantity of naproxen peptide-conjugated prodrug required to obtain a peptide-drug conjugated hydrogel.

The previously discussed, drug conjugation to col4VBC25 via the ninhydrin assay can only be accurately quantified if drug conjugation is below 18% of the AC total amino lysine groups. Therefore, as with sulfasalazine, a sample of AC was conjugated to NAPPCP at a 1 molar excess to determine the degree of functionalisation of AC. It was expected that the degree of functionalisation with SSZ and NAPPCP would be similar due to both compounds being readily reactive and only containing a single carboxylic group. The degree of functionalisation of AC with NAPPCP was calculated to be 35% (*Table 3.5.*) therefore it can be deduced that the total degree of functionalisation of col4VBC25 with NAPPCP was between 18 and

52%. The reason of synthesising col4VBC25-NAPPCP was to confirm whether or not successful UV induced network formation was possible following UV irradiation and if so alternative means of accurately quantifying the degree of functionalisation by NAPPCP were to be explored.

Following the successful coupling of NAPPCP to col4VBC25, UV induced crosslinking was carried out. As observed in both col4VBC25-SSZ and gel4VBC25-SSZ, col4VBC25-NAPPCP also exhibited no network formation in response to UV light in the presence of I2959 photoinitiator, despite the col4VBC25 control successfully forming a network. To confirm the photoinitiator batch was not a contributing factor to the lack of drug-conjugated network formation, an alternative batch was used in a repeat of the UV curing, with the same results obtained. Due to the NAPPCP-conjugated col4VBC25 sample also failing to form a hydrogel network, the possibility of molecular shielding seems a likely explanation for the unexpected lack of UV-induced network formation.

Ordinarily, UV irradiation generates free radicals causing the 4VBC molecule, to react with other strands of the AC or gelatin polymer, increasing the concentration of coupled strands, leading to a network formation as the coupled strands interact and react with other strands as well as other 4VBC molecules on the same strand (*Figure 3.7.*) [52, 286].

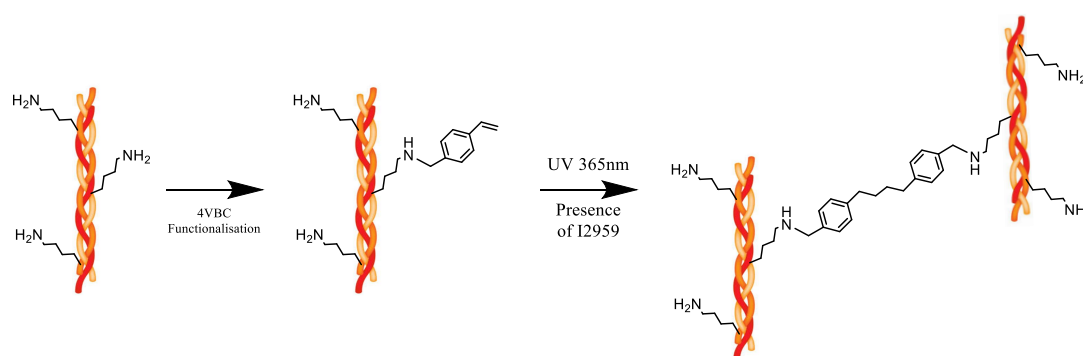


Figure 3.7. UV-induced Crosslinking of collagen-based biopolymers. Following 4VBC functionalisation collagen-based biopolymers were crosslinked in the presence of I2959 photoinitiator.

In the presence of a conjugated drug, it is thought the network formation due to UV-induced photoinitiation is blocked by a shielding effect, caused by the conjugation of the drug molecule. The specific type of shielding is thought to be due

to the steric hinderance of the molecules, which is known to slow chemical reactions due to the blocking of nucleophilic attacking molecules, in this case the free radicals created from UV irradiation. It could be said that the degree of functionalisation of 4VBC on gelatin is considerably larger (67%) than that of the coupled SSZ, however the size and structure of SSZ may be sufficient enough to considerably slow the reaction enough to appear as though no crosslinking was possible. To assess this samples were left overnight under UV light, which again exhibited no gel formation, over 12 times longer than the previous methods state. Steric shielding is shown to play roles within free radical reactions of nitroxide [287-289]. It is likely that steric shielding is the explanation behind the lack of gel formation in the presence of UV irradiated free radical molecules, however whether complete gel formation is prevented or the reaction is significantly slowed remains unclear.

As a result of the inability of col4VBC25-NAPPCP to form hydrogel networks under UV light, an alternative method of forming a NAPPCP conjugated biopolymer-based hydrogel was investigated.

3.4.4 UV crosslinking photo-active biopolymers to encapsulate drug-conjugated biopolymers

The utilisation of hydrogels for drug delivery often occurs by one of two methods 1) drug conjugation directly onto the hydrogel, the initial strategy proposed here, and 2) drug loading onto a hydrogel network [177, 290]. A method of drug loading involves the encapsulation of a drug within a hydrogel network [291]. Loading of a drug onto a hydrogel network, has a major flaw compared to a conjugation approach, in that, the drug has an increased chance of diffusing out of the hydrogel away from the target site, thus increasing the potential of off-target toxicity. Unless the loading of a drug is controlled by stimuli such as temperature or pH, a drug, if small enough, has the potential to diffuse out of the gel network.

The inability to synthesise a UV networked drug-conjugated col4VBC hydrogel, forced an alternative approach. This approach involved the functionalisation of two separate samples of AC, one functionalised with 4VBC at a 25-molar excess, as previously described and the other, a drug conjugated AC sample (colNAPPCP). The two samples were mixed and UV crosslinked. Successful network formation was observed indicating the ability to encapsulate a colNAPPCP material within the network of col4VBC25 during the UV curing process to form

col4VBC25encap-NAPPCP (Figure 3.8). The formation of a UV irradiated, drug-encapsulating hydrogel is in line with related literature where alternative drugs have been loaded onto a variety of photo-crosslinked hydrogels [292, 293], namely the work by Cao *et al* (2014). Cao *et al* encapsulated bone morphogenic protein-loaded nanoparticles within a gelatin-based photopolymerisable hydrogel, to deliver a sustained growth factor release to increase the rate of bone regeneration [294].

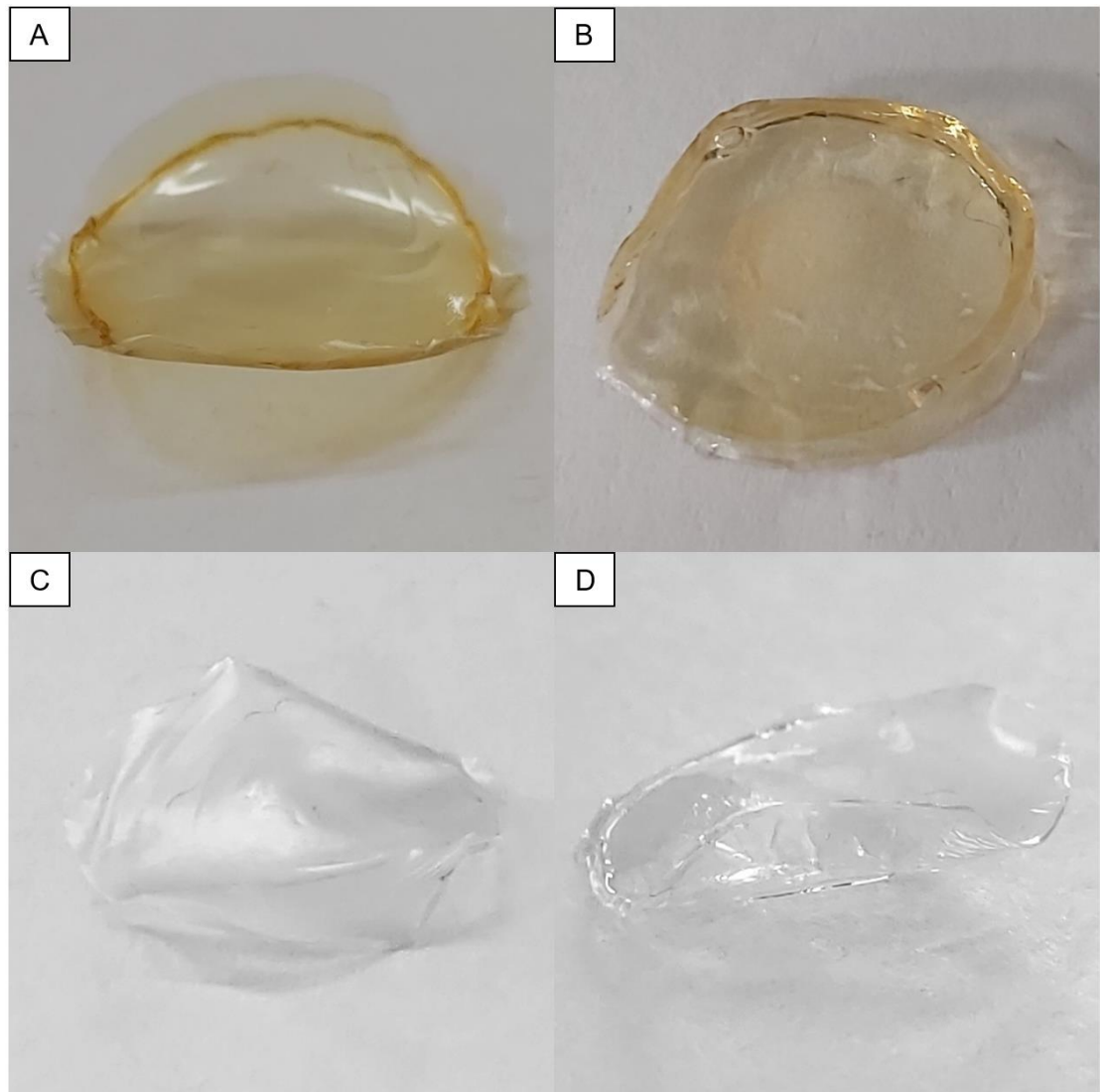


Figure 3.8. Confirmation of successful network formation of encapsulated hydrogels. Hydrogel network of col4VBC25 encapsulating either colSSZ or colNAPPCP A-B) colSSZ and C-D) colNAPPCP. Left side of figure depicts the encapsulated hydrogels in their dry state, whereas the right side shows the swollen state of the hydrogels.

Using a hydrogel as a drug delivery vehicle serves several key purposes, including a localised delivery, a selective form of release, whether by stimuli or other means and a greater drug therapeutic index. If encapsulating (a type of loading) a drug within a gel network decreases off-target toxicity compared to the drug alone, the drug requires a method of keeping it loaded to the gel, otherwise diffusion of the active drug may occur prematurely. In efforts to reduce the risk of premature diffusion-induced drug release, the NAPPCCP prodrug was conjugated to a separate sample of AC prior to encapsulation. It was expected that by conjugating to AC, it would prevent NAPPCCP from diffusing out of the gel network due to the gel network consisting of functionalised AC as well as the molecular size of AC (approximately 300kDa), being significantly larger than the prodrug alone.

3.4.5 MMP14 selective recombinant enzyme assay

After the successful formation col4VBC25encap-NAPPCCP hydrogels, the release of NAP from the NAPPCCP component, which relies on the selective cleavage by the proteolytic enzyme MMP14 was assessed using recombinant MMP14. Cleavage of the peptide-conjugate triggers drug release [295] leading to the deprotection of the peptide chain ends, allowing the remaining 4 amino acids to be easily metabolised and removed from naproxen to release the drug in an active state [103, 229]. The selection of a recombinant MMP14 assay over an *ex vivo* biological assay using homogenised tissue overexpressing MMP14 was pursued to confirm cleavage of the peptide-conjugate occurs through MMP14 activity. The recombinant enzyme demonstrates that MMP14, the target enzyme is capable of cleaving NAPPCCP between the Hof-Gly peptide bond. In an *ex vivo* assay of this type it would not be possible to identify which specific enzyme was cleaving the prodrug. Due to the nature of the study, proving the concept for the release of the active drug, naproxen from the hydrogel-NAPPCCP system, was thought to be the priority over, the assessment of the drug's half-life and breakdown after the initial release.

HPLC analysis of the MMP14 recombinant assay buffer was carried out to assess the release of the NAPPCCP cleavage metabolite (NAP-Arg-Ser-Cit-Gly) into the reaction buffer (*Figure 3.9.*) from within the hydrogel network.

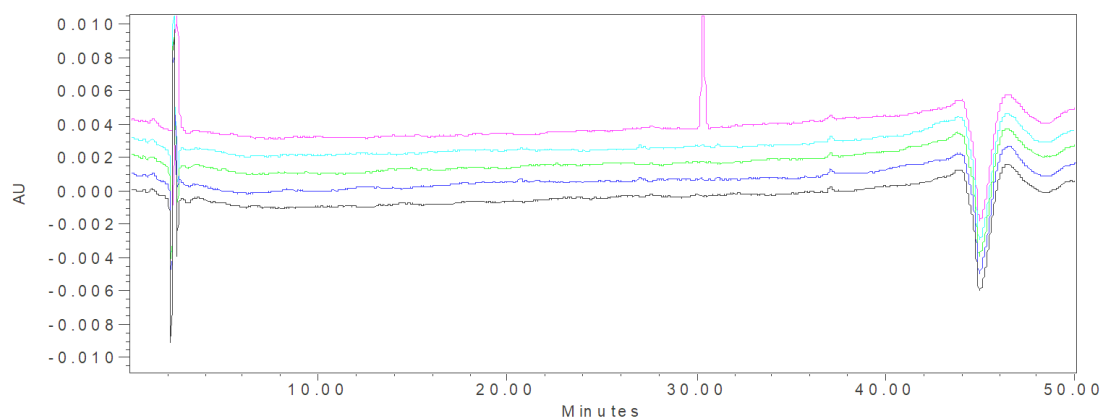


Figure 3.9. HPLC spectra (absorbance chromatograms at 330 nm) of reaction buffer for MMP14 recombinant assay. Assessment of the release of naproxen metabolites from a col4VBC25encap-NAPPCP hydrogel network: pink: naproxen drug control, cyan: col4VBC25encap-NAPPCP gel, green: col4VBC25 control, blue: col4VBC25encap-NAPPCP gel repeat, and black: reaction buffer negative control.

Unexpectedly no expected naproxen containing compound metabolite peaks were detected in the col4VBC25encap-NAPPCP samples, suggesting no release of NAP metabolites from the hydrogel networks. The naproxen control sample was calculated to be the maximum possible concentration of NAP on gel, within the reaction buffer, and the detection limits of the HPLC was $<0.1\mu\text{M}$, further suggesting no cleavage by MMP14 took place due to the high sensitivity of the HPLC equipment. To confirm the unsuccessful cleavage by MMP14, col4VBC25 and col4VBC25encap-NAPPCP networks were separately degraded in 6M HCl prior to preparation to analyse the sample solution in HPLC (*Figure 3.10.*)

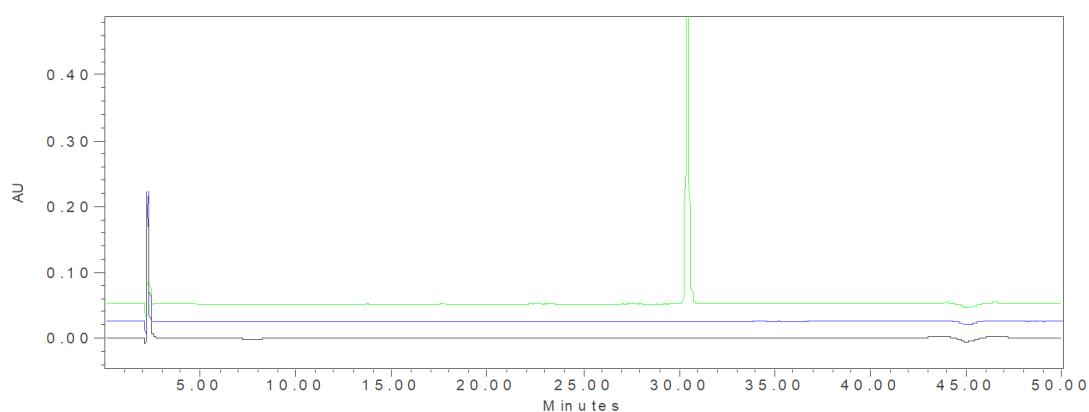


Figure 3.10. HPLC analysis of acid degradation assay (absorbance chromatograms at 330 nm). Green: naproxen drug control, blue: col4VBCencap-NAPPCP and black: col4VBC25 control.

As observed in the MMP14 recombinant assay, acid degradation produced no traces of naproxen-based compounds. An initial theory for this was the instability of NAPPCP occurring once conjugated to the AC biopolymer, or during the UV-crosslinking process. Ultraviolet light could have some effects upon the NAPPCP component as well as the collagen itself. In collagen, under UV light research has demonstrated an increased viscosity, compared to native collagen, thought to be due to the formation of intermolecular crosslinks via tyrosine dimers, shown by the production of blue fluorescence, with a peak of approximately 350nm [296]. A more recent study has shown UV irradiation of tyrosine and phenylalanine (and likely homophenylalanine) produces free radical residues that crosslink collagen fibres [297, 298]. In the case of the NAPPCP it is unlikely that subsequent crosslinking between tyrosine and other aromatic amino acid components of collagen occurred as this would result in the conjugation of NAPPCP to collagen during the photo-crosslinking process, anchoring naproxen to the hydrogel network. Given that the HPLC is capable of detecting concentrations of NAP $<0.1\mu\text{M}$, if any naproxen was present it is likely it would have been detected, when the gel was fully degraded in acid.

Tyrosine - an amino acid within the NAPPCP prodrug, is shown to be irradiated by UV light [299] shown to result in the inactivation of enzymes [300] which in NAPPCP, may have broken the peptide conjugate, releasing NAPPCP within the crosslinking solution, which when subsequently washed would allow the naproxen-metabolite to freely diffuse out through a hydrogel pore. These findings indicate the absence of colNAPPCP within the network prior to the start of the MMP14

recombinant assay which could only be explained by the unexpected diffusion of colNAPPCP or NAPPCP metabolites containing NAP from the col4VBC25 network during the washing and hardening phases after hydrogel formation. The wash step is a crucial step which cannot be avoided post-UV crosslinking, due to the acidic conditions required to initially dissolve col4VBC25 as well as the free radicals produced during network formation, which would not be safe to deliver into the disease site. Due to the remnants of the crosslinking solution mixture (and encapsulated colNAPPCP) remaining within the newly formed encapsulating hydrogel, when the wash step takes place it is possible that the dissolved colNAPPCP or NAP-based metabolites are washed out as it diffuses and mixes into the solution the hydrogel is washed with, in turn exhibiting no naproxen peaks on the HPLC spectra.

3.5 Conclusions

Photo-active 4VBC, collagen-based hydrogels appear to lack the ability to support drug attachment, observed in the inability of dual functionalised collagen and gelatin biopolymers to undergo UV-induced photo-crosslinking. The unexpected ability of colNAPPCP to remove itself from the encapsulating hydrogel further demonstrated photo-crosslinking 4VBC is not a suitable method to support a Hydrogel-PCP system. As a result, alternative approaches must be taken in order to synthesise a collagen-derived hydrogel delivery vehicle capable of delivering and anchoring NAPPCP at its' intended site.

Chapter 4
Chemically crosslinked biopolymer hydrogels

4.0 Chemically crosslinked biopolymer hydrogels

Here, the exploration into an alternative crosslinking strategy, to synthesise a more clinically relevant Hydrogel-PCP is undertaken. Chemical crosslinking by DMTMM, is employed to crosslink NAPP-CP-conjugated gelatin, under physiological conditions. Initial assessments of gel-NAPP-CP hydrogel properties are carried out through assessments of:

- *Gel content*
- *Swelling ratio*
- *Gelation kinetics*
- *Rheology.*

The release of naproxen, by MMP14 cleavage of the peptide-conjugate, as well as acid degradation, was analysed by Liquid Chromatography Mass Spectrometry (LCMS). Finally, preliminary investigations into a less invasive and more clinically desirable delivery strategy, injection, are carried out under physiological conditions.

4.1 Introduction

Extensive research into UV-curable gel networks, and their potential for drug delivery has been carried out, however UV-curing did not prove a suitable method to enable full solution gelation and the formation of mechanically competent covalently crosslinked hydrogel networks. Another widely investigated crosslinking method for medical therapies, is chemical crosslinking which has produced an alternative range of unique characteristics. Whereas UV-cured hydrogels often have the ability to withstand higher temperatures or greater mechanical pressure [301], chemically crosslinked hydrogels have the potential to be crosslinked in a crosslinking solution, without the need of an alternative source, such as a UV light, which in some environments is not possible without invasive surgery, i.e. deep within tissue or bone constructs. This feature alone, is a clinically desirable property, as in many cases the need for an invasive implantation can be substituted for an injectable form, which gels *in situ*, of which, several research groups have investigated the potential of these alternative hydrogels in a range of biomedical applications [302, 303]. Chemical crosslinking has a range of crosslinkers available, dependant on the polymer backbone used, for example a biopolymer such as gelatin, a carbodiimide reaction, activating free carboxylic groups to readily react with the free amino groups of gelatin, chemically crosslinking the polymer.

In some research areas, the use of hybrid hydrogels has arisen, enabling the modulation of microscale hydrogel properties as well as incorporating the tailoring of drug or gene delivery capabilities [304]. In 2015 a study by Qu *et al* demonstrated the use of a thermo-responsive hybrid hydrogel for the delivery of DOX in breast cancer through the incorporation of gold nanorods into the hydrogel itself [305]. However, there is still much potential for a solely chemically crosslinked hydrogel system that delivers a selective and localised drug delivery system whilst acting as a support network, when necessary.

The decision to exclude the AC biopolymer material at this stage of the research was made due to greater accessibility towards gelatin amino lysine groups when conjugating our peptide-conjugated prodrugs. When collagen is degraded, the triple-helix is broken into randomised, more linear coils known as gelatin. The degree of denaturation is relative to the amount of triple-helical structures, with lower amounts found in gelatin compared with collagen [306, 307]. The process of collagen denaturation into gelatin is attributed to hydrogen bonds and covalent crosslinks which break endothermically and exothermically, respectively [308]. The collapse of the triple helix, which is necessary to stabilise the collagen fibril ultrastructure [309] occurs, resulting in the unfolding and fragmentation of collagen, leaving functionalisation sites more accessible for conjugation of NAPPCP. The ratio of drug conjugated to the gelatin biopolymer, a 1 molar ratio to free amino groups, as previously used in AC, is no longer necessary to achieve the same degree of functionalisation, because of the increased lysine accessibility in gelatin. This is supported by the degree of functionalisation achieved in collagen versus the degree of functionalisation obtained in gelatin after 4VBC (at a 25-molar excess) functionalisation $17\% \pm 1$ and $67\% \pm 2$, respectively (*Table 3.4. and 3.5.*).

A revised strategy was employed after the previously discussed, unsuccessful coupling and loading of naproxen conjugated PCPs (NAPPCP) to collagen or gelatin UV-cured hydrogels. The revised strategy aims to chemically crosslink a drug conjugated form of the collagen-derived biopolymer, gelatin. The original aim of the study hoped the UV-curing method would bypass the non-selective delivery of naproxen by surgically implanting the NAPPCP-conjugated hydrogel network to lower the risk of off-target toxicity, as previously discussed. This chapter, focuses around the proposed concept surrounding: gelatin-NAPPCP chemically crosslinked hydrogels under physiological conditions and the drug release profile of naproxen. The change from photo-crosslinking to chemical crosslinking, as well as

the change in material streamlines the hydrogel synthesis procedure, both in the number of steps required and the time taken. Three steps are required in the photo-crosslinking method: monomer attachment, prodrug conjugation and UV curing, all of which, in collagen takes approximately 5-6 days if all materials are to hand, and in gelatin the same method takes roughly 3 days. On the other hand, the chemical crosslinking method in gelatin requires, prodrug conjugation followed by chemical crosslinking and takes 2 days to synthesis a Hydrogel-PCP. Therefore, the increased efficiency of the procedural change, works in favour of the production of a Hydrogel-PCP system. The new strategy also covalently couples the drug to the biopolymer which is in turn crosslinked, preventing the drug from escaping from the hydrogel after the crosslinking process, as observed in the UV-curing encapsulation experiments.

4.1.1 Delivery route – implantation versus injection

Drug development requires a suitable delivery route, tailored to the disease target. Common routes of delivery include: oral, transdermal, intravenous (IV), implantation and injection [310]. The most popular of these is oral delivery, however, many drugs are unsuitable via oral delivery due to compliance issues of the patient or degradation in acidic conditions within the stomach. These complications can be bypassed using IV delivery as an alternative. A disadvantage of IV is the need for a healthcare professional to administer the treatment. Similarly, transdermal delivery overcomes many oral delivery routes, yet it comes with further disadvantages. Few drug compounds possess the necessary properties, for example: good solubility, low molecular weight and high partition coefficient [311], required to pass through the outer barrier of the skin.

With these disadvantages, as well as the lack of localised delivery none of oral, IV or transdermal drug deliveries were selected to investigate as possible delivery routes for the novel Hydrogel-PCP system. Implantation of the Hydrogel-PCP was initially hypothesised to be the more suitable delivery route, due to the crosslinking method originally used. Photo-crosslinking requires light; therefore, an injectable device would not be suitable when targeting deep tissue disease such as osteosarcoma or rheumatoid arthritis. The major disadvantage of implantation is the invasive procedure it requires, increasing the risk of toxicity through infection. Collagen-based hydrogels however, are biodegradable [312], and once implanted would not require surgery to remove the device. The device could also be implanted

at the time of tumour removal in osteosarcoma [313] removing the need for a second surgical procedure.

The change in direction from the original crosslinking methodology, prompted a revision of the clinical delivery route. By using a chemical crosslinker, network formation can be triggered and the treatment administered, before the formation of the hydrogel network, without the need for an external activator (such as UV light). This allows the injectable delivery route, a non-invasive procedure, to be explored. As well as implanted hydrogels, injectable hydrogels are able to provide localised and selective drug release, with an added advantage of no required surgery. This is key in providing a more clinically desirable delivery route. The injectable method also allows for recurring treatments at regular intervals, where necessary, and unlike the implanted delivery, the injectable route could be administered at key sites to provide structural support to surrounding tissues [314, 315]. An example of this would be the site of cartilage degradation, between a joint in rheumatoid arthritis, helping to prevent bone erosion [316].

The revised crosslinking strategy provides a more clinically desirable therapeutic device, capable of *in situ* gelation to selectively release naproxen in a localised manner at a disease site, whilst acting as a tissue support structure (*Figure 4.1.*).

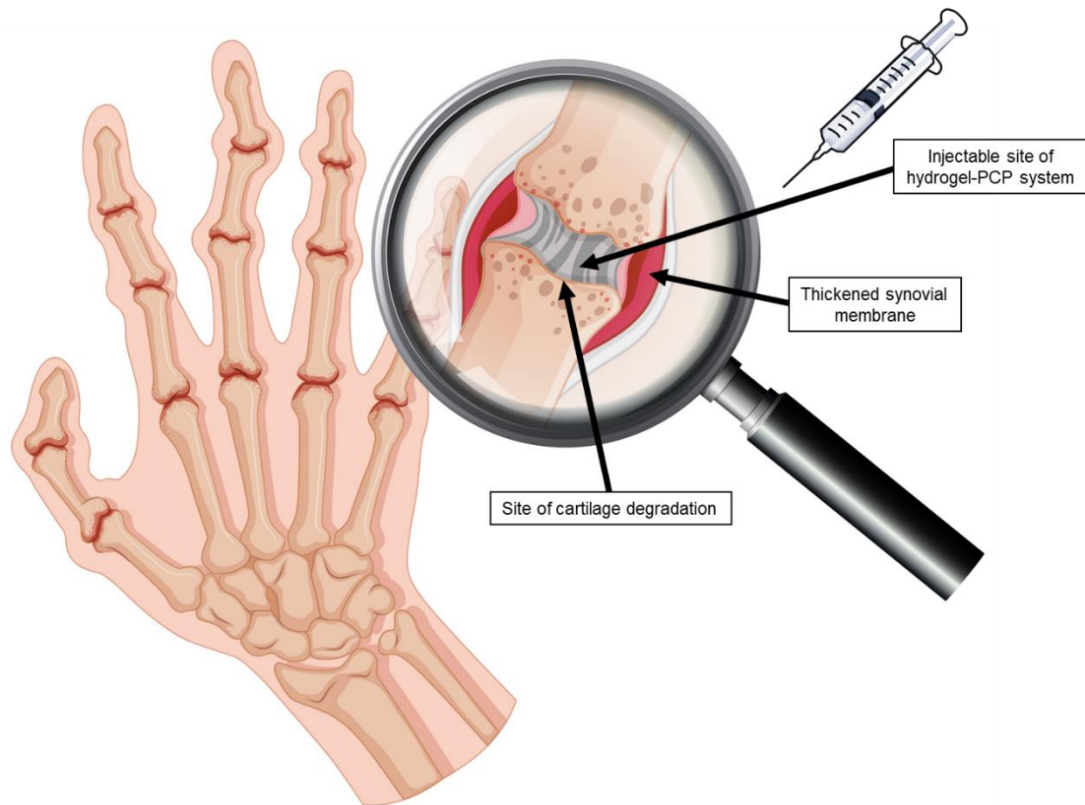


Figure 4.1. Injection delivery strategy. Gel-NAPPCP system, injected between the rheumatic joints, at the site of cartilage degradation, where *in situ* chemical crosslinking occurs to form a gel-NAPPCP hydrogel with a cartilage-like consistency. Structural support is provided by the hydrogel, whilst selectively releasing the anti-inflammatory drug, naproxen, through the cleavage of the peptide-conjugated sequence by MMP14.

Here, initial findings suggest the potential for the use of an injectable PCP-conjugated hydrogel as a suitable delivery vehicle for selectively released naproxen by proteolytic MMP14 cleavage. Further work is however required to optimise crosslinking potential and the efficiency of drug release by MMP14.

4.2 Materials

All non-conventional research materials and equipment information is listed in Chapter 3.2 (*Table 3.1. and 3.2.*).

4.3 Methods

4.3.1 *Synthesis and confirmation of naproxen peptide-conjugated prodrug*

Peptide-conjugated prodrug synthesis and confirmation of successful synthesis, followed the same methods as described in Chapters 3.3.5 and 3.3.6.

4.3.2 *Drug conjugation to native biopolymer material*

Naproxen and naproxen peptide-conjugated prodrugs were coupled to free amino lysine groups of gelatin biopolymers through EDC/NHS activation of free drug carboxylic groups (-COOH). The coupling drug was dissolved in minimal DMSO before molar ratio-dependent quantities of EDC and NHS were added to the solution and stirred for 1 hour at room temperature. Again, the volume of DMSO required to dissolve the drug is not sufficient enough to significantly impact the coupling reaction after which the compound is dried and washed, removing the DMSO used to initially dissolve the drug. The excess EDC was quenched by the addition of 2-Mercaptoethanol for 15 minutes before adding the solution to a 10% w/v solution of gelatin containing 10% v/v DMSO/PBS to prevent drug precipitation which was found to gradually occur in 100% PBS over the reaction time of 24 hours whilst stirring at 40°C. The resulting solution was precipitated in a 10-fold volume excess of ethanol for 5 hours, before collection and air drying of the drug-conjugated gelatin biopolymer occurred.

4.3.3 *Confirmation of drug conjugation to gelatin biopolymers*

Confirmation of successful drug-conjugation was carried out using the previously validated Ninhydrin methodology described in Chapter 3.3.2.2.

4.3.4 Chemically-induced gelatin network formation and gelation kinetics

After the successful conjugation of naproxen-based drugs to gelatin biopolymers, drug-conjugated and gelatin samples were dissolved separately at 10 w/v ratio in PBS solution at 40°C, before placing the solution in a 37°C incubator under stirring and the addition of DMTMM at a 2 molar ratio to remaining free amino lysine groups and dissolving for 5 minutes in a screw top vial. Once dissolved and mixed, the solution was plated out into well plates and left to gel at 37°C for 30 minutes to ensure total gelation had occurred (*Figure 4.2.*). After gelation, the resulting hydrogels were washed in 50% ethanol to remove unreacted activators and drug-conjugations and left to air dry.

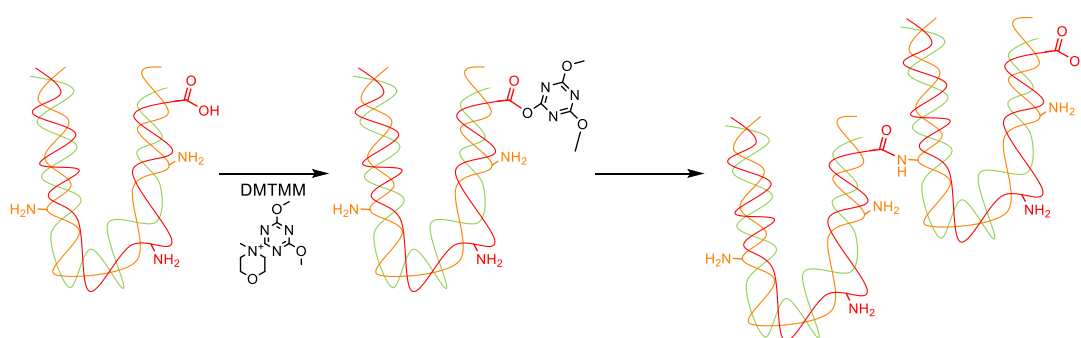


Figure 4.2. Chemical crosslinking of gelatin using DMTMM crosslinker. DMTMM activation of gelatin carboxylic groups, before reaction with free amino lysine groups of other gelatin strands, resulting in the formation of a hydrogel network.

Gelation kinetics were prepared in the same way, except the crosslinking solution was removed from stirring and left to crosslink at 37°C instead of being plated into well plates, allowing the samples to be angled to confirm liquid to solid transition progress, at given timepoints. Briefly, 0.5g sample was dissolved in 5 ml PBS at 40°C until completely dissolved. Gelatin control samples were mixed with a minimal amount of rhodamine to dye the gels pink to show the gelation clearly. Once completely dissolved, DMTMM fixed molar excesses were added (calculated using the equation in Chapter 3.3.1) and stirred at 37°C. At 5-minute time intervals, the mixture was held at approximately 45° to assess whether gelation had occurred. The time at which the solution no longer flowed was deemed to be the time of network formation.

4.3.5 Quantification of swelling ratio and gel content

Dry chemically crosslinked samples ($n = 4$) of known mass (m_d) from both gelatin-only and gel-NAPPCP hydrogels were individually incubated in 5 ml of 50mM Tris HCl (pH 7.5), 150mM NaCl, 5mM CaCl₂ and 0.025 wt.% Brij-35 (MMP reaction buffer) at room temperature for 24 h. The swelling ratio (SR) was calculated using the equation:

$$SR = \frac{m_s - m_d}{m_d} \times 100$$

where m_s is the mass of the DMTMM-crosslinked sample equilibrated in MMP reaction buffer (swollen sample) and m_d is the dry mass of sample.

Gel content was measured to assess the overall proportion of the covalent hydrogel network, insoluble in MMP reaction buffer. Dry chemically crosslinked samples ($n=4$) of known mass (m_d : 40 mg – 50 mg) were incubated in 3 ml of MMP reaction buffer for 3 days. MMP reaction buffer and a 3 day time scale were selected, to allow comparisons between gel content before and after the drug release assay to be made, to assess the stability of the network within the presence of MMP14. Resulting samples were air dried and weighed. The gel content (G) was calculated by the equation:

$$G = \frac{m_1}{m_d} \times 100$$

Where m_1 is the dry mass of the collected sample.

4.3.6 Rheological assessments

Rheological assessments involved amplitude and frequency sweeps on both gelatin-control and gelatin-NAPPCP conjugated hydrogels. Amplitude sweeps of newly formed hydrogels ($n=4$) were measured by a modular compact rotational rheometer from Anton Paar, at a fixed frequency of 1 rad·s⁻¹ at time interval increases of shear strain %. During the Frequency sweeps, frequency was increased, whilst the shear strain remained at a constant percentage of 10%, to accommodate the linear viscoelastic region of both gel sets. Both assessments were carried out at physiological temperatures (37°C) and a parallel plate ($\varnothing=8$ mm) was used to apply the shear force, with a plate gap of 1.8mm. Storage (G') and Loss (G'') modulus values were recorded throughout the sweeps.

4.3.7 MMP14-Selective Recombinant Enzyme Assay

MMP14 recombinant enzyme assay carried out as described in Chapter 3.3.7 and analysed as described in Chapter 3.3.6 using the same methods used to confirm naproxen peptide-conjugated prodrug synthesis.

4.3.8 Initial Investigations of Injectable Device and In Situ Gel Formation

Gelation solutions were prepared as described in Chapter 4.3.4, however rather than setting the crosslinking solution in well plates, the solution was taken up by syringe, and injected using a 0.3 mm outer diameter needle, into pre-prepared cavities of sawbone and left to crosslink under physiological temperatures. The resulting gels were photographed to demonstrate anchorage potential of the newly formed hydrogels. Similar to the investigation of gelation kinetics, gelatin control samples were mixed with a minimal amount of rhodamine to dye the gels pink to clearly show swelling within the cavities.

4.4 Results and Discussion

4.4.1 Confirmation of drug conjugation to native biopolymer material

Native gelatin was reacted with activated carboxylic groups of naproxen (NAP) (previously depicted in *Figure 3.3.*) or Naproxen peptide-conjugated prodrug (NAPPCP) compounds, through an EDC/NHS reaction [317]. Coupling of this nature occurs through a nucleophilic attack, whereby the free amino groups, for example the ones found in lysine react with the activated carboxylic groups of drug compounds.

Naproxen-conjugated gelatin biopolymers were synthesised and the degree of functionalisation with naproxen drug compounds was confirmed for each molar ratio sample (*Table 4.1.*) [275]. The design of the coupling reaction ensured the avoidance of unintentional activation of gelatin -COOH groups, evading unwanted crosslinking of gelatin during the coupling reaction [318]. Activating the single -COOH of NAP and later NAPPCP, before quenching EDC, prevented the activation of gelatin -COOH when mixing the separate solutions together.

Gelatin was first conjugated to naproxen, to act as a guide for NAPPCP coupling, molar ratio. As expected, doubling the molar ratio from 0.1 to 0.2, exhibited approximately double the degree of functionalisation, from 8% to 17%, however a molar ratio of 0.3 showed a degree of functionalisation of just 20%, suggesting approximately two thirds of the naproxen reacted with gelatin was successfully coupled compared with 80 and 85% in 0.1 and 0.2 molar ratio reactions respectively. The molar ratio of 0.2 was employed for gelatin functionalisation with NAPPCP, and yielded 17% functionalisation of free amino lysine groups. The selection of the molar ratio, 0.2, was made for two key reasons 1) the quantity of unreacted drug versus degree of functionalisation, as the results suggested an almost complete saturated degree of functionalisation of this coupling method in our gelatin system was 20% and 2) the 17% degree of functionalisation of gel-NAPPCP(0.2) was half that of the 35% of col-NAPPCP, equating to approximately 3 times the quantity of NAPPCP per gelatin hydrogels of equal networking solution mass compared to col-NAPPCP (due to the higher wt.% of gelatin used for crosslinking).

Table 4.7. Functionalisation of gelatin with naproxen and NAPPCCP. Naproxen peptide-conjugated prodrugs (n=3) at varying concentrations, confirmed by ninhydrin assays, quantifying the unreacted amino groups of gelatin biopolymers.

Sample ID	Amine Groups / mol·g ⁻¹ (x 10 ⁻⁴)	F / %
Native Gelatin	2.53 ± 0.006	N/A
Gel-NAP (0.1)	2.34 ± 0.004	8 ± 0.14
Gel-NAP (0.2)	2.10 ± 0.002	17 ± 0.08
Gel-NAP (0.3)	2.04 ± 0.003	20 ± 0.11
Gel-NAPPCCP (0.2)	2.08 ± 0.003	18 ± 0.11

The method of conjugating drugs to gelatin, provides a potentially significant advantage when attempting to overcome solubility issues of certain drugs in physiological solutions. The precipitation and washing steps between the coupling and crosslinking stages of hydrogel production, allows various different solutions to be used to dissolve drugs. Drugs can be dissolved in dimethyl sulfoxide (DMSO) and reacted with EDC/NHS to activate the carboxylic acid groups, before mixing with dissolved gelatin solution allowing the drug to stay in solution whilst reacting with free amine groups of gelatin, before washing out the DMSO during precipitation. Dimethyl sulfoxide is an aprotic solvent which is often capable of dissolving water insoluble therapeutic and toxic agents [319]. However, DMSO has significant penetration potential and can be detected in the blood 5 minutes after application to the skin and in 20 minutes DMSO can be detected in all organs of the body. Delivery of a drug, for example intravenously, requires the drug to be solubilised, however using DMSO to dissolve a water insoluble drug so that it can be intravenously administered could enhance the penetrative effects of the drug, therefore increasing the risk of off-target toxicity as well as causing DMSO-induced side effects including: erythema and in some cases systemic symptoms [320, 321]. In relation to drug-conjugation of gelatin biopolymers, DMSO allows less water insoluble drugs, for example sulfasalazine (SSZ) with a 0.2mg/ml water solubility, and a DMSO solubility of approximately 30mg/ml, to be dissolved in a high enough concentration (to achieve the desired degree of functionalisation) to limit the dilution of a dissolved gelatin solution when the two reaction mixtures are combined, without the added complications of enhanced drug penetration when delivered into the body in a drug-conjugated

hydrogel format. Any remaining DMSO is washed off the drug-conjugated biopolymer after the coupling reaction, allowing an insoluble drug to be coupled to a delivery vehicle precursor, without risking the enhanced risks which the use of DMSO brings.

4.4.2 Chemically-induced gelatin network formation

Upon successful drug conjugation to gelatin biopolymers, the newly NAP-conjugated gelatin and gelatin-control biopolymers were reacted separately with DMTMM to initiate chemical crosslinking, prior to the crosslinking of the gel-NAPPCP biopolymer. Chemical crosslinking, through DMTMM activity was observed in the native gelatin control and gelatin-naproxen sample, confirming the formation of drug-conjugated hydrogels. This agrees with other studies where DMTMM has been used to crosslink materials including recombinant human collagen type I [322], whilst also been used to ligate amines to modify and form hyaluronan hydrogels [323]. Following the successful network formation of both gel-CT and gel-NAP, chemical crosslinking of gel-NAPPCP biopolymer occurred (*Figure 4.3*).

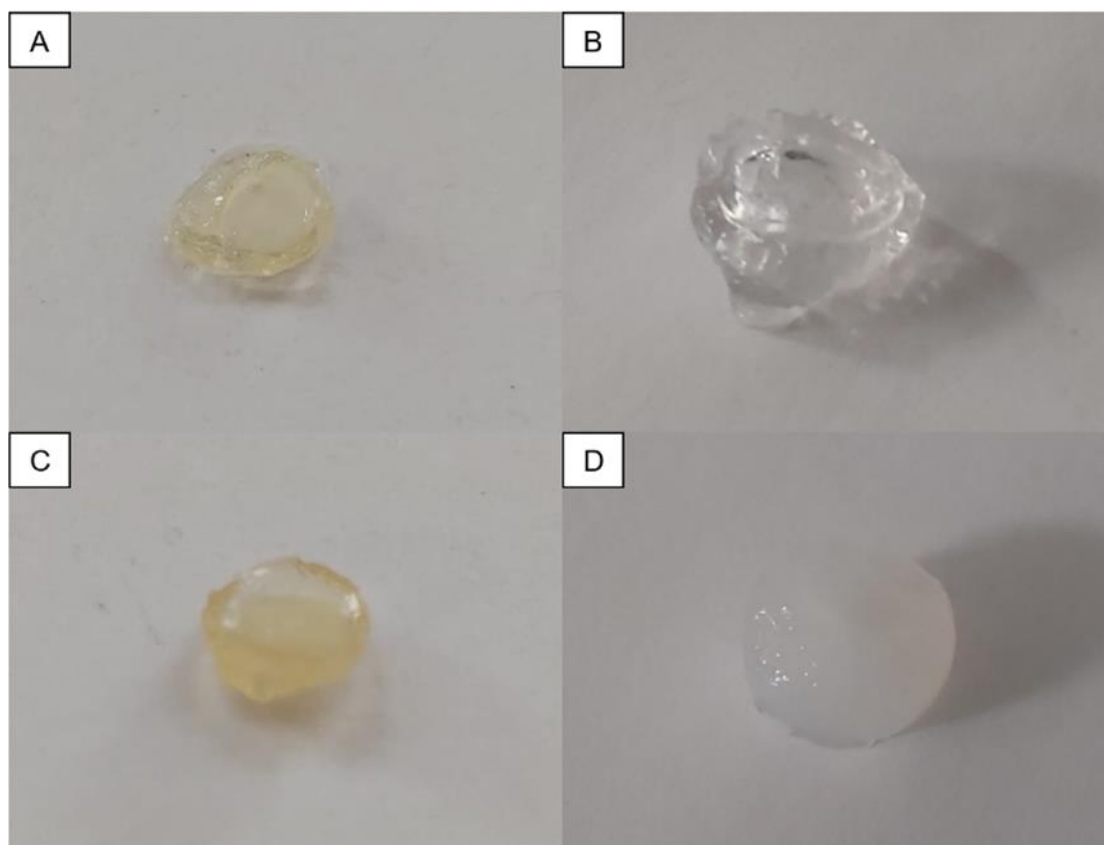


Figure 4.3. Hydrogel network formation by DMTMM-induced chemical crosslinking. Gelatin-control A) dry B) wet and gelatin-NAPPCP C) dry and D) wet.

The gel-CT hydrogels, appeared paler and more transparent, compared to gel-NAPPCP, which when swollen, appeared more clouded and greyer in colour. The successful formation of a gel-NAPPCP hydrogel, demonstrates the initial synthesis of a PCP-conjugated collagen-derived (gelatin) hydrogel material is possible through nucleophilic reactions. Chemical crosslinking enables the formation of gel-NAPPCP hydrogels, which when compared to the UV crosslinking strategy, is significant progress in proving the concept of providing a selective, localised peptide-conjugated prodrug hydrogel delivery system. The conjugation of NAPPCP to the gelatin backbone as opposed to an encapsulation method, significantly reduces the risk of the NAPPCP eluding the gel network. In an ideal crosslinking reaction, the 2-molar excess of DMTMM reacted with free or remaining amino lysine groups of the gelatin-based biopolymers would occupy every group. We observed from other functionalisation reactions that the applied molar ratio with respect to remaining amino lysine groups rarely achieves complete occupation (*Table 4.1.*) [52]. Further

ninhydrin assays were carried out on DMTMM chemically crosslinked gel-CT and gel-NAPPCP, however due to the low number of remaining lysine groups, falling outside of the linear region (Chapter 3.3.2.2) the ninhydrin results were inconclusive in determining the exact degree of crosslinking.

Gelation time of gel-CT and gel-NAPPCP was measured in PBS (*Figure 4.4.* and *4.5.* respectively) crosslinking solutions with DMTMM, and repeated 3 times for each sample. In both the control and drug conjugated samples, gelation time occurred in under 30 minutes and in each replicate gel-NAPPCP gelation times were 5 minutes faster than that of the gel-CT times and considerably quicker than some literature states, which may be due to a difference in crosslinker used [324, 325]. The gelation kinetics were repeated at higher volumes (10, 15 and 20 ml total volume) with no effect on the network formation times observed, indicating the size of the hydrogel produced does not hinder the gelation kinetics, which is unsurprising due to the same molar excess of DMTMM crosslinker to free amino lysine groups used, under the same conditions. In the initial crosslinking batch, the crosslinking solution contained, 10mM HCl pH 2.1, compared to future batches consisting of PBS and it was observed that in the presence of acidic conditions the crosslinking time approximately doubled, however this was not recorded due to the change in crosslinking solution. This result is in line with previous research, demonstrating prolonged crosslinking times in acidic conditions [275]. Liang *et al* observed slower gelation times in acidic crosslinking solutions, which is in line with previous work by Ratanavaraporn *et al* (2008) [326]. Native collagen is known to be altered depending on factors such as pH, ionic strength and salt concentrations, due to their effect upon amino acidic terminations (ionisation), as well as their secondary interactions [275, 327-329]. Given that the nature of gelatin is degraded and partially hydrolysed collagen, it is possible that these variations also occur in gelatin, explaining why the differences in gelation times may have been observed between HCl and PBS based crosslinking solutions. The change to PBS solution was made in pursuit of the possible injectable delivery strategy. The decision to use a 2 molar excess of DMTMM with respect to free Lys groups was made as a result of other gelation kinetic experiments, using gelatin-only polymers, aiming at injection as the ideal clinical delivery route. Other molar ratios of DMTMM used were 0.1, 0.5, 1 and 3, the figures for which are not displayed due to the repetition of data. The 0.1 DMTMM molar ratio, failed to form a solid gel, instead appearing as a viscous liquid, due to the partial network formation that likely occurred. The ratios of 0.5 and 1 formed hydrogels however the time taken was considerably longer than that observed in the 2 molar

excess experiments, taking 70 and 45 minutes respectively. Using a 3 molar excess of DMTMM yielded a hydrogel, in the same time as the 2 molar excess for hydrogels (*Figure 4.4.*). As a result of the varying molar ratios of DMTMM, a 2 molar excess was selected as a hydrogel was formed in under 30 minutes which is thought to be a suitable enough time to mix and deliver the Hydrogel-PCP system and allow gelation to occur with minimal disruption to the patient's daily routine.

Unfortunately, gelation kinetics using DMTMM crosslinked gelatin or gelatin-NAPPCP was not possible using a rheometer. Evaporation of the crosslinking solution occurred when attempting gelation kinetics on the rheometer at 37°C, despite countering the humidity. A lower temperature to reduce evaporation was rejected, due to the auto-crosslinking nature of gelatin below 30-35°C, resulting in the reassembly of the triple helical structures [258, 330]. Additionally, a higher temperature than 37°C was not assessed either, due to the increased evaporation that would be observed, as well as the overall delivery of the Hydrogel-PCP system aiming to be an injectable solution, physiological temperatures more relevant than higher temperatures and therefore kinetics were assessed at 37°C in a vial-based assay.

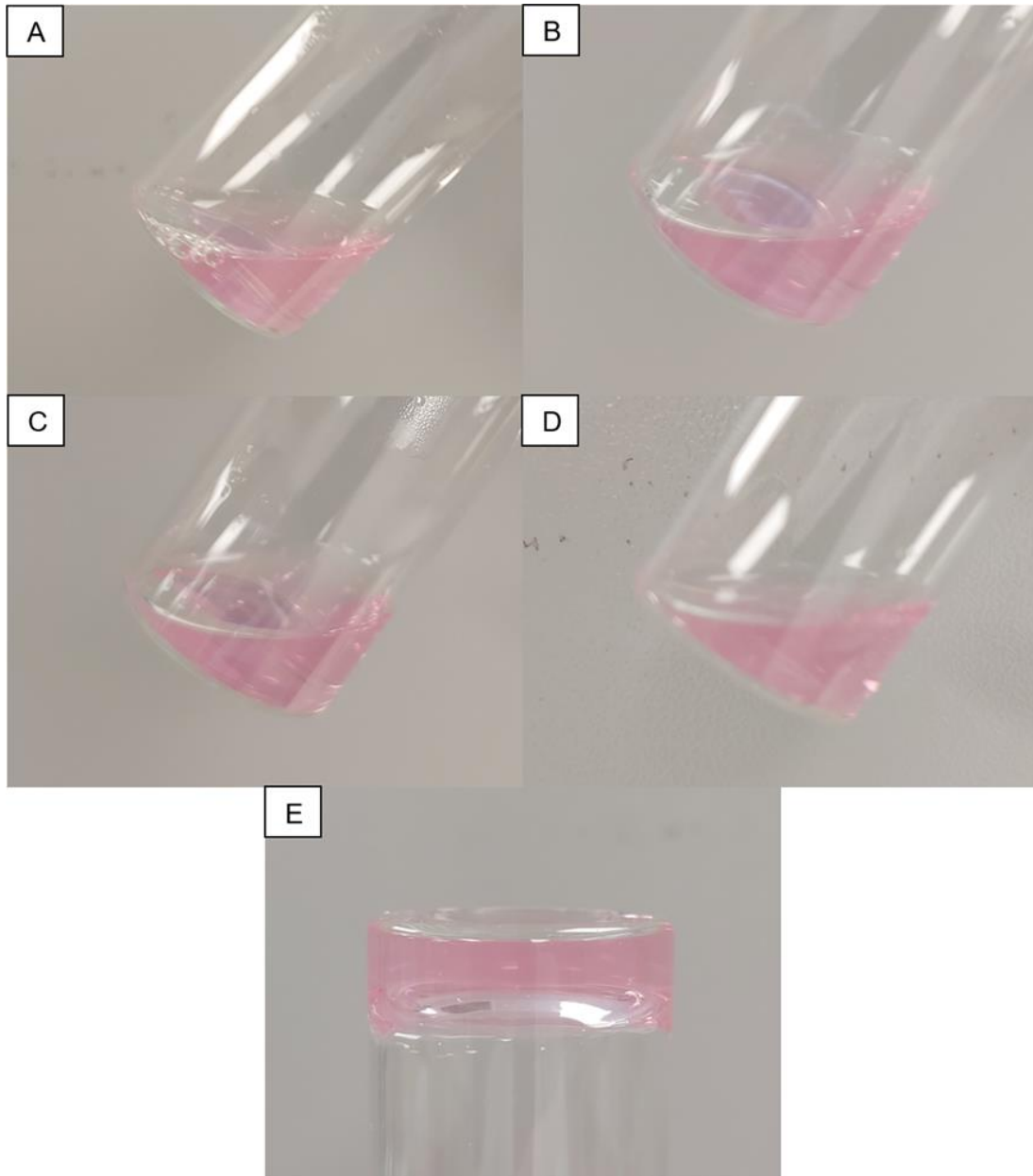


Figure 4.4. Gelation kinetics of chemically crosslinking gel-CT. Mixed with phosphate buffer saline and DMTMM crosslinker at A) 5 minutes B) 10 minutes C) 15 minutes D) 20 minutes and E) 25 minutes after.

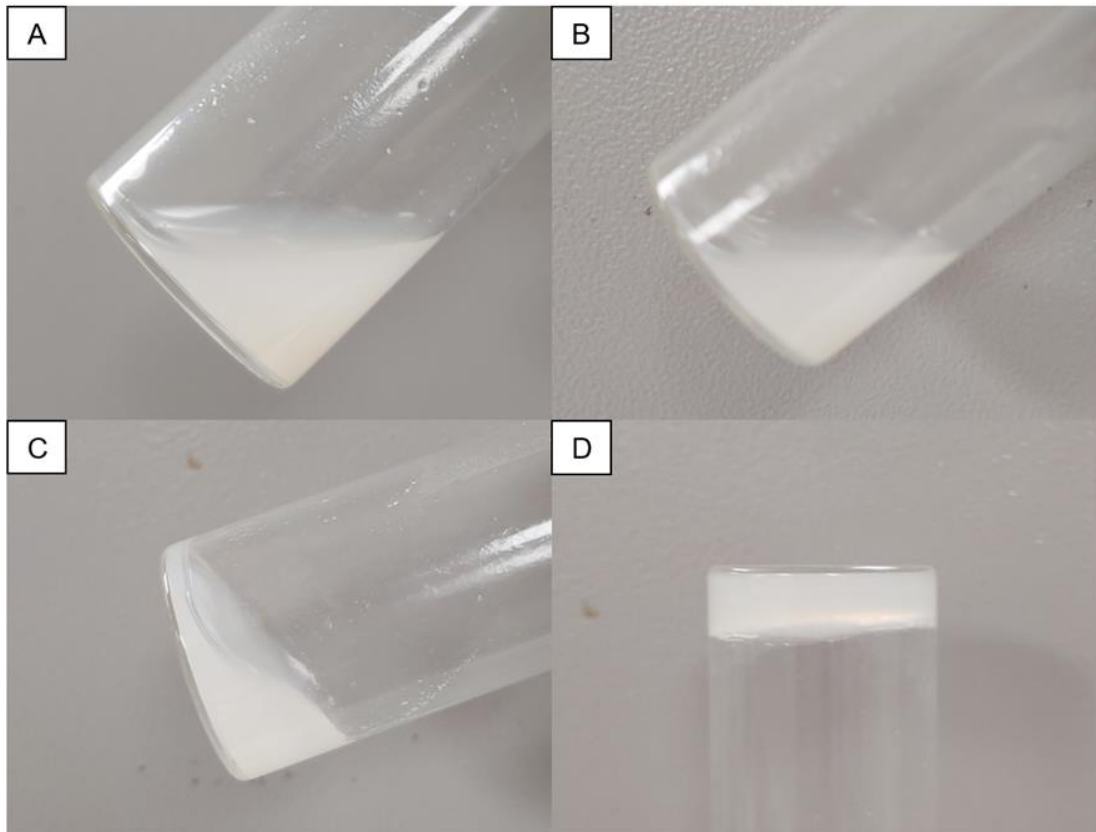


Figure 4.5. Gelation kinetics of chemically crosslinking gel-NAPPCP. Mixed with phosphate buffer saline and DMTMM crosslinker at A) 5 minutes B) 10 minutes C) 15 minutes and D) 20 minutes after.

The decreased crosslinking time of the NAPPCP-conjugated gelatin biopolymer, compared to the control gel, provides stronger support of an injectable delivery method. Additional support for the injectable delivery route is the ability for the system to undergo network formation in physiological conditions. Furthermore, the biodegradable nature of the hydrogel system [331], allows for a simple end to treatment, without the need to invasively remove the hydrogel network. The formation of PCP-conjugated hydrogels, is a crucial step towards obtaining a novel, selective and localised drug release, whilst providing structural support within the targeted disease site.

4.4.3 Assessment of gel content, swelling ratio and rheological properties

Following the quantification of functionalisation degree, the gel content (GC) and swelling ratio (SR) were measured to further assess the structural characteristics of the chemically crosslinked gelatin networks. All chemically crosslinked networks displayed an average gel content above 90% in MMP reaction buffer (*Figure 4.6*). Both the gel-CT and gel-NAPPCP showed high gel contents with minor variations observed between samples, confirming conjugation of NAPPCPP to gelatin had little effect on the GC and resulted in a highly crosslinked network, above the accepted criteria of other studies [275].

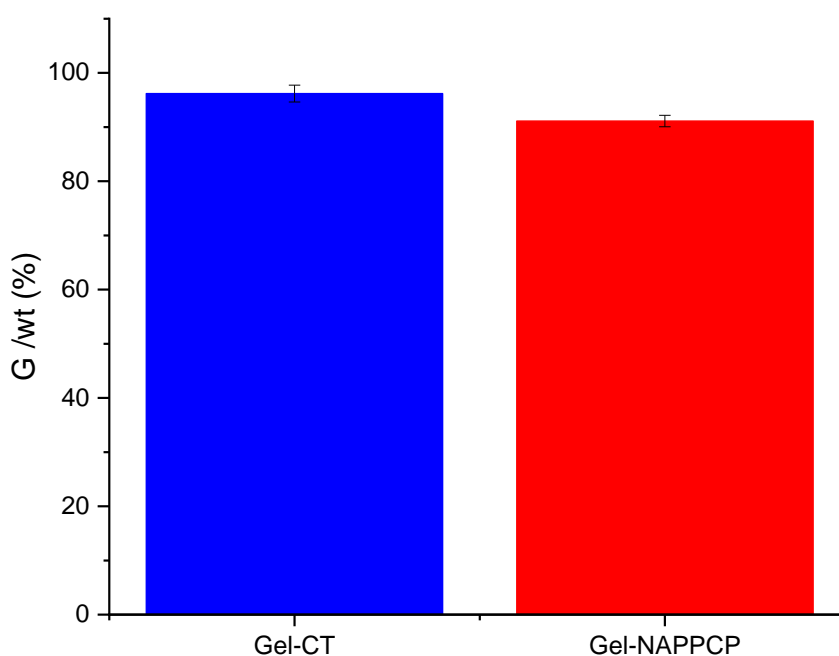


Figure 4.6. Gel content (GC) chemically crosslinked hydrogels. Gel-CT (96.18 ± 1.55 %) and gel-NAPPCP (91.11 ± 1.05 %) hydrogels ($n=4$). A statistical difference ($p<0.05$) between gel-CT and gel-NAPPCP gel contents was observed using a T-test analysis.

To assess other characteristics NAPPCP coupling may have had upon the gel-NAPPCP hydrogel, the swelling ratio (SR) was also determined (*Figure 4.7*). The conjugation of NAPPCP, again showed little variation in SR compared to gel-CT, exhibiting a non-significant decrease in the swelling ratio of gel-NAPPCP. Both

hydrogels on averaged swelled to over 900% (9 times) their dry weight. The evidence suggests that NAPPCCP conjugation to gelatin carries only minor decreases in SR when conjugated to gelatin.

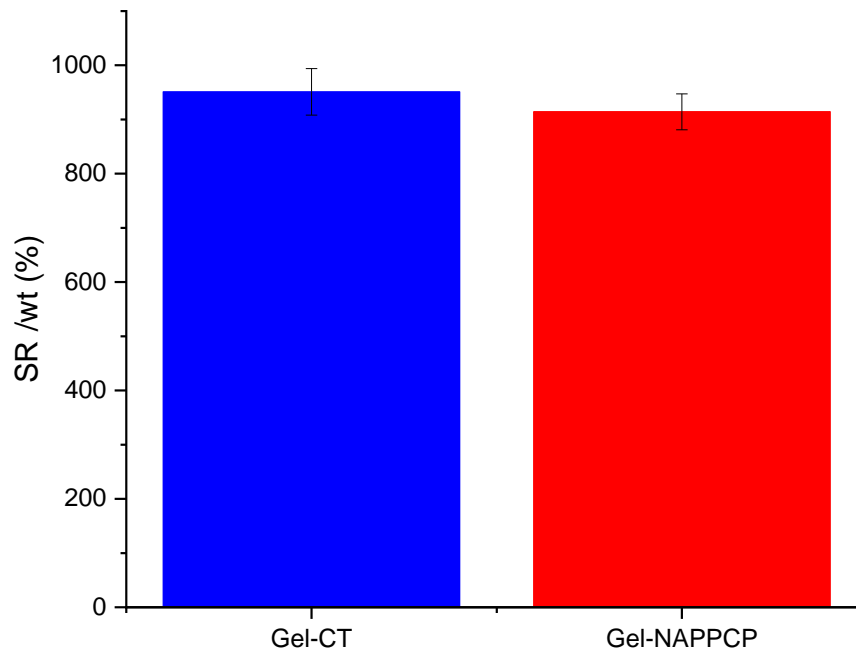


Figure 4.7. Swelling Ratio of chemically crosslinked hydrogels. Gel-CT (950.98 ± 43.02 %) and gel-NAPPCCP (914.19 ± 33.06 %) hydrogels (n=4), using DMTMM as a crosslinking activator. No statistical difference was observed ($p>0.05$) from a T-test statistical analysis, comparing gel-CT and gel-NAPPCCP.

The combination of GC and SR provide evidence, suggesting conjugation of NAPPCCP has little effect on network formation when chemically crosslinked with DMTMM, or the ability of the hydrogel to absorb liquid during the swelling process, at least when conjugated at a 0.2 molar ratio to free amino lysine groups of gelatin. Although the assessment of gel content and swelling ratio demonstrate the retention of network formation and swelling properties in NAPPCCP conjugated hydrogels, it doesn't confirm whether network formation occurred in the same way, for example whether NAPPCCP acted as a linker during the crosslinking process or whether it played no part in the network formation.

To further investigate the potential effects NAPPCCP conjugation has, initial rheological assessments were employed, namely, amplitude and frequency sweeps. Amplitude sweeps were used to assess the percentage shear strain that can be exerted on the gel before minor cracks in the network begin to show, unto the point at which these cracks result in major network damage, ultimately leading to the collapse of the hydrogel network. Gel-CT and gel-NAPPCCP samples were assessed at a constant frequency of $1 \text{ rad}\cdot\text{s}^{-1}$, under increasing shear strain. The loss modulus (G'') linear viscoelastic (LVE) region of gel-CT was found to be between 6 and 30% shear strain (*Figure 4.8.*). Comparing this to the LVE region of gel-NAPPCCP (9-30% shear strain) it can be deduced, gel-NAPPCCP is more resilient at than gel-CT, before the gel network begins to exhibit minor cracks - the beginning of the LVE region. During this time the network remains largely intact, maintaining an overall structure as only a small proportion of bonds in the network rupture, whilst the surrounding network remains intact. The minor cracks described are a result of internal friction during shearing which increases the G'' modulus linearly [332]. In *Figure 4.8.*, G'' is displayed, indicating the loss modulus of the respective hydrogels, as increasing shear strain is exerted upon them. The loss modulus was selected to measure the LVE region, as gels were put under increasing deformation amplitude until the point at which the gels exhibit significant structural damage, causing a plateau of the G'' curve. G' was not displayed due to the presence of large fluctuations between each sample, however, the amplitude sweep was used to determine the percentage shear strain of the LVE region which can be determined from the loss modulus curve. The fluctuations of G' may be a result of the DMTMM crosslinked gelatin gel's consistency and viscosity allowing the gel to flow in response applied shear strain, however this would also be expected to some degree in the loss modulus curve. Further, more in-depth investigations, once confirmation of selective drug release is achieved, are required to investigate the fluctuations observed in the G' curve.

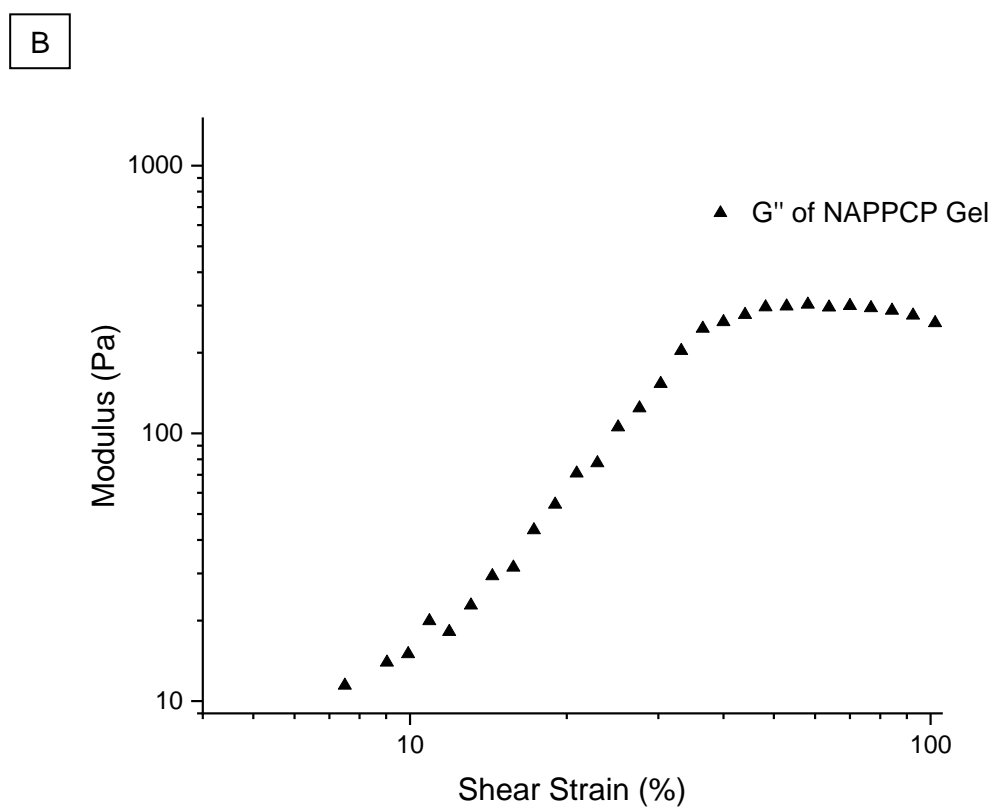
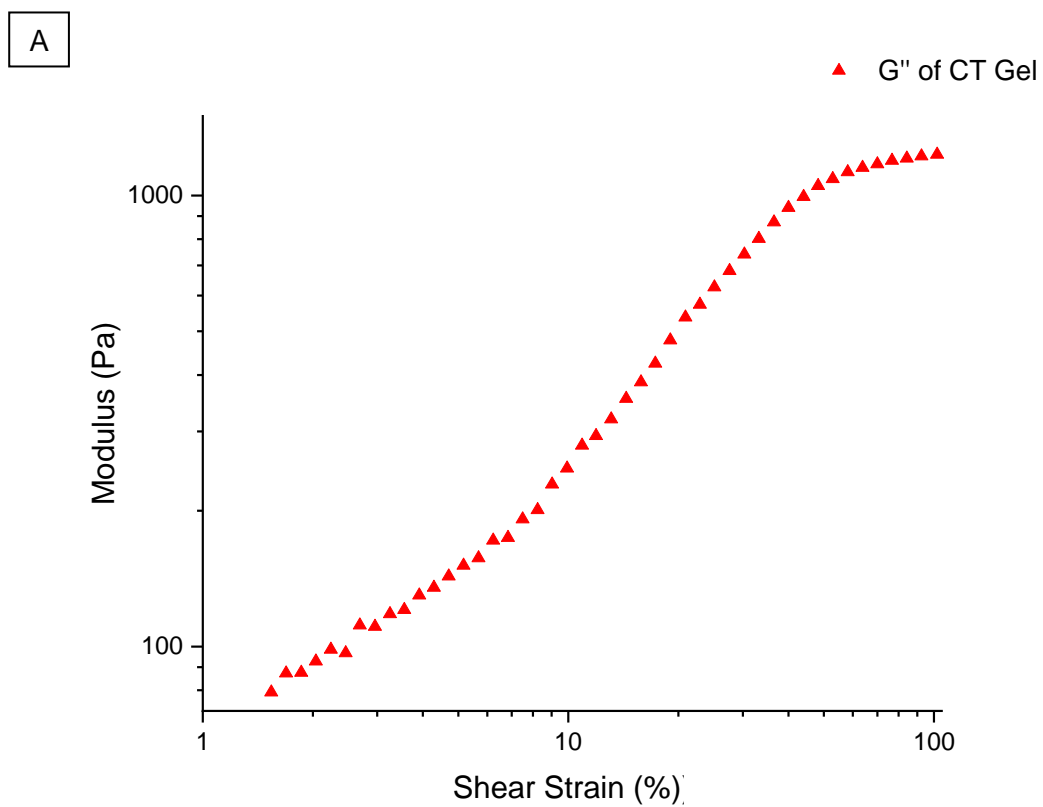


Figure 4.8. Amplitude sweep showing the loss modulus G'' LVE region. A) gel-CT and B) gel-NAPPCP, under constant frequencies of 1 rad-s⁻¹.

Conjugation of NAPP-CP to gelatin appears to strengthen the hydrogel, allowing it to resist greater shear strain force than gelatin control hydrogels before the network begins to break. The G'' plateau, or the end of the LVE region, observed in both hydrogel types occurred at approximately 30% shear strain, at which point it can be assumed that the minor cracks had grown to form a continuous macro crack running through the samples, causing the gel to break and begin to flow, exhibiting total network collapse [333]. Interestingly, although gel-NAPP-CP withstood greater shear strain before beginning to display network breakage, the point at which total network collapse is similar to that of gel-CT suggesting NAPP-CP conjugation only strengthens the gel at lower shear strain force, and network collapse occurs at the same point in both hydrogels.

The frequency sweeps were carried out at a constant shear strain of 10%, within the LVE region of both gel-CT and gel-NAPP-CP, and describes the behaviours of the gels within the non-destructive deformation range in increasing frequencies [334]. At lower frequencies both gel types remained undamaged by the increasing frequency, likely due to the vibrations failing to oscillate through the network, causing it to remain rigid. At approximately $8 \text{ rad}\cdot\text{s}^{-1}$ gel-CT began to crack under the vibrational force leading to a total network collapse around $10.5 \text{ rad}\cdot\text{s}^{-1}$ (*Figure 4.9*). Gel-NAPP-CP remained intact up until $10 \text{ rad}\cdot\text{s}^{-1}$, however once the network began to crack, gel-NAPP-CP broke down rapidly as the total network collapsed at $11 \text{ rad}\cdot\text{s}^{-1}$. The results of the frequency sweeps suggest, similarly to that observed in the amplitude sweep, gel-NAPP-CP is capable of withstanding greater force (vibrational force in frequency sweeps) before the network begins to crack compared to gel-CT. However, the point at which the networks collapse remained approximately equal in each of the hydrogel types, indicating gel-NAPP-CP is more resistant to lower frequencies than gel-CT.

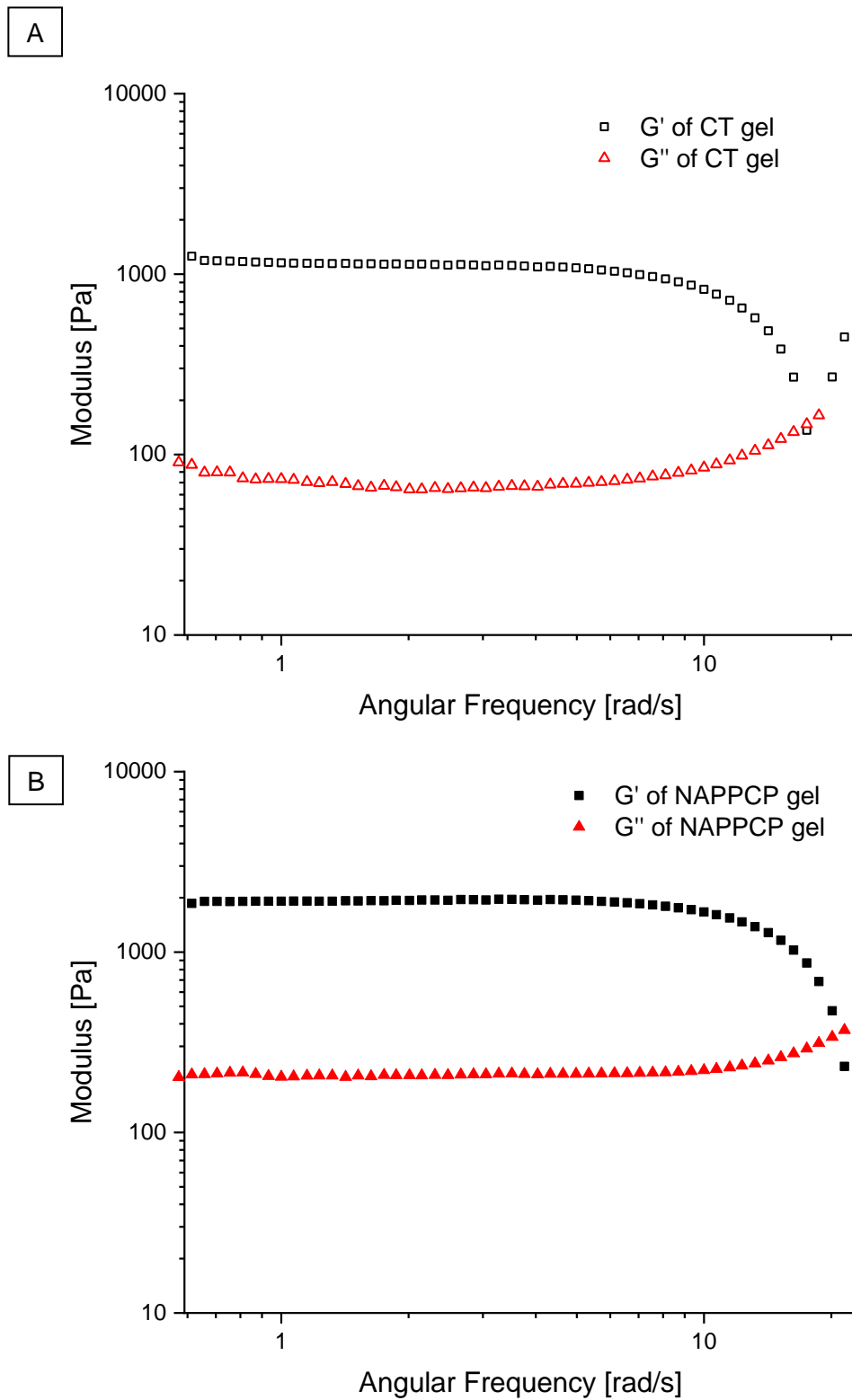


Figure 4.9. Frequency sweep showing storage (G') and loss modulus (G''). A) gel-CT and B) gel-NAPPCP, under a constant shear strain of 10%, a value within the linear viscoelastic region of both gel types.

Overall, the data collected from the gel content, swelling ratio and rheology suggests no negative impact from the conjugation of NAPP-CP to gelatin occurred, for the application the gel-NAPP-CP hydrogel would be intended. Conjugation of NAPP-CP maintains the swelling potential of the hydrogel, allowing it to swell to fill a cavity, as well as the network forming potential, when compared to chemically crosslinked gelatin control gels. Furthermore, although NAPP-CP, fails to enhance the maximum gel strength in relation to shear strain and frequency, NAPP-CP achieves increased resilience to both shear strain and frequencies before initial network cracking occurs. The non-detrimental characteristics of NAPP-CP conjugation provide support for the continuation of research into the novel system. In depth assessments into the unique properties of the hydrogel, will however, be delayed until a proof of concept to confirm drug release is carried out to avoid lost research time. It remains unclear, the role, if any, that NAPP-CP plays in DMTMM induced chemical crosslinking. That said, the minor enhancements observed from the rheological data provide some insight into how functionalisation of biopolymers with PCPs may provide beneficial and unique characteristics in the future.

4.4.4 MMP14 selective recombinant enzyme assay

After the successful network formation of NAPP-CP-conjugated gelatin biopolymers to form, gel-NAPP-CP hydrogels, the drug release capabilities by MMP14 were assessed. As previously discussed, the peptide sequence, donated by the research team at the University of Bradford, UK is selective to MMP14, a matrix metalloproteinase, found overexpressed in multiple diseases due to the key role it plays in a variety of cellular functions [335, 336]. MMP14 is shown to selectively cleave the peptide sequence at the Hof-Gly peptide bond [229]. A recombinant enzyme assay was employed to confirm the release of NAP-based metabolites through the activity of MMP14.

After 72 hours incubation, observational differences were noticeable between the gel-CT and gel-NAPP-CP assay hydrogels (*Figure 4.10*). In the gel-CT gel, the reaction buffer showed no visible deposits, whereas in the gel-NAPP-CP drug gels grey-white specs were visible, indicating initial degradation of the network. In line with the observations, the gel-NAPP-CP hydrogel appeared to have lost structural integrity and had flattened in shape, further indicating the beginning of a collapsed network. It is well known that MMP14 degrades various extracellular matrix components, including fibrillar collagen types I, II, III and gelatin [337], amongst many other

extracellular matrix macromolecules [338]. Gelatin degradation can occur as a result of MMP14 activity, either by direct cleavage or through the activation of other gelatinase MMPs. The 2013 study by Albrechtsen *et al* demonstrated activation of MMP14 in breast cancer resulted in gelatin degradation, reduced apoptosis and increased tumour growth [339]. It was shown that inhibition of MMP14 halts gelatin degradation, demonstrating a direct link between MMP14 and gelatin degradation. Due to the MMP14 cleavage sites of gelatin, as well as MMP14's ability to activate gelatinase MMPs, there was a risk that MMP14 would be more selective towards the gelatin network than the NAPPCCP peptide conjugate. However, the gel-CT appeared to maintain the structural integrity, remaining of similar shape and size as they did prior to the start of the recombinant enzyme assay, indicating MMP14 has little cleavage activity upon the DMTMM crosslinked gel-CT gel.

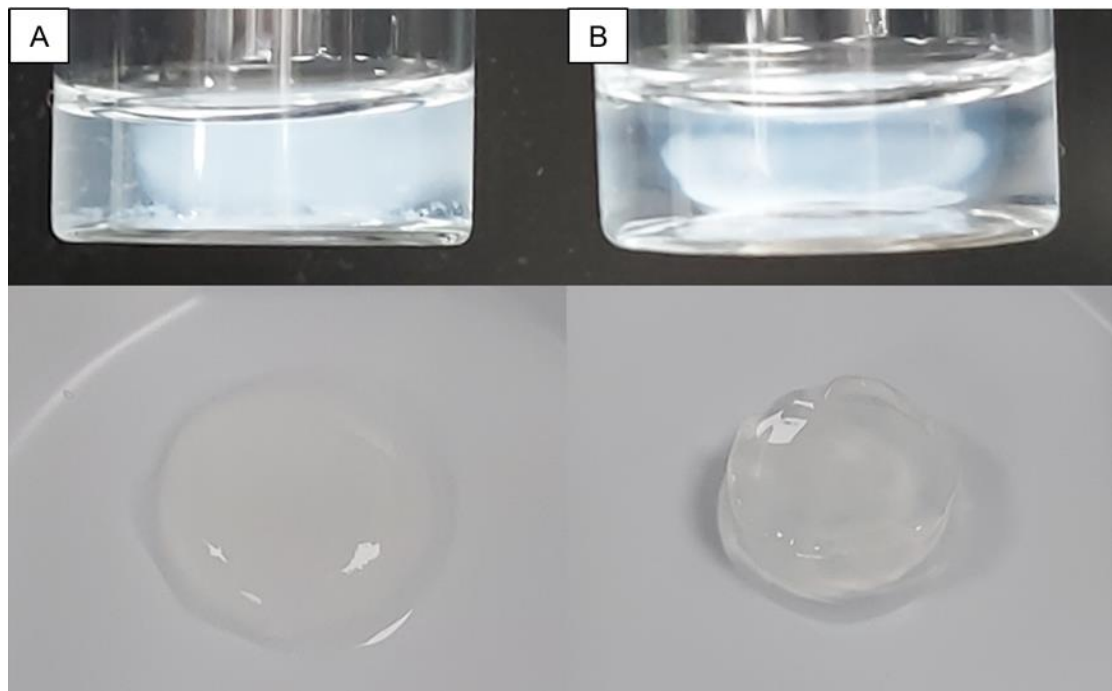


Figure 4.10. Photographic depiction of hydrogels after MMP14 assay. The deposits and sunken appearance of the A) gel-NAPPCCP hydrogel after 72 hours in the presence of recombinant MMP14, compared to the structurally intact B) gel-CT hydrogel.

Initial observations indicated MMP14 more readily attacks the gel-NAPPCP hydrogel, compared to the gel-CT, however why this occurs is unclear due to both hydrogels consisting largely of gelatin. The addition of the NAPPCP to the biopolymer, may alter how network formation occurs, exposing more MMP14 degradation sites on the gelatin backbone. This remains unlikely due to the significantly larger molecular size of gelatin, which can be up to 125 KDa [340] compared to that of NAPPCP at approximately 1.3 KDa, however further investigation would be required to rule this out as intermolecular forces play key roles in biopolymers participating in biological functions such as molecular assembly, self-assembly and the selectivity of enzymes [341].

The collection of deposits from the MMP reaction buffer were dissolved in methanol and analysed by LCMS to identify any drug release that had occurred. The gel-CT, as expected exhibited no naproxen-based metabolites, tracked using the photo diode array at 330nm. The NAPPCP prodrug control sample displayed only one peak at 7.43 minutes, which was later identified using mass spectrometry (MS) as the un-cleaved NAPPCP and unexpectedly no naproxen-based metabolites were detected, suggesting no successful cleavage by MMP14 occurred. In the gel-NAPPCP a small peak around 7.43 minutes was present which is the same elution time as the NAPPCP prodrug. Similarly, at 17.33 minutes a metabolite containing naproxen eluted which was later confirmed, using MS, to be a mass of 384.43 which correlates to the naproxen-arginine metabolites (*Figure 4.11.*).

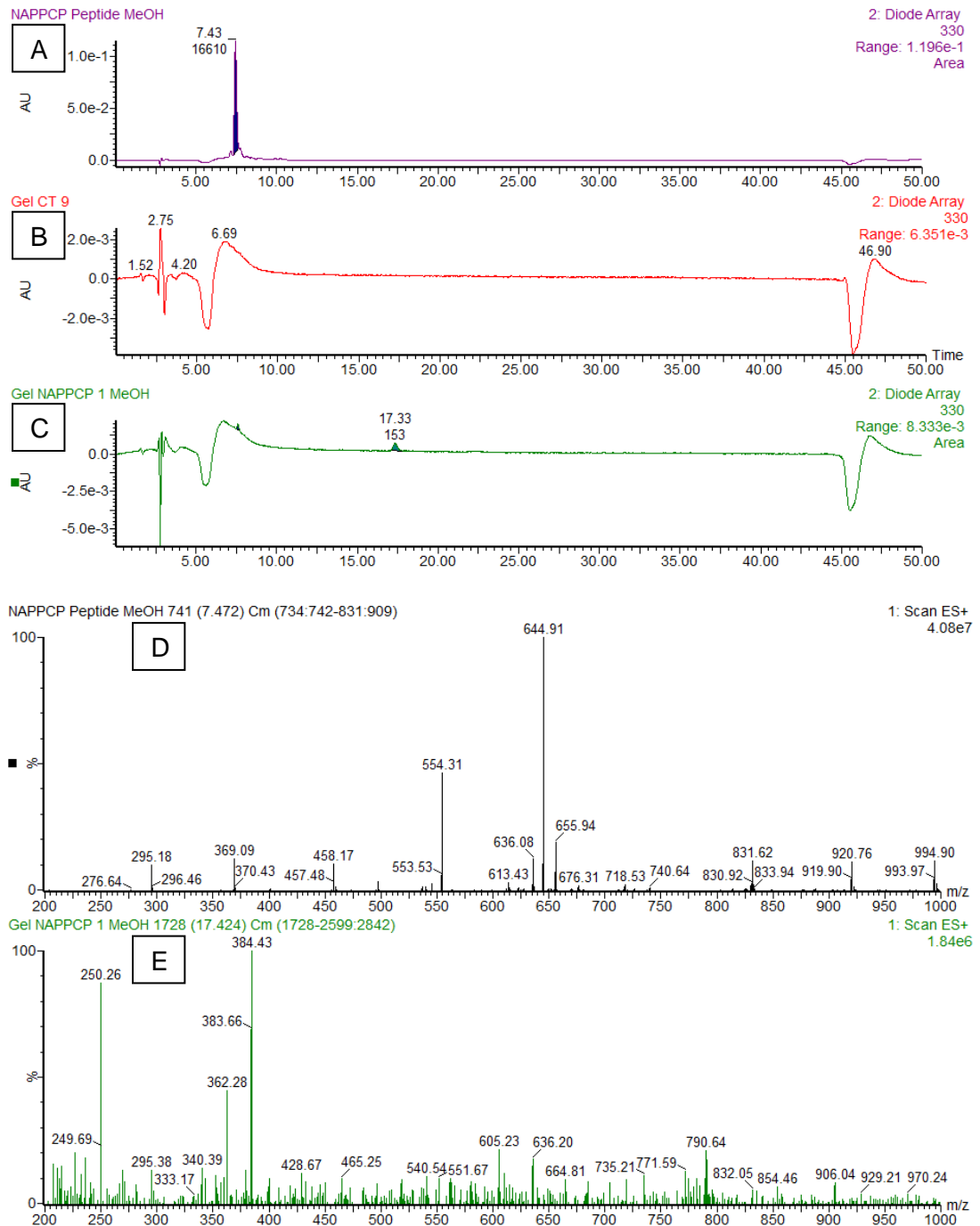


Figure 4.11. LCMS analysis of MMP14 recombinant assay. Tracking the release of naproxen peptide-conjugated prodrug metabolites A) NAPPCP control B) gel-CT control gel and C) gel-NAPPCP gel. Confirmation of key peaks confirmed by Mass Spectrometry D) 7.43 MS of NAPPCP peak shown by MH²⁺ charged mass and E) 17.28 MS of NAPPCP metabolite peak of MH charged mass of NAP-Arg metabolite (384 m/z).

The expected metabolite from the MMP14 recombinant enzyme assay was NAP-Arg-Ser-Cit-Gly which has an MH mass charge of 686.35 m/z. The metabolite observed, NAP-Arg was unexpected and interestingly not observed in the NAPPCP control, suggesting coupling NAPPCP to gelatin may enhance the drug release by means other than MMP14. NAPPCP showed no successful cleavage by MMP14 at the expected scissile bond, as demonstrated by Atkinson *et al* (2010) [103]. This was a possibility, as the conjugated sequence is an MMP14 cleavable sequence for the prodrug known as ICT2588, a vascular disrupting agent with an azademethylcolchicine drug warhead [103] and as discussed, changing a single amino acid or the drug itself can alter the release profile. The substitution of azademethylcolchicine for naproxen and the removal of the Fluorescein Isothiocyanate (FITC) endcap may have prevented NAPPCP cleavage from occurring. Whether the substitution of the drug warhead or removal of the FITC endcap has the stabilising effect (or shielding of the cleavage site to MMP14) is unknown as altering the endcap also has the potential to change the properties of the compound [342]. The removal of the FITC endcap was a necessary step to couple NAPPCP to the gelatin biopolymer, as it lacks a free carboxylic group to couple to the free amino groups of gelatin. One key difference between the NAPPCP and ICT2588 is the position in which the drug warhead is conjugated, in NAPPCP, NAP is coupled to the N-terminus of the peptide conjugate, whereas in ICT2588, azademethylcolchicine is coupled to the C-terminus, which may impact the rate of cleavage by MMP14 (*Figure 4.12.*). The structure of NAPPCP differs from ICT2588, and due to PCPs being 3D structures, it is possible that the expected cleavage site is still recognisable but inaccessible to MMP14 because of the altered structure.

At this time, it is not possible to know which, or to what extent the modifications of ICT2588 to form NAPPCP had upon the MMP14 recognition and proteolytic activity of the Hof-Gly cleavage site. Structural analysis and sequence modifications could enhance the MMP14 activity around the cleavage site in the future to increase the rate of drug release, as even a single amino acid change can drastically alter the recognition by MMP14 [343]. Cleavage may also be possible through an alternative MMP or protease, which could be identified using an *ex vivo* assay or a series of recombinant enzyme assays against a panel of MMPs, which may allow selective release using an alternative proteolytic enzyme target.

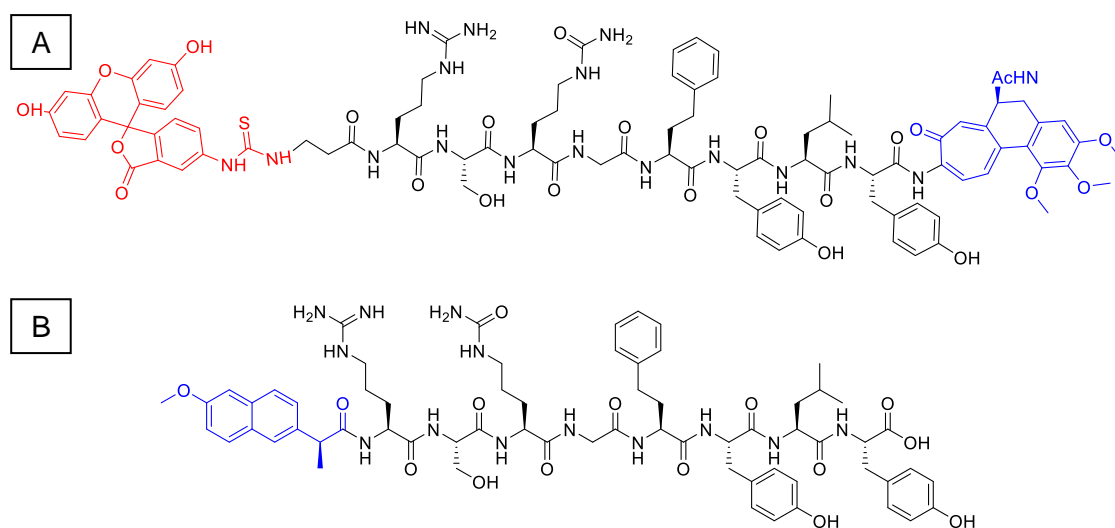


Figure 4.12. Structural differences between A) ICT2588 and B) NAPPCP. Demonstrating the active drug components (blue) are coupled to alternative ends of the peptide conjugate with azademethylcolchicine coupled to the C-terminus and naproxen coupled to the N-terminus. The N-terminus of ICT2588 is occupied by the FITC endcap (red).

The NAP-Arg metabolite, released from gel-NAPPCP, confirms the release of naproxen from the hydrogel network, although this metabolite was unexpected, even more so due to the metabolite being undetectable in the NAPPCP drug control sample. MMP14 may be responsible for the cleavage between Arg and Ser in gel-NAPPCP, but not in the NAPPCP drug control due to a key difference between the two structures; gel-NAPPCP contains the gelatin biopolymer network as an endcap which as previously discussed can alter the release profile of a drug. It was initially hypothesised that NAPPCP conjugation to gelatin, or the crosslinking process, causes a previously inaccessible MMP14 cleavage site to become accessible, however this theory is doubtful because the degradation of gel-NAPPCP and gel-CT hydrogels in 6M HCl (and no MMP14 presence) exhibited the NAP-Arg metabolite in a higher quantity compared to the MMP14 enzyme assay (*Figure 4.13.*).

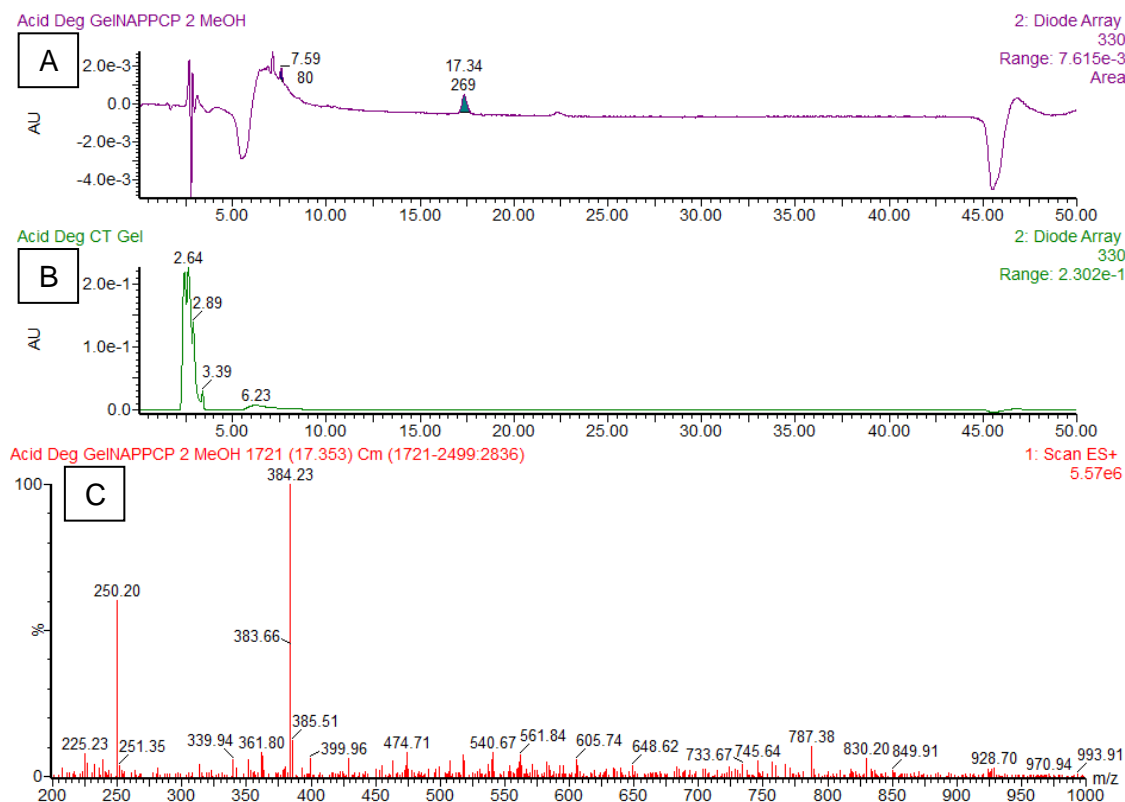


Figure 4.13. Acid degradation analysis using LCMS. A) gel-NAPPCP B) gel-CT and C) using MS to identify the peak located at 17.34 minutes in gel-NAPPCP, identified as NAP-Arg.

The release of the NAP-Arg metabolite observed in both the gel-NAPPCP MMP14 recombinant assay and the acid degradation assay indicate that release of the metabolite from the hydrogel network is unlikely to have occurred through enzymatic cleavage as first thought. The most likely explanation as to why, in both MMP14 recombinant assays carried out (Collagen, Chapter 3.4.5 and Gelatin, here) it appeared no cleavage of the NAPPCP occurred at the known MMP14 cleave site (Hof-Gly) was initially attributed to the inactivity of the supplied MMP14 enzyme itself. This however is ruled out by the delivery of the active MMP14 arriving with confirmation of activity as well as internal investigations of the active enzyme using an ICT2588 variant peptide, donated by the University of Bradford, UK, cleaving at the Hof-Gly cleave site as expected. The spectra of the confirmed cleavage were requested not to be displayed due to ongoing research surrounding variants of the ICT2588 prodrug.

A theory which would support the presence of NAP-Arg in both the MMMP14 recombinant enzyme assay and acid degradation but not in the NAPPCP drug

control, is that conjugation of NAPPCCP to gelatin and/or network formation by DMTMM causes the NAPPCCP component to become unstable and degrade naturally. Testing this theory would be possible through a series of gel content-like assays, on both gel-NAPPCCP biopolymer and gel-NAPPCCP hydrogels, by synthesising and submerging both the biopolymer and hydrogel forms at varying time points after synthesis, in weak acid or ethanol so not to degrade the gelatin, before neutralising and analysing through LCMS to assess changes in NAP-Arg metabolite vs NAPPCCP or NAP-only peaks. If instability of NAPPCCP is affected by conjugation or network formation, it would be expected that increasing quantities of NAP-Arg or NAP-metabolites would be observed as time went on. Due to the lack of cleavage of the NAPPCCP drug itself, resources would be more suited towards optimising the cleavage by MMP14, to continue to develop a selective and localised drug release. The degradation theory however, poses another potential release strategy for the hydrogel network. A greater peak area was observed in the acid degradation of 1.76 times compared to the MMP14 recombinant enzyme assay, indicating acidic conditions further contributes to release of NAP-Arg.

Another, likely possibility is that the conjugation of NAPPCCP, partially hinders the chemical crosslinking process, so that acidic degradation or MMP14 cleavage became more favourable in the gel-NAPPCCP hydrogel compared to the gel-CT, causing the degradation of gelatin. This would account for the increased gel-NAPPCCP debris observed after the MMP14 recombinant assay, as MMP14 would have more accessibility to degrade the gelatin network, releasing NAP-Arg as a result.

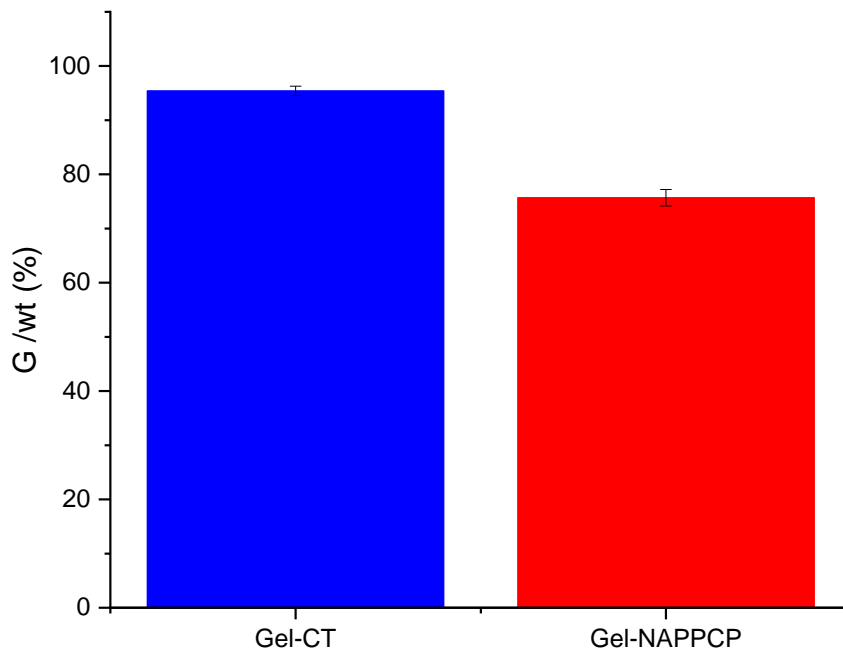
The NAP-Arg metabolite identified may have also occurred as a result of crosslinking in PBS solution, due to the guanidium group of arginine carrying a positive charge under physiological conditions [344, 345] and therefore may readily have reacted with DMTMM activated carboxylic groups on the gelatin biopolymer leading to NAPPCCP acting as a linker within the crosslinking process. Armstrong *et al* (2016) discuss the hydrogen bonding potential between the Arg guanidinium group is satisfied by oxygen hydrogen bond acceptors of the carboxylate (-COO⁻) containing amino acids, which is the same method by which DMTMM activated -COOH groups to enable chemical crosslinking [346]. This would cause NAPPCCP to be conjugated both at the tyrosine end chain -COOH and the arginine guanidium side chain. Drug release would then rely on two cleavage locations on the peptide-conjugate as opposed to one, making this theory less probable, considering MMP14, the only

proteolytic enzyme present in the MMP reaction buffer appears to not cleave NAPPCP at the previously shown cleavage site. Furthermore, if successful cleavage of both sites were to occur, evidence of this would likely be observed in the NAPPCP spectra and would be expected in larger quantities, than that detected in the gel-NAPPCP MMP14 recombinant enzyme assay. The small peak of NAPPCP detected in gel-NAPPCP is likely due to MMP14 degradation of the hydrogel network which appeared to have collapsed under visual observations (*Figure 4.10.*). Alternative, future sequences could exclude the use of Arg to eliminate the possible risk of crosslinking at the Arg guanidium site.

It is possible that, NAPPCP acting as a linker during network formation, may have indirectly caused the observed collapse in the network, if MMP14 attacked the gelatin biopolymer around the NAPPCP linker regions, causing NAPPCP to elute, identified as a small peak of NAPPCP and NAP-Arg, which may occur as a result of natural break down once the sequence is deprotected. The observed network collapse of the gel-NAPPCP hydrogel is further supported by the gel content carried out on the MMP14 recombinant enzyme assay gels (*Figure 4.14.*). No statistical difference was found in the gel content of gel-CT hydrogels before and after the MMP14 recombinant assay, which supports the findings displayed in *Figure 4.10.* demonstrating an intact network. On the other hand, from the observations, the Gel-NAPPCP network appeared to collapse over the 3-day assay and as a result a decrease of 15.42% was observed in gel content, which was found to be statistically significant. The significant reduction in gel content could be a result of the hypothesised steric hinderance of the coupled NAPPCP, preventing total chemical crosslinking by DMTMM, instead catering for a physical crosslinking of the hydrogel. This method has been observed in a study by Yu *et al* (2020) where they overcame polymer low grafting degree of functional groups and steric hinderance by designing a novel hydrogel through non-covalent interactions [347]. It is possible that non-covalent crosslinking of gelatin (which is capable of auto-crosslinking) occurred as a result of inhibited chemical crosslinking because of steric hinderance. Over several days in solution with MMP14 the gel-NAPPCP hydrogel may breakdown due to MMP attack, but also naturally as a result of the weaker non-covalent bonds present, unable to support a swollen structure. This could be investigated by comparing the gel content of auto-crosslinked gelatin hydrogels with DMTMM crosslinked gels, over a several days in solution to assess the changes in GC. The non-significant change observed earlier in the swelling ratios support the theory of steric hinderance. Ordinarily, a more crosslinked hydrogel swells less than a less crosslinked hydrogel

because of a more tightly compact network preventing large amounts of solution from expanding the network. The hydrophobicity of the aromatic rings within the NAPPCP prodrug, may prevent additional swelling by repelling water from the network, thus reducing the swelling ratio [348].

A



B

Gel Type	Before/After Assay	G /wt (%)
Gel-CT	Before	96.18 ± 1.55
Gel-CT	After	95.42 ± 0.86
Gel-NAPPCP	Before	91.11 ± 1.05
Gel-NAPPCP	After	75.69 ± 0.86

Figure 4.14. Gel content carried out on gel-CT and gel-NAPPCP hydrogels. A) after 3-day MMP14 recombinant enzyme assay and B) table exhibiting percentage values of gel content before and after the assay. Statistical analysis between gel-CT and gel-NAPPCP hydrogels before and after were compared using a T-test. No significant difference was observed between the gel-CT hydrogels, however a statistical difference in gel-NAPPCP was observed, between before and after samples.

Gel content in the gel-CT remains consistent with the content observed prior to the MMP14 recombinant enzyme assay, however gel-NAPPCP exhibited a 15.4% decrease in gel content on average, suggesting a sixth of the network had collapsed or being degraded. The decreased gel content confirms the start of network collapse within the gel-NAPPCP hydrogel, however if MMP14 were responsible for this collapse, a more decreased gel content for gel-CT would have been expected, however NAPPCP conjugation may cause MMP14 cleavage sites on the gelatin biopolymer to become more recognisable for cleavage. The network collapse may be due to instability of the NAPPCP prodrug acting as a linker molecule in part, during the crosslinking process. This theory would require further assessment of the structural integrity of the network to confirm the presence of NAPPCP as a partial linker within the gel network, combine with the previously discussed time-dependent stability assessment of the gel-NAPPCP biopolymer and hydrogels. The decrease in gel content following the assay may be attributed to secondary interactions established between the NAPPCP and the gelatin biopolymer and/or other NAPPCP compounds, however future investigations are necessary to confirm which of the theories is correct, if any.

4.4.5 Investigating the clinical delivery route – injectability

Clinically, the advantage of being able safely and effectively deliver therapeutic agents via non-invasive means is crucial when developing a new therapeutic treatment. In some instances, surgery is a necessary feat, for example the implantation of stents, or the removal of a tumour mass that it is too high risk to leave in place and reduce with chemo/radio therapy. However, where possible, the use of surgery as a therapy should be avoided, particularly in drug delivery. If a drug can only be delivered to the site of disease by surgical implantation, the risk of disease site toxicity, through infection significantly increases [349]. Many drugs can be delivered by non-surgical means, including taking drugs orally or by intravenous methods. It is not possible to deliver every therapeutic drug via these methods, as part of, or whole drugs, such as the tail of peptide-conjugated prodrugs would be degraded by stomach acid if taken orally. Similarly, not all drugs can be delivered intravenously, for example, using the NAPPCP or a methotrexate-PCP (MTXPCP) to target osteosarcoma, activation and release is triggered by MMP14 cleavage, which is overexpressed in some off-target healthy regions, due to MMP14 involvement in bone development and regulation [18]. Therefore, intravenously delivering a drug

similar to MTXPCP which has the potential to release the cytotoxic MTX at a high concentration within healthy tissue, away from the osteosarcoma site, from a clinical perspective is not viable. A need for a selective, localised and non-invasive method of drug delivery is clinically appealing for the more complex drug deliveries, as well as those where efficacy can be improved. The hydrogel system established here has the potential to selectively release a drug whilst remaining anchored at the disease site.

There are two obvious delivery strategies for the gel-NAPPCP hydrogel system 1) surgical implantation and 2) network mixture injection. The biodegradable nature of collagen and collagen-derived hydrogels remain stable, as a support network for approximately 7-10 days within the body and therefore initial implantation of a hydrogel system would be suitable as part of a surgical procedure such as removing an osteosarcoma mass. This method however, would not be viable as a long-term therapy because surgery every 7 to 10 days, to provide continued drug release is not possible, due to time it takes for surgical wounds to heal after surgery which would take two to six weeks if implanted during an arthroscopy [350]. Also, the surgical implantation again would not be an effective strategy in diseases that often do not require surgery, including rheumatoid arthritis (RA). The second delivery strategy, the injection of a network mixture, allows for a non-invasive drug delivery system and at a more frequent rate, weekly or fortnightly perhaps, although this would depend on the drug dosage conjugated to the hydrogel. The advantage of an *in situ* network formation enables a straight forward delivery route and due to the consistency of the gelatin-based hydrogel network, being similar to that of cartilage and other connective tissues, structural support could be provided in several diseases including RA, where cartilage degradation occurs and MMP14 overexpression can be observed [351]. The chemically crosslinked nature of the gel-NAPPCP hydrogels, allows network formation to occur under physiological conditions within 20-25 minutes, once mixed with the DMTMM crosslinker. Therefore, the injectable delivery system wouldn't be hindered by long network formation times, relying on the patient resting for prolonged periods of time post-injection to allow gelation to occur. A question to be answered in future research is whether or not the crosslinking reaction is toxic to cells, however DMTMM is shown to be a non-toxic compound [352], and therefore the components involved in crosslinking all possess low levels of toxicity and therefore can be hypothesised that the crosslinking reaction should be safe.

Although shorter gelation times of a hydrogel are an advantage, gelation to fill a cavity or anchor themselves within the disease environment is critical to avoid potential gelation within a healthy tissue environment as this could lead to, no drug release or unwanted off-target toxicity due to the release of the drug within healthy tissues, naturally expressing MMP14. To investigate the anchorage potential of gelation, cavities were created within solid sawbone pieces to replicate femur bone ends, where cartilage degradation would be most prevalent in RA, and network forming mixtures injected into the cavity to gel under physiological conditions. Both gel-CT and gel-NAPPCP network forming mixtures underwent successful chemical crosslinking with DMTMM in sawbone cavity holes (*Figure 4.15.*), however only gel-CT was displayed due to clarity of the newly formed hydrogel sample, as the control was dyed using rhodamine. Both hydrogel types, 25 minutes after cavity injection were able to be stood vertically on end and turned upside (not displayed), remaining intact, anchored within both cavity hole shapes.

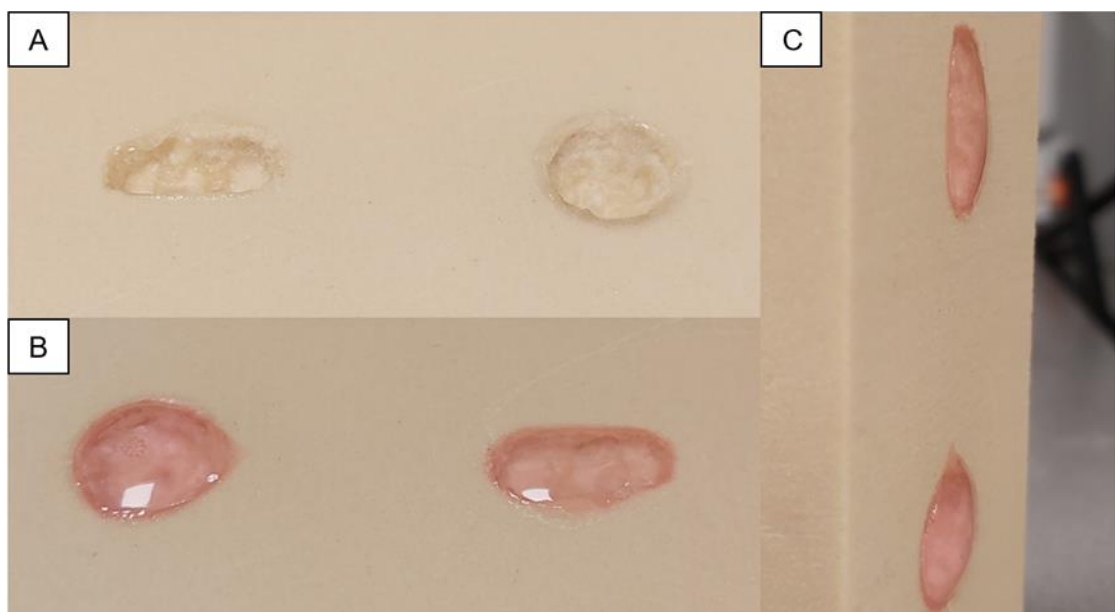


Figure 4.15. Gelation of gelatin-control hydrogels in polyurethane synthetic bone. Crosslinked with DMTMM under physiological conditions A) horizontal image of cavities prior to network forming mixture injection B) horizontal image of cavities 25 minutes post network forming mixture injection and C) vertical image of cavities 25 minutes post network forming mixture injection. Polyurethane synthetic bone (40PCF).

The consistency when handling the hydrogels within the cavities, compared to those conventionally formed in a well plate, appeared the same, as did the anchoring; when turned vertically or upside-down the hydrogels remained firmly anchored in place, with no indication of leaking out of the cavity.

After observing gel anchoring within cavities, anchoring through the sawbone was investigated to give an indication of how gelation might occur within a joint (*Figure 4.16*). Gelation through the sawbone was observed in both the control and NAPP-CP conjugated hydrogels, providing further evidence for the theory of *in situ* network formation to anchor a PCP-conjugated hydrogel within a disease site.

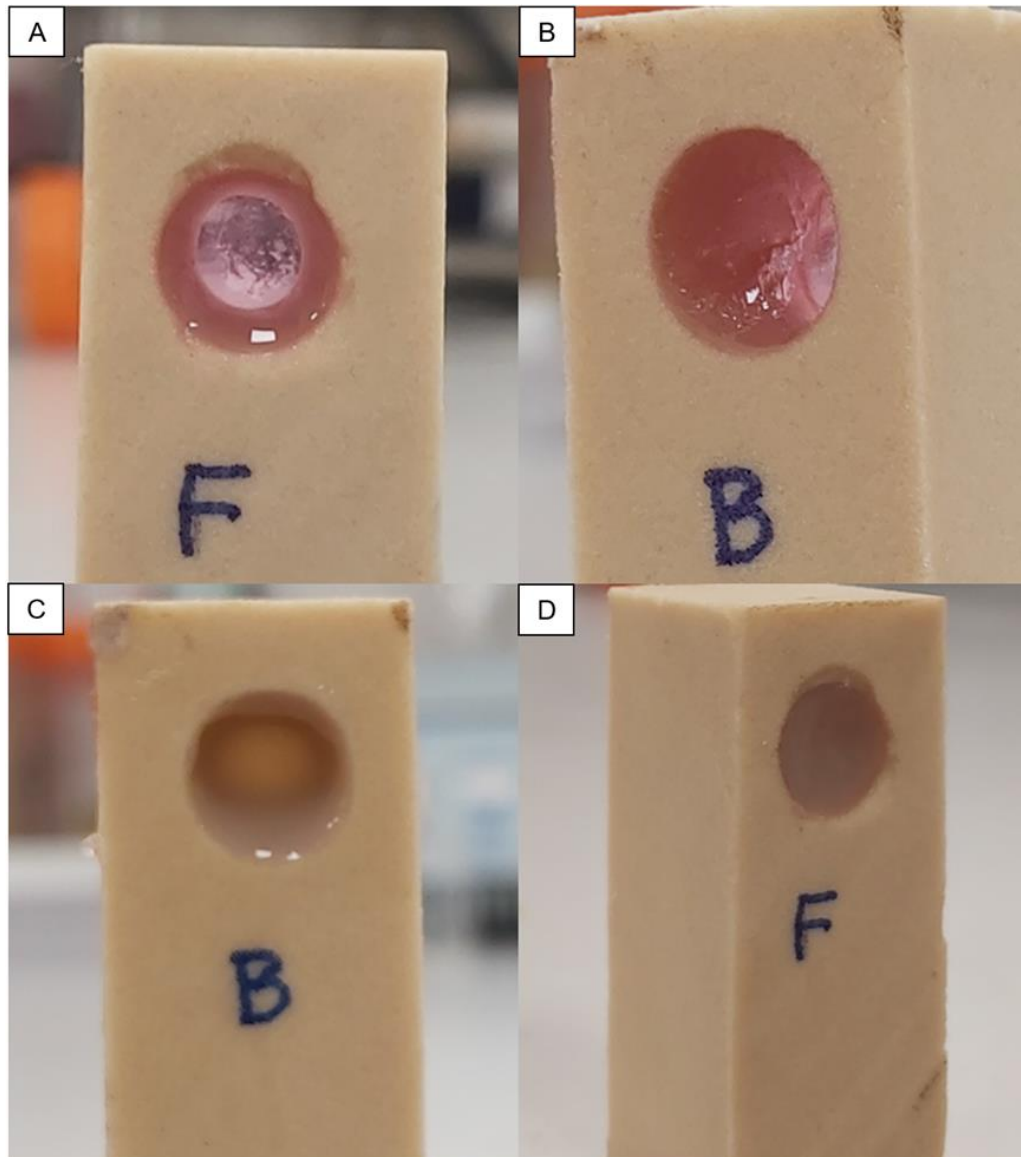


Figure 4.16. Hydrogel gelation through polyurethane synthetic bone tunnel cavity. Gelatin-control A) front-facing B) side profile and gelatin-NAPPCP C) back-facing and D) side profile.

The results demonstrate the clinical delivery potential for an injectable, *in situ* crosslinking hydrogel to provide a selective and localised release of a therapeutic drug to lower the risk of unwanted off-target toxicity within the body. An injectable strategy enables a non-invasive delivery route that is applicable to a broad range of diseases that can be reached by injectable means. The concept of using an injectable hydrogel to anchor a peptide-conjugated prodrug at a disease site and provide structural support where needed, is a novel approach, one that requires further work to confirm the suitability of the delivery approach, with regards to the diversity of the hydrogel anchoring ability in different tissue types.

4.5 Conclusions

Drug delivery can play a major role in the amount of associated off-target toxicity of a therapeutic drug, reduced by controlling the release, activation of a prodrug, or by changing the physical delivery method, i.e. orally or localised injection. Here, successful gel-NAPPCP hydrogels were synthesised using a DMTMM chemical crosslinker, capable of crosslinking in physiological conditions within sawbone cavities. The release of NAP triggered by MMP14, appeared unsuccessful however release of a NAP-Arg metabolite was observed in both the recombinant enzyme and acid degradation assays. Future work is required to develop the selective NAP release triggered by MMP14 cleavage.

Chapter 5
Final Discussions

5.0 Final Discussions

The thesis describes the fusion of two well researched scientific fields, biomaterials and medicinal chemistry to propose the concept of a selective and localised form of drug delivery. Biomaterials design as a research field has shown advances in tissue scaffolding and regenerative medicine in recent years [353-355], whereas medicinal chemistry has demonstrated key alternatives to current therapeutics aiming to reduce toxicity associated with certain disease treatments, leading to improved clinical success [356]. It is therefore unsurprising that the combination of structural tissue support and less toxic therapeutic agents would be desirable and advantageous when treating diseases such as rheumatoid arthritis or osteosarcoma. The study aimed to prove the concept of peptide-conjugated prodrugs coupled to a biopolymer which then undergoes network formation (crosslinking) to produce a hydrogel system with selective means of releasing the drug component.

The initial network formation strategy focused around the UV-induced network formation due to the wealth of knowledge obtained through previous work within the research group into collagen and the 4VBC molecule, not to mention the patent that the University of Leeds, UK currently holds on collagen and collagen derived photo-active functionalised polymers [189]. Although the project focused, initially around collagen and collagen-derived biopolymers (4VBC functionalised and UV crosslinked) which were in used studies as previous work [52, 275], this project differed, as it took the previously characterised collagen-derived biopolymers and applied them towards using them as therapeutic drug delivery systems whilst incorporating a novel peptide-conjugated prodrug. The novelty of the system described here, sheds new light on the therapeutic stalemate RA and OS have seen in recent years and aims to bring forward new therapies which provide tissue support in the form of a selective drug release hydrogel system.

The results showed that collagen and gelatin biopolymers, when sequentially coupled to a drug and the photo-active molecule, 4-vinylbenzyl chloride (4VBC), do not lead to network formation, by UV crosslinking. It is hypothesised that this is due to molecular shielding (prodrug-induced steric hinderance), preventing the combination of free radical-propagation chains of the 4VBC-functionalised biopolymer. The method of UV crosslinking would have been a desirable system, allowing for efficient curing methods, whilst including the possibility to cure *in situ* whilst implanting the system, allows for an enhanced variety of cavities or areas to be filled prior to curing, enabling increased delivery accuracy compared to injectable

methods. Injectable methods, as previously discussed have more significant advantages including minimally invasiveness and reduced risk of infection. The advantage of using a peptide-conjugated prodrug (PCP) is that it could be applied to any disease, overexpressing a proteolytic enzyme, with changes to the peptide-conjugated sequence made to make it selectively recognisable by the new target enzyme [357]. This allows for a wide variety of different diseases to be targeted, drugs that can be administered and polymer materials that can be used, which all together provide a unique and tailored therapeutic approach to many disease conditions.

After the unexpected inability to form a PCP-conjugated hydrogel system, the encapsulation of col-NAPPCP within a crosslinked network of col4VBC25 was carried out and successful network formation was accomplished following UV irradiation. However, it appeared that the col-NAPPCP molecules impregnated in the 4VBC-functionalised collagen network diffused out of the system following sample incubation in aqueous environment. This was confirmed when complete acid degradation of the col4VBC25encap-NAPPCP showed no naproxen-based peaks during HPLC analysis.

The change in strategy from a photo-crosslinked Hydrogel-PCP system to a chemically crosslinked system was therefore employed in light of the potential prodrug-induced steric hinderance effect during UV irradiation preventing combination of free radical propagating chains and successful biopolymer network formation. By chemically crosslinking the biomaterial, the use of a photo-active molecule was no longer necessary, allowing NAPPCP to be conjugated directly onto a biomaterial as the suspected steric shielding was no longer present. Gelatin was deployed as the frontline material to synthesis a Hydrogel-PCP system from, using the chemical crosslinker DMTMM, due to the increased ease of functionalisation discussed previously. The successful conjugation of NAPPCP to gelatin was confirmed using a ninhydrin assay prior to network formation. The success of network formation under physiological temperatures, accomplished the key objective for the proof of concept study by synthesising a Hydrogel-PCP system that was capable of undergoing network formation in physiological conditions. Further, initial investigative assessments were carried out, including gel content and swelling ratio as well as rheology, comparing the gel-NAPPCP with a gelatin control gel. The results of the hydrogel properties investigated, displayed no significant detrimental effects from the coupling of NAPPCP to gelatin, further supporting the suggestion of a Hydrogel-PCP

system. The decision to carry out rheology and other investigative experiments on the chemically crosslinked systems and not the UV-crosslinked systems was due to resources available at the time of each development. The collagen-based UV-crosslinked systems produced finite quantities of conjugated PCP systems, of which the MMP14 enzyme assay was deemed more crucial to assess over the investigative experimental work. The MMP14 assay was a critical step in the aims of the study, demonstrating the release of NAP from the hydrogel system. If the collagen-based systems had demonstrated drug release from the hydrogels, a larger quantity of drug-conjugated biopolymer would have been synthesised to allow further investigative work to be carried out. The lack of drug release from collagen systems at a crucial stage in the research project favoured the change in crosslinking method, to establish a Hydrogel-PCP system, as opposed to carrying out characterisation of a hydrogel system which would require further modifications, likely altering the characteristics which would have already been investigated, thus using up the finite resources at hand.

Following the investigative analysis, drug release was assessed in an MMP14 recombinant enzyme assay. No cleavage between the Hof-Gly site was detected using LCMS, however a NAP-Arg metabolite was released from the structure. It is unlikely that MMP14 is responsible for the release of NAP-Arg, as the NAPP-CP-only control did not produce the NAP-Arg metabolite, however conjugation to gelatin may allow MMP14 to target the Arg-Ser site. Although the attempt to confirm drug release through MMP14 cleavage, appeared to fail, the overall results of the project are promising as the peptide-conjugate sequence is known to be cleaved by MMP14 [229], therefore suggesting that slight alterations to the peptide sequence are required to accommodate the change in active drug used. Furthermore, acidic conditions appeared to display larger quantities of the NAP-Arg metabolite, suggesting potential for an alternative selective release strategy, triggered in response to a decrease in pH [358, 359].

Another key aspect of the project was the establishment of a delivery strategy for the proposed Hydrogel-PCP system to address the needs of RA and OS, whilst being as minimally invasive as possible. Many well researched diseases already have established therapeutic treatments to cure them, however therapies for more complex diseases such as RA, focus around managing the disease. Some, but not all of these therapeutic treatments could be further enhanced by either: alternative

drug delivery routes or the alteration of the treatment compound to reduce the chance of unwanted off-target toxicity, for example using a prodrug. Osteosarcoma and rheumatoid arthritis are two complex diseases requiring clinical intervention to improve the therapeutic index of current treatments.

The development and approval of any new treatment must be clinically viable, a treatment is null and void if significant systemic toxicity is associated or the therapeutic cannot be delivered effectively [360]. Cytotoxic or chemotherapeutic drugs in particular, are therapeutic agents where reducing off-target toxicity is crucial [361]. This can be achieved by reducing the administered dose, which may result in a less effective treatment, limiting the spread of the therapy, either by anchoring it at the treatment site or making the treatment more selective [98, 362]. Another area to consider is the delivery strategy, even the most effective treatments won't gain approval if the clinical delivery route is not viable and safe.

Here, the proof of concept study addressed the key areas which oppose a new therapeutic strategy by combining several research fields to suggest the release of a selective therapeutic prodrug, anchored at the disease site by a tissue support structure, delivered by injectable means, negating the need to surgically implant the device. No proof of concept study of this nature produces a finalised therapeutic product, however, the progress made here paves the way for future studies to adapt and fine-tune the novel Hydrogel-PCP concept to produce an effective therapeutic system.

The particular concept in this study demonstrated its' clinical potential by being able to temporarily disable the active drug through conjugation of a peptide sequence, as well as being injectable as part of an *in situ* forming tissue scaffold. Furthermore, by bypassing the oral administration of naproxen, off-target toxicity, peptic ulceration - a common side effect of prolonged NSAID treatments, may be avoidable. The drug release profiling, requires further work, however the initial aims as well as a delivery route have been achieved. Overall, the described study lays the foundations for future work across a vast variety of diseases, through the alteration of a peptide-conjugate sequence, to target and exploit the overexpression of proteolytic enzymes within the disease.

As the study developed the versatility of the system was further highlighted, demonstrating the potential to incorporate the system into several future study designs, not only using PCPs but to investigate other selective release methods such as in pH responsive, but also, using a peptide-conjugate as an anchoring chain to

the hydrogel. This diversifies the variety of diseases that could be targeted using a Hydrogel-PCP system. The research focussed heavily around meeting the clinical needs of OS and RA, as both diseases require updated therapeutic treatments. Osteosarcoma, in the form of more targeted treatments displaying reduced off-target toxicity and reduced patient side-effects. Whereas RA requires a localised and selective drug delivery within a structural support network, reducing the risk of bone erosion. Both of these disease treatments are possible through the use of a hydrogel as a drug delivery vehicle, administered by injection to meet another desirable clinical attribute, reducing the need for invasive procedures to deliver a therapeutic treatment.

A concept with desirable clinical attributes, such as reducing the associated off-target toxicity, providing a non-invasive delivery or the provision of a tissue support structure are favourable treatment methods [363]. The combination of these attributes makes the discussed study a clinically advantageous strategy to reduce off-target toxicity when treating rheumatoid arthritis and osteosarcoma in the future.

Chapter 6
Conclusions

6.0 Conclusions

The project described here has demonstrated a need for new research into the therapeutic targeting of rheumatoid arthritis and osteosarcoma, to break the deadlock of currently used, outdated therapies. The outlining of new knowledge brought forward through the development of novel drug delivery system to kick start a resurgence in RA and OS therapeutics, was achieved following research objectives, described in Chapter 1.1. Key objectives met included:

- *The establishment of a novel Hydrogel-PCP system
Synthesis of the Hydrogel-PCP system is the first system to our knowledge to conjugate PCP to a biopolymer prior to network formation.*
- *The use of DMTMM as a chemical crosslinker
Traditionally, the carbodiimide, EDC alongside NHS, has been used in the activation of carboxylic acid groups and chemical crosslinking. The emerging use of DMTMM in literature has been strengthened here, demonstrating itself as a substantial alternative to EDC/NHS.*
- *A substantial and credible delivery strategy for the newly synthesised Hydrogel-PCP system
The establishment of a minimally invasive, injectable device, which is capable of in situ network formation under physiological temperatures, looks to overcome the complications of surgical implantation, which was originally proposed as a delivery strategy at the beginning of the research project.*

Peptide-conjugated prodrugs have become advantageous drug delivery compounds, which have demonstrated a selective release and a much-reduced risk of drug associated off-target toxicity. A key example of this would be ICT2588, demonstrating no significant off-target cardiotoxicity *in vivo* [229]. The use of a hydrogel to deliver and anchor a PCP in place at a disease site, was proposed here and is thought to further enhance the PCP drug release whilst providing a structural tissue support.

Here, the key objective of the project, to synthesis a novel Hydrogel-PCP system was established, through chemically crosslinking a collagen-derived

hydrogel, after exhausting crosslinking capabilities in the UV-induced Hydrogel-PCP systems. Aiming to the use of a Hydrogel-PCP system, identification of a clinically desirable delivery route was another significantly important objective. The establishment of an injectable Hydrogel-PCP system, capable of crosslinking under physiological temperatures, which provides a novel drug delivery system with a targeted and minimally invasive delivery route, whilst crosslinking to provide structural support, is possibly the most exciting result of this study, open up several future directions of work to expand knowledge within the research field.

Further investigations are required to define the ideal peptide sequence and release mechanism of NAPP-CP (Chapter 7), however, the concept of developing an *in situ* forming Hydrogel-PCP system has been demonstrated as well as initial investigations into the properties and clinical delivery routes.

In all, the study provides insights into the design of a novel concept to provide, localised and selective drug delivery using a tissue support network as an anchor for the drug, which in theory can be applied to the treatment of any disease, not only rheumatoid arthritis and osteosarcoma, but indeed any disease overexpressing a proteolytic enzyme such as MMP14.

Chapter 7
Future Works

7.0 Future works

The proof of concept study, discussed here provides a strategy foundation for several therapeutic directions involving the use of DMTMM-crosslinked gelatin hydrogel systems. In this sub-chapter the individual directions will be outlined to provide a base from which future work can be carried out.

5.3.1 Peptide-conjugated prodrug functionalised gelatin hydrogels

The most obvious of the future strategies is the continuation of a Hydrogel-PCP system research using a proteolytic enzyme to trigger drug release. The alterations made to the ICT2588 sequence to accommodate synthesis of the gelatin-NAPPCP system led to the stabilisation of the prodrug in regards to MMP14 cleavage. The stabilised condition can be altered to produce a more cleavable peptide-conjugate by adjusting the peptide sequence [364], allowing for increased NAP metabolite release due to MMP14 activity. The establishment of an MMP14 cleavable NAPPCP would allow for a selective release within a disease, increasing the therapeutic index, by reduction of off-target toxicity [365]. Substitution of a single amino acid can cause significant effects on the rate of drug release as previously seen in MTX-PCPs. Previous work, demonstrated the substitution of β -Ala for Cit causes the rate of drug release to increase across all three assessed tissues which is an undesirable trait in healthy tissues, such as the liver and kidneys [21]. A balance between effective drug release in diseased tissues and the degree of off-target toxicity caused to healthy tissues must be established, with the degree of off-target toxicity being lower than that of existing therapeutic treatments in order to be clinically desirable.

The design of future Hydrogel-PCP systems of the concept described here, requires a careful and systematic approach, using the basis of ICT2588's peptide sequence as a starting point. Initial work, removing the hydrogel component of the system may be useful to establish a peptide-conjugate sequence that when coupled to naproxen is selectively released by MMP14. This would confirm whether the sequence, when conjugated to the hydrogel is unrecognisable due to the hydrogel and not the change in drug component to the sequence, reducing the amount of resources lost. Batches of PCP sequences containing single changes could be simultaneously synthesised using the SyroXP fully automated peptide synthesiser, used here.

After successful synthesis and purification, if required, release assessments will be carried out either through an MMP14 recombinant assay or an ex vivo assay using homogenised tissue with an overexpression of MMP14. Both assays have advantages over the other. The recombinant assay demonstrates MMP14 is capable of cleaving the peptide sequence releasing a drug metabolite, which in the body would be deprotected and open to metabolism, leading to the release of the active drug. Selectivity of MMP14 could be determined by follow-up recombinant enzyme assays using alternative MMPs. The ex vivo assay would assess release in a tissue environment, and could be carried out in a variety of tissues, both healthy and diseased to indicate the drug release profile and potential associated toxicity of the NAPP-PCP. The analysis of both assays could be carried out using LCMS and the drug, half-life calculated. The biological assay, as a suggestion would be used initially to determine peptide cleavage and drug release to efficiently identify the more successful PCP release sequences before confirming which expressed MMP carries out the initial cleavage – likely to be MMP14 due to the modified ICT2588 sequence. If an alternative MMP was identified for the initial cleavage then diseases overexpressing the newly identified protease could be investigated further to establish a therapeutic treatment.

With regards to the sequence modifications from the ICT2588 sequence, Arg would be an ideal starting point to substitute for an alternative amino acid, due to the previously discussed guanidinium group of arginine, which would remove the risk of the PCP acting as a linker molecule during hydrogel network formation. The successful NAPP-PCP sequences would then be coupled to gelatin and chemically crosslinked to form a hydrogel before reassessing the drug release assays to compare the changes, if any to the drug release. Should drug-release remain unchanged the following steps would involve the hydrogel characterisation, including but not limited to, techniques such as rheology, swelling ratio and gel content. Ordinarily, assessments of hydrogel properties are carried out prior to the drug release assays, shown here, however due to the results and nature of the Hydrogel-PCP system the logical route is to assess drug release first. If drug release from the Hydrogel-PCP system was not possible then there would be no reason to carry out hydrogel characterisation as the PCP sequence would require further modifications which could affect the hydrogel properties.

5.3.2 Acidic release investigation

As the results of this study confirmed, a drug metabolite, NAP-Arg was released in more acidic conditions. Although the method of drug release appears to be in response to pH changes, further investigations are required to confirm this. Changes in the pH can trigger drug release [366], due to the changing of molecular charges. Investigations into the effect pH changes have on drug release from the gel-NAPPCP system could allow for a new range of applications to be explored, including wound healing. Furthermore, further investigations into the structure of gel-NAPPCP may provide insight into the discussed theories surrounding the role NAPPCP plays, if any, during network formation. Minor alterations to the peptide sequence could enhance the pH-selective release of NAP, should confirmation of pH-sensitive drug release be confirmed.

Exposure of equal mass gel-CT and gel-NAPPCP hydrogels to varying pH levels across a range of time points, incubated at 37°C, prior to neutralisation and analysis, using LCMS to measure the release of NAP metabolites, would confirm the optimal pH for drug release. The effects of alkaline conditions may also be assessed in this manner as NAP metabolites may also be released in alkaline conditions.

Should a pH induced drug release be proven, the system may be deployed in an *in vitro* or *in vivo* model to further assess the drug release and provide an idea of the degree of off-target toxicity associated with this form of drug delivery. Comparisons between current NAP treatments and the hypothesised pH-induced NAP release could be made in *in vivo* models to determine whether the pH-induced release strategy is more beneficial, clinically, than current NAP treatments.

5.3.3 Clinical device developmental investigations

The third direction of future research, is the development of the clinical delivery device – the injectable, *in situ* crosslinking Hydrogel-PCP system. Here, we have shown the initial steps towards an injectable system by demonstrating that network formation is possible under physiological conditions using a networking solution of phosphate buffer saline, dissolved gel-NAPPCP and DMTMM, as well as injecting it within sawbone to visualise and depict the gelling capability within a bone cavity or between two bones. Future research could expand on the progress made here, using bovine bone and drilling a series of different cavities to assess gelation in a more dynamic range of cavity sizes, whilst assessing gelation in other solution

types to optimise gelation times and strength, as the use of a gelation solution may affect the strength of the networked hydrogel. Once assessment of *in situ* gelation from an injectable hydrogel solution has been made *ex vivo* bone, the investigation could be carried out *in vivo* by injecting a series of hydrogel solutions into cavities to assess gelation within the model, however this would likely only be at a stage when the drug release strategy was ready for *in vivo* assessments too.

The investigation into the development of a clinical device is future work which would be suitable alongside one of the other two described research directions as there is little need to assess the delivery without a means of releasing the therapeutic treatment once established within the model.

5.3.4 Peptide-conjugated photo-crosslinked hydrogels

Future work may also involve the investigations into the failings of the photo-crosslinking strategy to gain further insight into why the dual functionalisation of collagen with 4VBC and NAPPCP led to an inhibition of network formation. Furthermore, the theory of how the encapsulated col-NAPPCP yielded no drug after complete acid degradation of the encapsulating hydrogel still remains unanswered.

It may be that dual functionalisation with a photo-active molecule that doesn't contain an aromatic ring such as methacrylate (MA) [54] may be a sufficient enough change to allow network formation to occur under UV light, however it is likely that due to the suspected steric effects and UV effects on certain amino acids as previously described, a complete resequencing of the PCP sequence may be required to enable photo-crosslinking capabilities.

Steric shielding could be investigated using solvent accessible surface area analysis [367] and has been used to determine the effect of steric shielding on another popular biopolymer, polyethylene glycol (PEG) by Mu *et al* [368]. This could be applied in future works to investigate and confirm the role steric shielding may have played in the prevention of network formation through photo-crosslinking methods.

If photo-crosslinking can be achieved, to form a Hydrogel-PCP system, similar steps to the 'Peptide-Conjugated Prodrug Functionalised Gelatin Hydrogels' direction could be carried out produce an implantable clinical delivery route for applications such as dentistry. Photo-crosslinking is possible under visible light and has gained

much attention in recent years [262] and may be of greater use than a chemically crosslinked hydrogel in certain applications, however investigations would be required to confirm this.

6.0 References

1. Messerschmitt, P.J., et al., *Osteosarcoma*. JAAOS - Journal of the American Academy of Orthopaedic Surgeons, 2009. **17**(8).
2. Trieb, K., *Treatment of the Wrist in Rheumatoid Arthritis*. The Journal of Hand Surgery, 2008. **33**(1): p. 113-123.
3. Schiff, M.H. and A. Whelton, *Renal toxicity associated with disease-modifying antirheumatic drugs used for the treatment of rheumatoid arthritis*. Seminars in Arthritis and Rheumatism, 2000. **30**(3): p. 196-208.
4. Kundu, P., S. Das, and N. Chattopadhyay, *Managing efficacy and toxicity of drugs: Targeted delivery and excretion*. International Journal of Pharmaceutics, 2019. **565**: p. 378-390.
5. Ashton, S., et al., *Aurora kinase inhibitor nanoparticles target tumors with favorable therapeutic index in vivo*. Science Translational Medicine, 2016. **8**(325): p. 325ra17.
6. Allen, T.M. and P.R. Cullis, *Liposomal drug delivery systems: From concept to clinical applications*. Advanced Drug Delivery Reviews, 2013. **65**(1): p. 36-48.
7. Ćwierkot, J. and J. Szechiński, *Methotrexate in rheumatoid arthritis*. Pharmacological reports, 2006. **58**(473): p. 473-492.
8. Wahed, M., et al., *Efficacy of methotrexate in Crohn's disease and ulcerative colitis patients unresponsive or intolerant to azathioprine/mercaptopurine*. Alimentary Pharmacology & Therapeutics, 2009. **30**(6): p. 614-620.
9. Friedman, B. and B. Cronstein, *Methotrexate mechanism in treatment of rheumatoid arthritis*. Joint Bone Spine, 2019. **86**(3): p. 301-307.
10. Liu, J., et al., *Heat-triggered drug release systems based on mesoporous silica nanoparticles filled with a maghemite core and phase-change molecules as gatekeepers*. Journal of Materials Chemistry B, 2014. **2**(1): p. 59-70.
11. Wang, Y., et al., *Temperature-triggered redox-degradable poly(ether urethane) nanoparticles for controlled drug delivery*. Journal of Materials Chemistry, 2012. **22**(48): p. 25217-25226.
12. Barot, M., et al., *Prodrug strategies in ocular drug delivery*. Medicinal chemistry (Sharjah (United Arab Emirates)), 2012. **8**(4): p. 753-768.
13. Zaal, E.A. and C.R. Berkers, *The Influence of Metabolism on Drug Response in Cancer*. Frontiers in oncology, 2018. **8**: p. 500-500.
14. Deeks, E.D., *Polatuzumab Vedotin: First Global Approval*. Drugs, 2019. **79**(13): p. 1467-1475.
15. Stancu, I.C., A. Lungu, and H. Iovu, *3 - Hydrogels for bone regeneration, in Biomaterials for Bone Regeneration*, P. Dubrue and S. Van Vlierberghe, Editors. 2014, Woodhead Publishing. p. 62-86.
16. Kamath, K.R. and K. Park, *Biodegradable hydrogels in drug delivery*. Advanced Drug Delivery Reviews, 1993. **11**(1): p. 59-84.
17. Tanan, W., J. Panichpakdee, and S. Saengsuwan, *Novel biodegradable hydrogel based on natural polymers: Synthesis, characterization, swelling/reswelling and biodegradability*. European Polymer Journal, 2019. **112**: p. 678-687.
18. Delgado-Calle, J., et al., *MMP14 is a novel target of PTH signaling in osteocytes that controls resorption by regulating soluble RANKL production*. FASEB J, 2018. **32**(5): p. 2878-2890.
19. Shamji, M.F., et al., *Development and characterization of a fusion protein between thermally responsive elastin-like polypeptide and interleukin-1 receptor antagonist: Sustained release of a local antiinflammatory therapeutic*. Arthritis & Rheumatism, 2007. **56**(11): p. 3650-3661.

20. Wang, Y., et al., *Peptide-drug conjugates as effective prodrug strategies for targeted delivery*. *Adv Drug Deliv Rev*, 2017. **110-111**: p. 112-126.
21. Perkins, E., *Development of novel MMP-activated prodrugs*, in *Institute of Cancer Therapeutics, Faculty of Life Sciences*. 2016, University of Bradford. p. 1-67.
22. Dong, J. and H. Chen, *Cardiotoxicity of Anticancer Therapeutics*. *Frontiers in cardiovascular medicine*, 2018. **5**: p. 9-9.
23. Clezardin, P., *Recent insights into the role of integrins in cancer metastasis*. *Cellular and Molecular Life Sciences CMLS*, 1998. **54(6)**: p. 541-548.
24. Desgrosellier, J.S. and D.A. Cheresh, *Integrins in cancer: biological implications and therapeutic opportunities*. *Nature Reviews Cancer*, 2010. **10(1)**: p. 9-22.
25. Cox, N., et al., *Integrin-Targeting Knottin Peptide-Drug Conjugates Are Potent Inhibitors of Tumor Cell Proliferation*. *Angewandte Chemie International Edition*, 2016. **55(34)**: p. 9894-9897.
26. Conibear, A.C., et al., *Multifunctional $\alpha\beta6$ Integrin-Specific Peptide-Pt(IV) Conjugates for Cancer Cell Targeting*. *Bioconjugate Chemistry*, 2017. **28(9)**: p. 2429-2439.
27. Böhme, D. and A.G. Beck-Sickinger, *Drug delivery and release systems for targeted tumor therapy*. *J Pept Sci*, 2015. **21(3)**: p. 186-200.
28. Gilad, Y., M. Firer, and G. Gellerman, *Recent Innovations in Peptide Based Targeted Drug Delivery to Cancer Cells*. *Biomedicines*, 2016. **4(2)**: p. 11.
29. Siemoneit, U., et al., *Acrylic/cyclodextrin hydrogels with enhanced drug loading and sustained release capability*. *International journal of pharmaceutics*, 2006. **312(1-2)**: p. 66-74.
30. Rathna, G.V.N., *Gelatin hydrogels: enhanced biocompatibility, drug release and cell viability*. *Journal of Materials Science: Materials in Medicine*, 2008. **19(6)**: p. 2351-2358.
31. reza Saboktakin, M. and R.M. Tabatabaei, *Supramolecular hydrogels as drug delivery systems*. *International journal of biological macromolecules*, 2015. **75**: p. 426-436.
32. El-Sherbiny, I.M. and M.H. Yacoub, *Hydrogel scaffolds for tissue engineering: Progress and challenges*. *Glob Cardiol Sci Pract*, 2013. **2013(3)**: p. 316-42.
33. Zhao, F., M.L. Ma, and B. Xu, *Molecular hydrogels of therapeutic agents*. *Chemical Society Reviews*, 2009. **38(4)**: p. 883-891.
34. Xing, R., et al., *Self-Assembled Injectable Peptide Hydrogels Capable of Triggering Antitumor Immune Response*. *Biomacromolecules*, 2017. **18(11)**: p. 3514-3523.
35. Altunbas, A., et al., *Encapsulation of curcumin in self-assembling peptide hydrogels as injectable drug delivery vehicles*. *Biomaterials*, 2011. **32(25)**: p. 5906-5914.
36. Syng-ai, C., A.L. Kumari, and A. Khar, *Effect of curcumin on normal and tumor cells: Role of glutathione and bcl-2*. *Molecular Cancer Therapeutics*, 2004. **3(9)**: p. 1101.
37. Ravindran, J., S. Prasad, and B.B. Aggarwal, *Curcumin and Cancer Cells: How Many Ways Can Curry Kill Tumor Cells Selectively?* *The AAPS Journal*, 2009. **11(3)**: p. 495-510.
38. Pandit, G., et al., *Self-Assembly Mechanism of a Peptide-Based Drug Delivery Vehicle*. *ACS Omega*, 2018. **3(3)**: p. 3143-3155.
39. Vu, T.D. and T. Kofidis, *6 - Biomaterials and cells for cardiac tissue engineering*, in *Cardiac Regeneration and Repair*, R.-K. Li and R.D. Weisel, Editors. 2014, Woodhead Publishing. p. 127-179.
40. Schneider, A., J.A. Garlick, and C. Egles, *Self-assembling peptide nanofiber scaffolds accelerate wound healing*. *PLoS one*, 2008. **3(1)**: p. e1410-e1410.
41. Li, Y., et al., *Multi-functional hydrogels prepared by dual-ion crosslinking for chronic wound healing*. *ACS Appl Mater Interfaces*, 2017.

42. Kamoun, E.A., E.S. Kenawy, and X. Chen, *A review on polymeric hydrogel membranes for wound dressing applications: PVA-based hydrogel dressings*. J Adv Res, 2017. **8**(3): p. 217-233.
43. Lai, W.F. and A.L. Rogach, *Hydrogel-Based Materials for Delivery of Herbal Medicines*. ACS Appl Mater Interfaces, 2017. **9**(13): p. 11309-11320.
44. Nguyen, H., et al., *Lipid-based submicron capsules as a strategy to include high concentrations of a hydrophobic lightening agent in a hydrogel*. Int J Cosmet Sci, 2017.
45. O, W. and L. D, *Hydrophilic gels for biological use*. Nature, 1960. **185**: p. 117-118.
46. Shingel, K.I., et al., *Inflammatory inert poly(ethylene glycol)--protein wound dressing improves healing responses in partial- and full-thickness wounds*. Int Wound J, 2006. **3**(4): p. 332-42.
47. Jeon, O., et al., *Affinity-based growth factor delivery using biodegradable, photocrosslinked heparin-alginate hydrogels*. J Control Release, 2011. **154**(3): p. 258-66.
48. Lee, S., et al., *Self-Assembling Peptides and Their Application in the Treatment of Diseases*. International journal of molecular sciences, 2019. **20**(23): p. 5850.
49. Ahsan, A., M.A. Farooq, and A. Parveen, *Thermosensitive Chitosan-Based Injectable Hydrogel as an Efficient Anticancer Drug Carrier*. ACS Omega, 2020. **5**(32): p. 20450-20460.
50. Date, P., et al., *Biodegradable and biocompatible agarose-poly (vinyl alcohol) hydrogel for the in vitro investigation of ibuprofen release*. Chemical Papers, 2020. **74**(6): p. 1965-1978.
51. Dadsetan, M., et al., *A stimuli-responsive hydrogel for doxorubicin delivery*. Biomaterials, 2010. **31**(31): p. 8051-62.
52. Tronci, G., et al., *Multi-scale mechanical characterization of highly swollen photo-activated collagen hydrogels*. J R Soc Interface, 2015. **12**(102): p. 20141079.
53. Tronci, G., et al., *Protease-sensitive atelocollagen hydrogels promote healing in a diabetic wound model*. Journal of Materials Chemistry B, 2016. **4**(45): p. 7249-7258.
54. Nichol, J.W., et al., *Cell-laden microengineered gelatin methacrylate hydrogels*. Biomaterials, 2010. **31**(21): p. 5536-5544.
55. Sun, M., et al., *Synthesis and Properties of Gelatin Methacryloyl (GelMA) Hydrogels and Their Recent Applications in Load-Bearing Tissue*. Polymers, 2018. **10**(11): p. 1290.
56. Huang, J., et al., *Tunable sequential drug delivery system based on chitosan/hyaluronic acid hydrogels and PLGA microspheres for management of non-healing infected wounds*. Materials Science and Engineering: C, 2018. **89**: p. 213-222.
57. Eiselt, P., K.Y. Lee, and D.J. Mooney, *Rigidity of Two-Component Hydrogels Prepared from Alginate and Poly(ethylene glycol)-Diamines*. Macromolecules, 1999. **32**(17): p. 5561-5566.
58. Wang, M., et al., *Radiation synthesis of PVP/CMC hydrogels as wound dressing*. Nuclear Instruments and Methods in Physics Research Section B: Beam Interactions with Materials and Atoms, 2007. **265**(1): p. 385-389.
59. Ma, H., et al., *Localized Co-delivery of Doxorubicin, Cisplatin, and Methotrexate by Thermosensitive Hydrogels for Enhanced Osteosarcoma Treatment*. ACS Appl Mater Interfaces, 2015. **7**(49): p. 27040-8.
60. Zentner, G.M., et al., *Biodegradable block copolymers for delivery of proteins and water-insoluble drugs*. J Control Release, 2001. **72**(1-3): p. 203-15.
61. Welzel, P.B., et al., *Modulating Biofunctional starPEG Heparin Hydrogels by Varying Size and Ratio of the Constituents*. Polymers, 2011. **3**(1).

62. Galler, K.M., et al., *Self-Assembling Multidomain Peptide Hydrogels: Designed Susceptibility to Enzymatic Cleavage Allows Enhanced Cell Migration and Spreading*. Journal of the American Chemical Society, 2010. **132**(9): p. 3217-3223.
63. Liu, J., et al., *Self-Assembling Peptide of d-Amino Acids Boosts Selectivity and Antitumor Efficacy of 10-Hydroxycamptothecin*. ACS Applied Materials & Interfaces, 2014. **6**(8): p. 5558-5565.
64. Fabiano, A., R. Bizzarri, and Y. Zambito, *Thermosensitive hydrogel based on chitosan and its derivatives containing medicated nanoparticles for transcorneal administration of 5-fluorouracil*. Int J Nanomedicine, 2017. **12**: p. 633-643.
65. Patel, P., et al., *Thermosensitive hydrogel-based drug delivery system for sustained drug release*. Journal of Polymer Research, 2019. **26**(6): p. 131.
66. Vermonden, T., et al., *Photopolymerized thermosensitive hydrogels: synthesis, degradation, and cytocompatibility*. Biomacromolecules, 2008. **9**(3): p. 919-26.
67. Nam, K., J. Watanabe, and K. Ishihara, *The characteristics of spontaneously forming physically cross-linked hydrogels composed of two water-soluble phospholipid polymers for oral drug delivery carrier I: hydrogel dissolution and insulin release under neutral pH condition*. Eur J Pharm Sci, 2004. **23**(3): p. 261-70.
68. Nehate, C., et al., *Combinatorial delivery of superparamagnetic iron oxide nanoparticles ($\gamma\text{Fe}_2\text{O}_3$) and doxorubicin using folate conjugated redox sensitive multiblock polymeric nanocarriers for enhancing the chemotherapeutic efficacy in cancer cells*. Mater Sci Eng C Mater Biol Appl, 2017. **75**: p. 1128-1143.
69. Chaudhari, U., et al., *Metabolite signatures of doxorubicin induced toxicity in human induced pluripotent stem cell-derived cardiomyocytes*. Amino Acids, 2017.
70. Howard, S.C., et al., *Preventing and Managing Toxicities of High-Dose Methotrexate*. Oncologist, 2016. **21**(12): p. 1471-1482.
71. Madeddu, C., et al., *Pathophysiology of cardiotoxicity induced by nonanthracycline chemotherapy*. J Cardiovasc Med (Hagerstown), 2016. **17** Suppl 1 Special issue on **Cardiotoxicity from Antiblastic Drugs and Cardioprotection**: p. e12-e18.
72. Nishioka, Y., et al., *Cisplatin suppository: preparation, release characteristics and clinical evaluation*. Chem Pharm Bull (Tokyo), 1991. **39**(6): p. 1518-21.
73. Peng, M., et al., *Thermosensitive injectable hydrogel enhances the antitumor effect of embelin in mouse hepatocellular carcinoma*. J Pharm Sci, 2014. **103**(3): p. 965-73.
74. Sheu, M.T., et al., *Codelivery of doxorubicin-containing thermosensitive hydrogels incorporated with docetaxel-loaded mixed micelles enhances local cancer therapy*. Colloids Surf B Biointerfaces, 2016. **143**: p. 260-70.
75. Liang, Y., et al., *A reconstituted thermosensitive hydrogel system based on paclitaxel-loaded amphiphilic copolymer nanoparticles and antitumor efficacy*. Drug Dev Ind Pharm, 2017: p. 1-29.
76. Nazli, C., et al., *Targeted delivery of doxorubicin into tumor cells via MMP-sensitive PEG hydrogel-coated magnetic iron oxide nanoparticles (MIONPs)*. Colloids Surf B Biointerfaces, 2014. **122**: p. 674-83.
77. Meenach, S.A., et al., *Characterization of PEG-iron oxide hydrogel nanocomposites for dual hyperthermia and paclitaxel delivery*. J Biomater Sci Polym Ed, 2013. **24**(9): p. 1112-26.
78. Zhu, X., et al., *Functionalized graphene oxide-based thermosensitive hydrogel for magnetic hyperthermia therapy on tumors*. Nanotechnology, 2015. **26**(36): p. 365103.
79. Mahdavinia, G.R., et al., *Magnetic- and pH-responsive kappa-carrageenan/chitosan complexes for controlled release of methotrexate anticancer drug*. Int J Biol Macromol, 2017. **97**: p. 209-217.

80. Marquez, F., et al., *Preparation of hollow magnetite microspheres and their applications as drugs carriers*. *Nanoscale Res Lett*, 2012. **7**(1): p. 210.
81. Davaran, S., et al., *Physicochemical characteristics of Fe₃O₄ magnetic nanocomposites based on Poly(N-isopropylacrylamide) for anti-cancer drug delivery*. *Asian Pac J Cancer Prev*, 2014. **15**(1): p. 49-54.
82. Ouasti, S., et al., *Network connectivity, mechanical properties and cell adhesion for hyaluronic acid/PEG hydrogels*. *Biomaterials*, 2011. **32**(27): p. 6456-70.
83. Koehler, K.C., K.S. Anseth, and C.N. Bowman, *Diels-Alder mediated controlled release from a poly(ethylene glycol) based hydrogel*. *Biomacromolecules*, 2013. **14**(2): p. 538-47.
84. Phelps, E.A., et al., *Vasculogenic bio-synthetic hydrogel for enhancement of pancreatic islet engraftment and function in type 1 diabetes*. *Biomaterials*, 2013. **34**(19): p. 4602-11.
85. Garland, S.P., et al., *Photopatternable and photoactive hydrogel for on-demand generation of hydrogen peroxide in cell culture*. *Biomaterials*, 2014. **35**(5): p. 1762-70.
86. Schmedlen, R.H., K.S. Masters, and J.L. West, *Photocrosslinkable polyvinyl alcohol hydrogels that can be modified with cell adhesion peptides for use in tissue engineering*. *Biomaterials*, 2002. **23**(22): p. 4325-32.
87. Bako, J., et al., *Composition and characterization of in situ usable light cured dental drug delivery hydrogel system*. *J Mater Sci Mater Med*, 2013. **24**(3): p. 659-66.
88. Hu, J., et al., *Visible light crosslinkable chitosan hydrogels for tissue engineering*. *Acta Biomater*, 2012. **8**(5): p. 1730-8.
89. Enriquez-Navas, P.M., et al., *Exploiting evolutionary principles to prolong tumor control in preclinical models of breast cancer*. *Sci Transl Med*, 2016. **8**(327): p. 327ra24.
90. Lv, W., L. Cheng, and B. Li, *Development and evaluation of a novel TPGS-mediated paclitaxel-loaded PLGA-mPEG nanoparticle for the treatment of ovarian cancer*. *Chem Pharm Bull (Tokyo)*, 2015. **63**(2): p. 68-74.
91. Luo, C.Q., et al., *Curcumin-coordinated nanoparticles with improved stability for reactive oxygen species-responsive drug delivery in lung cancer therapy*. *Int J Nanomedicine*, 2017. **12**: p. 855-869.
92. Tyagi, P., et al., *Urodynamic and immunohistochemical evaluation of intravesical capsaicin delivery using thermosensitive hydrogel and liposomes*. *J Urol*, 2004. **171**(1): p. 483-9.
93. Wang, W., et al., *An anti-inflammatory cell-free collagen/resveratrol scaffold for repairing osteochondral defects in rabbits*. *Acta Biomater*, 2014. **10**(12): p. 4983-95.
94. Li, I.C., A.N. Moore, and J.D. Hartgerink, *"Missing Tooth" Multidomain Peptide Nanofibers for Delivery of Small Molecule Drugs*. *Biomacromolecules*, 2016. **17**(6): p. 2087-95.
95. Fu, C., et al., *Injectable micellar supramolecular hydrogel for delivery of hydrophobic anticancer drugs*. *J Mater Sci Mater Med*, 2016. **27**(4): p. 73.
96. Tanigo, T., R. Takaoka, and Y. Tabata, *Sustained release of water-insoluble simvastatin from biodegradable hydrogel augments bone regeneration*. *J Control Release*, 2010. **143**(2): p. 201-6.
97. Nitta, K., A. Kimoto, and J. Watanabe, *Design and synthesis of an amphiphilic graft hydrogel having a hydrophobic domain formed by multiple interactions*. *Mater Sci Eng C Mater Biol Appl*, 2016. **68**: p. 65-9.
98. Wolinsky, J.B., Y.L. Colson, and M.W. Grinstaff, *Local drug delivery strategies for cancer treatment: gels, nanoparticles, polymeric films, rods, and wafers*. *J Control Release*, 2012. **159**(1): p. 14-26.

99. Prausnitz, M.R. and R. Langer, *Transdermal drug delivery*. Nat Biotechnol, 2008. **26**(11): p. 1261-8.
100. Hoppenz, P., S. Els-Heindl, and A.G. Beck-Sickinger, *Peptide-Drug Conjugates and Their Targets in Advanced Cancer Therapies*. Frontiers in chemistry, 2020. **8**: p. 571-571.
101. Stintzing, S., et al., *Overexpression of MMP9 and tissue factor in unstable carotid plaques associated with Chlamydia pneumoniae, inflammation, and apoptosis*. Ann Vasc Surg, 2005. **19**(3): p. 310-9.
102. Narvekar, M., et al., *Nanocarrier for poorly water-soluble anticancer drugs--barriers of translation and solutions*. AAPS PharmSciTech, 2014. **15**(4): p. 822-833.
103. Atkinson, J.M., et al., *Development of a novel tumor-targeted vascular disrupting agent activated by membrane-type matrix metalloproteinases*. Cancer Res, 2010. **70**(17): p. 6902-12.
104. Choi, K.Y., et al., *Protease-activated drug development*. Theranostics, 2012. **2**(2): p. 156-178.
105. Hanahan, D. and R.A. Weinberg, *The hallmarks of cancer*. Cell, 2000. **100**(1): p. 57-70.
106. Corno, C., et al., *Role of the Receptor Tyrosine Kinase Axl and its Targeting in Cancer Cells*. Curr Med Chem, 2016. **23**(15): p. 1496-512.
107. Wang, H., et al., *HER4 promotes cell survival and chemoresistance in osteosarcoma via interaction with NDRG1*. Biochim Biophys Acta Mol Basis Dis, 2018. **1864**(5 Pt A): p. 1839-1849.
108. Weinberg, R.A., *The retinoblastoma protein and cell cycle control*. Cell, 1995. **81**(3): p. 323-30.
109. Green, D.R. and J.C. Reed, *Mitochondria and apoptosis*. Science, 1998. **281**(5381): p. 1309-12.
110. Liu, B., et al., *RACK1 induces chemotherapy resistance in esophageal carcinoma by upregulating the PI3K/AKT pathway and Bcl-2 expression*. Onco Targets Ther, 2018. **11**: p. 211-220.
111. Pruefer, F.G., et al., *Participation of Omi Htra2 serine-protease activity in the apoptosis induced by cisplatin on SW480 colon cancer cells*. J Chemother, 2008. **20**(3): p. 348-54.
112. Counter, C.M., et al., *Telomere shortening associated with chromosome instability is arrested in immortal cells which express telomerase activity*. Embo j, 1992. **11**(5): p. 1921-9.
113. Hayashi, M.T., et al., *Cell death during crisis is mediated by mitotic telomere deprotection*. Nature, 2015. **522**(7557): p. 492-6.
114. Shay, J.W. and S. Bacchetti, *A survey of telomerase activity in human cancer*. Eur J Cancer, 1997. **33**(5): p. 787-91.
115. Bryan, T.M., et al., *Telomere elongation in immortal human cells without detectable telomerase activity*. Embo j, 1995. **14**(17): p. 4240-8.
116. Reddel, R.R., *Telomere maintenance mechanisms in cancer: clinical implications*. Curr Pharm Des, 2014. **20**(41): p. 6361-74.
117. Huang, F.W., et al., *Highly recurrent TERT promoter mutations in human melanoma*. Science, 2013. **339**(6122): p. 957-9.
118. Hanahan, D. and J. Folkman, *Patterns and Emerging Mechanisms of the Angiogenic Switch during Tumorigenesis*. Cell, 1996. **86**(3): p. 353-364.
119. Zanolli, M.R. and C.A. Reinhart-King, *Mechanical Forces in Tumor Angiogenesis*. Advances in experimental medicine and biology, 2018. **1092**: p. 91-112.
120. Senger, D.R., et al., *Angiogenesis promoted by vascular endothelial growth factor: regulation through alpha1beta1 and alpha2beta1 integrins*. Proceedings of the

- National Academy of Sciences of the United States of America, 1997. **94**(25): p. 13612-13617.
121. Basu, A., et al., *Overexpression of vascular endothelial growth factor and the development of post-transplantation cancer*. Cancer research, 2008. **68**(14): p. 5689-5698.
 122. Volpert, O.V., K.M. Dameron, and N. Bouck, *Sequential development of an angiogenic phenotype by human fibroblasts progressing to tumorigenicity*. Oncogene, 1997. **14**(12): p. 1495-1502.
 123. Han, K.-Y., et al., *MT1-MMP modulates bFGF-induced VEGF-A expression in corneal fibroblasts*. Protein and peptide letters, 2012. **19**(12): p. 1334-1339.
 124. Yao, G., et al., *MT1-MMP in breast cancer: induction of VEGF-C correlates with metastasis and poor prognosis*. Cancer cell international, 2013. **13**(1): p. 98-98.
 125. Qiao, B., N.W. Johnson, and J. Gao, *Epithelial-mesenchymal transition in oral squamous cell carcinoma triggered by transforming growth factor-beta1 is Snail family-dependent and correlates with matrix metalloproteinase-2 and -9 expressions*. Int J Oncol, 2010. **37**(3): p. 663-8.
 126. Christofori, G. and H. Semb, *The role of the cell-adhesion molecule E-cadherin as a tumour-suppressor gene*. Trends Biochem Sci, 1999. **24**(2): p. 73-6.
 127. Ferrari, S. and E. Palmerini, *Adjuvant and neoadjuvant combination chemotherapy for osteogenic sarcoma*. Curr Opin Oncol, 2007. **19**(4): p. 341-6.
 128. Mirabello, L., R.J. Troisi, and S.A. Savage, *Osteosarcoma incidence and survival rates from 1973 to 2004: data from the Surveillance, Epidemiology, and End Results Program*. Cancer, 2009. **115**(7): p. 1531-1543.
 129. Huang, X., et al., *Risk and clinicopathological features of osteosarcoma metastasis to the lung: A population-based study*. Journal of bone oncology, 2019. **16**: p. 100230-100230.
 130. Feugeas, O., et al., *Loss of heterozygosity of the RB gene is a poor prognostic factor in patients with osteosarcoma*. Journal of Clinical Oncology, 1996. **14**(2): p. 467-472.
 131. Belchis, D.A., et al., *Loss of Heterozygosity and Microsatellite Instability at the Retinoblastoma Locus in Osteosarcomas*. Diagnostic Molecular Pathology, 1996. **5**(3).
 132. Bieging, K.T., S.S. Mello, and L.D. Attardi, *Unravelling mechanisms of p53-mediated tumour suppression*. Nature reviews. Cancer, 2014. **14**(5): p. 359-370.
 133. Varley, J.M., *Germline TP53 mutations and Li-Fraumeni syndrome*. Hum Mutat, 2003. **21**(3): p. 313-20.
 134. Zhou, R., et al., *Li-Fraumeni Syndrome Disease Model: A Platform to Develop Precision Cancer Therapy Targeting Oncogenic p53*. Trends in Pharmacological Sciences, 2017. **38**(10): p. 908-927.
 135. Rubio, R., et al., *Bone environment is essential for osteosarcoma development from transformed mesenchymal stem cells*. Stem Cells, 2014. **32**(5): p. 1136-48.
 136. Velletri, T., et al., *P53 functional abnormality in mesenchymal stem cells promotes osteosarcoma development*. Cell Death & Disease, 2016. **7**(1): p. e2015-e2015.
 137. Kundu, Z.S., *Classification, imaging, biopsy and staging of osteosarcoma*. Indian journal of orthopaedics, 2014. **48**(3): p. 238-246.
 138. Canale, S.T. and J.H. Beaty, *Campbell's operative orthopaedics e-book*. 2012: Elsevier Health Sciences.
 139. Moore, T.M., et al., *Closed biopsy of musculoskeletal lesions*. J Bone Joint Surg Am, 1979. **61**(3): p. 375-80.
 140. Pollock, R.C. and P.D. Stalley, *Biopsy of musculoskeletal tumours – beware*. ANZ Journal of Surgery, 2004. **74**(7): p. 516-519.

141. Wu, J.S., et al., *Bone and Soft-Tissue Lesions: What Factors Affect Diagnostic Yield of Image-guided Core-Needle Biopsy?* Radiology, 2008. **248**(3): p. 962-970.
142. Righi, A., et al., *High-grade focal areas in low-grade central osteosarcoma: high-grade or still low-grade osteosarcoma?* Clinical sarcoma research, 2015. **5**: p. 23-23.
143. Fletcher, C.D.M., K.K. Unni, and F. Mertens, *Pathology and genetics of tumours of soft tissue and bone*. Vol. 4. 2002: Iarc.
144. Bielack, S., D. Carrle, and P.G. Casali, *Osteosarcoma: ESMO clinical recommendations for diagnosis, treatment and follow-up*. Ann Oncol, 2009. **20 Suppl 4**: p. 137-9.
145. Isakoff, M.S., et al., *Osteosarcoma: Current Treatment and a Collaborative Pathway to Success*. Journal of clinical oncology : official journal of the American Society of Clinical Oncology, 2015. **33**(27): p. 3029-3035.
146. Jaffe, N., *Osteosarcoma: review of the past, impact on the future. The American experience*. Cancer Treat Res, 2009. **152**: p. 239-62.
147. Delepine, N., et al., *Importance of age and methotrexate dosage: prognosis in children and young adults with high-grade osteosarcomas*. Biomed Pharmacother, 1988. **42**(4): p. 257-62.
148. Winkler, K., et al., *Neoadjuvant chemotherapy of osteosarcoma: results of a randomized cooperative trial (COSS-82) with salvage chemotherapy based on histological tumor response*. J Clin Oncol, 1988. **6**(2): p. 329-37.
149. Provisor, A.J., et al., *Treatment of nonmetastatic osteosarcoma of the extremity with preoperative and postoperative chemotherapy: a report from the Children's Cancer Group*. J Clin Oncol, 1997. **15**(1): p. 76-84.
150. Gurpinar, E., W.E. Grizzle, and G.A. Piazza, *NSAIDs inhibit tumorigenesis, but how?* Clinical cancer research : an official journal of the American Association for Cancer Research, 2014. **20**(5): p. 1104-1113.
151. Urakawa, H., et al., *Cyclooxygenase-2 overexpression predicts poor survival in patients with high-grade extremity osteosarcoma: a pilot study*. Clinical orthopaedics and related research, 2009. **467**(11): p. 2932-2938.
152. Wang, S., et al., *Cyclooxygenase-2 expression correlates with development, progression, metastasis, and prognosis of osteosarcoma: a meta-analysis and trial sequential analysis*. FEBS open bio, 2019. **9**(2): p. 226-240.
153. Zarghi, A. and S. Arfaei, *Selective COX-2 Inhibitors: A Review of Their Structure-Activity Relationships*. Iranian journal of pharmaceutical research : IJPR, 2011. **10**(4): p. 655-683.
154. Pereira-Silva, M., et al., *Nanomedicine in osteosarcoma therapy: Micelleplexes for delivery of nucleic acids and drugs toward osteosarcoma-targeted therapies*. European Journal of Pharmaceutics and Biopharmaceutics, 2020. **148**: p. 88-106.
155. Shan, H., et al., *Locally Controlled Release of Methotrexate and Alendronate by Thermo-Sensitive Hydrogels for Synergistic Inhibition of Osteosarcoma Progression*. Frontiers in Pharmacology, 2020. **11**: p. 573.
156. Jabłońska-Trypuć, A., M. Matejczyk, and S. Rosochacki, *Matrix metalloproteinases (MMPs), the main extracellular matrix (ECM) enzymes in collagen degradation, as a target for anticancer drugs*. Journal of Enzyme Inhibition and Medicinal Chemistry, 2016. **31**(sup1): p. 177-183.
157. Rundhaug, J.E., *Matrix metalloproteinases and angiogenesis*. Journal of cellular and molecular medicine, 2005. **9**(2): p. 267-285.
158. Quintero-Fabián, S., et al., *Role of Matrix Metalloproteinases in Angiogenesis and Cancer*. Frontiers in oncology, 2019. **9**: p. 1370-1370.
159. Smolen, J.S., et al., *New therapies for treatment of rheumatoid arthritis*. The Lancet, 2007. **370**(9602): p. 1861-1874.

160. WHO. *World Health Organisation - Chronic rheumatic conditions*. 2020; Available from: <https://www.who.int/chp/topics/rheumatic/en/>.
161. Ishiguro, N., [*Cartilage degradation in rheumatoid arthritis*]. *Clin Calcium*, 2009. **19**(3): p. 347-54.
162. Jimenez-Boj, E., et al., *Interaction between synovial inflammatory tissue and bone marrow in rheumatoid arthritis*. *The Journal of Immunology*, 2005. **175**(4): p. 2579-2588.
163. Smolen, J.S. and G. Steiner, *Therapeutic strategies for rheumatoid arthritis*. *Nature Reviews Drug Discovery*, 2003. **2**(6): p. 473-488.
164. McInnes, I.B. and G. Schett, *Cytokines in the pathogenesis of rheumatoid arthritis*. *Nature Reviews Immunology*, 2007. **7**(6): p. 429-442.
165. De Benedetti, F., et al., *Impaired skeletal development in interleukin-6–transgenic mice: A model for the impact of chronic inflammation on the growing skeletal system*. *Arthritis & Rheumatism*, 2006. **54**(11): p. 3551-3563.
166. Sattar, N., et al., *Explaining How “High-Grade” Systemic Inflammation Accelerates Vascular Risk in Rheumatoid Arthritis*. *Circulation*, 2003. **108**(24): p. 2957-2963.
167. Choy, E., *Understanding the dynamics: pathways involved in the pathogenesis of rheumatoid arthritis*. *Rheumatology*, 2012. **51**(suppl_5): p. v3-v11.
168. Bresnihan, B., *Pathogenesis of joint damage in rheumatoid arthritis*. *J Rheumatol*, 1999. **26**(3): p. 717-9.
169. McInnes, I.B. and G. Schett, *The pathogenesis of rheumatoid arthritis*. *N Engl J Med*, 2011. **365**(23): p. 2205-19.
170. Yin, N., et al., *Intra-articular injection of indomethacin–methotrexate in situ hydrogel for the synergistic treatment of rheumatoid arthritis*. *Journal of Materials Chemistry B*, 2020. **8**(5): p. 993-1007.
171. Seo, J., et al., *Injectable Click-Crosslinked Hyaluronic Acid Depot To Prolong Therapeutic Activity in Articular Joints Affected by Rheumatoid Arthritis*. *ACS Applied Materials & Interfaces*, 2019. **11**(28): p. 24984-24998.
172. Kim, K.S., et al., *Injectable hyaluronic acid–tyramine hydrogels for the treatment of rheumatoid arthritis*. *Acta Biomaterialia*, 2011. **7**(2): p. 666-674.
173. Beddoes, C.M., et al., *Hydrogels as a Replacement Material for Damaged Articular Hyaline Cartilage*. *Materials (Basel, Switzerland)*, 2016. **9**(6): p. 443.
174. Tronci, G., et al., *Influence of 4-vinylbenzylation on the rheological and swelling properties of photo activated collagen hydrogels*. *Cambridge University Press*, 2016. **1**(8): p. 533-538.
175. Phelps, E.A., et al., *Maleimide cross-linked bioactive PEG hydrogel exhibits improved reaction kinetics and cross-linking for cell encapsulation and in situ delivery*. *Advanced materials (Deerfield Beach, Fla.)*, 2012. **24**(1): p. 64-2.
176. Lutolf, M.P., et al., *Synthetic matrix metalloproteinase-sensitive hydrogels for the conduction of tissue regeneration: engineering cell-invasion characteristics*. *Proceedings of the National Academy of Sciences of the United States of America*, 2003. **100**(9): p. 5413-5418.
177. Ashley, G.W., et al., *Hydrogel drug delivery system with predictable and tunable drug release and degradation rates*. *Proceedings of the National Academy of Sciences*, 2013. **110**(6): p. 2318.
178. Patterson, S.J., C.C. Scott, and K.B.E. Tucker, *Nonionic detergent degradation: III. Initial mechanism of the degradation*. *Journal of the American Oil Chemists' Society*, 1970. **47**(2): p. 37-41.
179. Mero, A. and M. Campisi, *Hyaluronic acid bioconjugates for the delivery of bioactive molecules*. *Polymers*, 2014. **6**(2): p. 346-369.

180. Roth, A., et al., *Intra-articular injections of high-molecular-weight hyaluronic acid have biphasic effects on joint inflammation and destruction in rat antigen-induced arthritis*. Arthritis research & therapy, 2005. **7**(3): p. R677-R686.
181. Davidenko, N., et al., *Biomimetic collagen scaffolds with anisotropic pore architecture*. Acta Biomaterialia, 2012. **8**(2): p. 667-676.
182. Boateng, J.S., et al., *Wound Healing Dressings and Drug Delivery Systems: A Review*. Journal of Pharmaceutical Sciences, 2008. **97**(8): p. 2892-2923.
183. Ricard-Blum, S., *The collagen family*. Cold Spring Harbor perspectives in biology, 2011. **3**(1): p. a004978-a004978.
184. Krakow, D., *105 - Heritable Diseases of Connective Tissue*, in *Kelley's Textbook of Rheumatology (Ninth Edition)*, G.S. Firestein, et al., Editors. 2013, W.B. Saunders: Philadelphia. p. 1719-1739.e3.
185. Esposito, C. and I. Caputo, *Mammalian transglutaminases*. The FEBS Journal, 2005. **272**(3): p. 615-631.
186. Avery, N.C. and A.J. Bailey, *The effects of the Maillard reaction on the physical properties and cell interactions of collagen*. Pathologie Biologie, 2006. **54**(7): p. 387-395.
187. Eyre, D.R. and J.-J. Wu, *Collagen Cross-Links*, in *Collagen: Primer in Structure, Processing and Assembly*, J. Brinckmann, H. Notbohm, and P.K. Müller, Editors. 2005, Springer Berlin Heidelberg: Berlin, Heidelberg. p. 207-229.
188. Pahoff, S., et al., *Effect of gelatin source and photoinitiator type on chondrocyte redifferentiation in gelatin methacryloyl-based tissue-engineered cartilage constructs*. Journal of Materials Chemistry B, 2019. **7**(10): p. 1761-1772.
189. Tronci, G., S.J. Russell, and D.J. Wood, *Improvements in and relating to collagen based materials*. 2013.
190. Chuang, C.-H., et al., *Enzymatic regulation of functional vascular networks using gelatin hydrogels*. Acta biomaterialia, 2015. **19**: p. 85-99.
191. Yue, K., et al., *Synthesis, properties, and biomedical applications of gelatin methacryloyl (GelMA) hydrogels*. Biomaterials, 2015. **73**: p. 254-271.
192. Klein, T. and R. Bischoff, *Physiology and pathophysiology of matrix metalloproteases*. Amino acids, 2011. **41**(2): p. 271-290.
193. Yamauchi, M. and M. Sricholpech, *Lysine post-translational modifications of collagen*. Essays in biochemistry, 2012. **52**: p. 113-133.
194. Courts, A., *The N-terminal amino acid residues of gelatin. 1. Intact gelatins*. The Biochemical journal, 1954. **58**(1): p. 70-74.
195. Kany, S., J.T. Vollrath, and B. Relja, *Cytokines in Inflammatory Disease*. International journal of molecular sciences, 2019. **20**(23): p. 6008.
196. Moudgil, K.D. and D. Choubey, *Cytokines in autoimmunity: role in induction, regulation, and treatment*. Journal of interferon & cytokine research : the official journal of the International Society for Interferon and Cytokine Research, 2011. **31**(10): p. 695-703.
197. Hahn, M.E. and N.C. Gianneschi, *Enzyme-directed assembly and manipulation of organic nanomaterials*. Chemical communications (Cambridge, England), 2011. **47**(43): p. 11814-11821.
198. Sinclair And, R.D. and T.J. Ryan, *PROTEOLYTIC ENZYMES IN WOUND HEALING: THE ROLE OF ENZYMATIC DEBRIDEMENT*. Australasian Journal of Dermatology, 1994. **35**(1): p. 35-41.
199. Bedford, M.R., *The Effect of Enzymes on Digestion*. Journal of Applied Poultry Research, 1996. **5**(4): p. 370-378.
200. Walter, R., W.H. Simmons, and T. Yoshimoto, *Proline specific endo- and exopeptidases*. Molecular and Cellular Biochemistry, 1980. **30**(2): p. 111-127.

201. Shuja, S., K. Sheahan, and M.J. Murnane, *Cysteine endopeptidase activity levels in normal human tissues, colorectal adenomas and carcinomas*. International Journal of Cancer, 1991. **49**(3): p. 341-346.
202. Rawlings, N.D. and A.J. Barrett, [2] *Families of serine peptidases*, in *Methods in Enzymology*. 1994, Academic Press. p. 19-61.
203. Mantle, D., et al., *Comparison of proline endopeptidase activity in brain tissue from normal cases and cases with Alzheimer's disease, Lewy body dementia, Parkinson's disease and Huntington's disease*. Clinica Chimica Acta, 1996. **249**(1): p. 129-139.
204. Vargová, V., M. Pytliak, and V. Mechírová, *Matrix metalloproteinases*. Exp Suppl, 2012. **103**: p. 1-33.
205. Li, Z., et al., *Regulation of collagenase activities of human cathepsins by glycosaminoglycans*. J Biol Chem, 2004. **279**(7): p. 5470-9.
206. Korenč, M., B. Lenarčič, and M. Novinec, *Human cathepsin L, a papain-like collagenase without proline specificity*. Febs j, 2015. **282**(22): p. 4328-40.
207. Cunnane, G., et al., *Collagenase, cathepsin B and cathepsin L gene expression in the synovial membrane of patients with early inflammatory arthritis*. Rheumatology (Oxford), 1999. **38**(1): p. 34-42.
208. Skoumal, M., et al., *Serum cathepsin K levels of patients with longstanding rheumatoid arthritis: correlation with radiological destruction*. Arthritis Res Ther, 2005. **7**(1): p. R65-70.
209. Husmann, K., et al., *Cathepsins and osteosarcoma: Expression analysis identifies cathepsin K as an indicator of metastasis*. Mol Carcinog, 2008. **47**(1): p. 66-73.
210. Lu, P., et al., *Extracellular matrix degradation and remodeling in development and disease*. Cold Spring Harbor perspectives in biology, 2011. **3**(12): p. a005058.
211. Caley, M.P., V.L.C. Martins, and E.A. O'Toole, *Metalloproteinases and Wound Healing*. Advances in wound care, 2015. **4**(4): p. 225-234.
212. Bergers, G., et al., *Matrix metalloproteinase-9 triggers the angiogenic switch during carcinogenesis*. Nature cell biology, 2000. **2**(10): p. 737-744.
213. Strauss Bradley, H., et al., *In Vivo Collagen Turnover Following Experimental Balloon Angioplasty Injury and the Role of Matrix Metalloproteinases*. Circulation Research, 1996. **79**(3): p. 541-550.
214. Parks, W.C., C.L. Wilson, and Y.S. López-Boado, *Matrix metalloproteinases as modulators of inflammation and innate immunity*. Nature Reviews Immunology, 2004. **4**(8): p. 617-629.
215. Mort, J.S. and C.J. Billington, *Articular cartilage and changes in Arthritis: Matrix degradation*. Arthritis Research & Therapy, 2001. **3**(6): p. 337.
216. Okada, A., et al., *Expression of matrix metalloproteinases during rat skin wound healing: evidence that membrane type-1 matrix metalloproteinase is a stromal activator of pro-gelatinase A*. The Journal of cell biology, 1997. **137**(1): p. 67-77.
217. Knäuper, V., et al., *Cellular mechanisms for human procollagenase-3 (MMP-13) activation. Evidence that MT1-MMP (MMP-14) and gelatinase a (MMP-2) are able to generate active enzyme*. J Biol Chem, 1996. **271**(29): p. 17124-31.
218. Dong, W., et al., *Matrix metalloproteinase 2 promotes cell growth and invasion in colorectal cancer*. Acta Biochimica et Biophysica Sinica, 2011. **43**(11): p. 840.
219. Knäuper, V., et al., *Biochemical characterization of human collagenase-3*. J Biol Chem, 1996. **271**(3): p. 1544-50.
220. Uchibori, M., et al., *Increased expression of membrane-type matrix metalloproteinase-1 is correlated with poor prognosis in patients with osteosarcoma*. Int J Oncol, 2006. **28**(1): p. 33-42.

221. Liu, B., et al., *A furin inhibitor downregulates osteosarcoma cell migration by downregulating the expression levels of MT1-MMP via the Wnt signaling pathway*. *Oncol Lett*, 2014. **7**(4): p. 1033-1038.
222. Miller, M.C., et al., *Membrane type 1 matrix metalloproteinase is a crucial promoter of synovial invasion in human rheumatoid arthritis*. *Arthritis Rheum*, 2009. **60**(3): p. 686-97.
223. Fosang, A.J., et al., *Membrane-type 1 MMP (MMP-14) cleaves at three sites in the aggrecan interglobular domain*. *FEBS Lett*, 1998. **430**(3): p. 186-90.
224. Kajita, M., et al., *Membrane-Type 1 Matrix Metalloproteinase Cleaves Cd44 and Promotes Cell Migration*. *Journal of Cell Biology*, 2001. **153**(5): p. 893-904.
225. Nikitovic, D., et al., *Lumican expression is positively correlated with the differentiation and negatively with the growth of human osteosarcoma cells*. *The FEBS Journal*, 2008. **275**(2): p. 350-361.
226. Niewiarowska, J., et al., *Lumican inhibits angiogenesis by interfering with $\alpha 2\beta 1$ receptor activity and downregulating MMP-14 expression*. *Thrombosis Research*, 2011. **128**(5): p. 452-457.
227. Wu, D., et al., *Screening of diagnostic markers for osteosarcoma*. *Mol Med Rep*, 2014. **10**(5): p. 2415-20.
228. Ho, X.D., et al., *Whole transcriptome analysis identifies differentially regulated networks between osteosarcoma and normal bone samples*. *Experimental biology and medicine (Maywood, N.J.)*, 2017. **242**(18): p. 1802-1811.
229. Gill, J.H., et al., *Tumor-targeted prodrug ICT2588 demonstrates therapeutic activity against solid tumors and reduced potential for cardiovascular toxicity*. *Mol Pharm*, 2014. **11**(4): p. 1294-300.
230. Mamdani, M., et al., *Effect of Selective Cyclooxygenase 2 Inhibitors and Naproxen on Short-term Risk of Acute Myocardial Infarction in the Elderly*. *Archives of Internal Medicine*, 2003. **163**(4): p. 481-486.
231. Farkouh, M.E., et al., *Cardiovascular outcomes in high risk patients with osteoarthritis treated with ibuprofen, naproxen or lumiracoxib*. *Annals of the Rheumatic Diseases*, 2007. **66**(6): p. 764.
232. Kunnumakkara, A.B., et al., *Chronic diseases, inflammation, and spices: how are they linked?* *Journal of translational medicine*, 2018. **16**(1): p. 14-14.
233. Silverstein, F.E., et al., *Misoprostol reduces serious gastrointestinal complications in patients with rheumatoid arthritis receiving nonsteroidal anti-inflammatory drugs. A randomized, double-blind, placebo-controlled trial*. *Ann Intern Med*, 1995. **123**(4): p. 241-9.
234. Drini, M., *Peptic ulcer disease and non-steroidal anti-inflammatory drugs*. *Australian prescriber*, 2017. **40**(3): p. 91-93.
235. Choi, B.-H., et al., *Aspirin-induced Bcl-2 translocation and its phosphorylation in the nucleus trigger apoptosis in breast cancer cells*. *Experimental & molecular medicine*, 2013. **45**(10): p. e47-e47.
236. Liu, H.F., P.W. Hsiao, and J.I. Chao, *Celecoxib induces p53-PUMA pathway for apoptosis in human colorectal cancer cells*. *Chem Biol Interact*, 2008. **176**(1): p. 48-57.
237. Benamouzig, R., et al., *Cyclooxygenase-2 expression and recurrence of colorectal adenomas: effect of aspirin chemoprevention*. *Gut*, 2010. **59**(5): p. 622-9.
238. Williams, C.S., M. Mann, and R.N. DuBois, *The role of cyclooxygenases in inflammation, cancer, and development*. *Oncogene*, 1999. **18**(55): p. 7908-7916.
239. Crofford, L.J., *The Role of COX-2 in Rheumatoid Arthritis Synovial Tissues*. *Arthritis Research*, 2000. **1**(Suppl 1): p. S30-S30.

240. Wu, X., et al., *The impact of COX-2 on invasion of osteosarcoma cell and its mechanism of regulation*. *Cancer cell international*, 2014. **14**: p. 27-27.
241. Mowat, A.G., et al., *Naproxen in rheumatoid arthritis. Extended trial*. *Annals of the rheumatic diseases*, 1976. **35**(6): p. 498-501.
242. Correia, I., et al., *Effects of naproxen on cell proliferation and genotoxicity in MG-63 osteosarcoma cell line*. *J Toxicol Environ Health A*, 2014. **77**(14-16): p. 916-23.
243. Naruse, T., et al., *Meloxicam inhibits osteosarcoma growth, invasiveness and metastasis by COX-2-dependent and independent routes*. *Carcinogenesis*, 2006. **27**(3): p. 584-92.
244. Nejadmoghaddam, M.-R., et al., *Antibody-Drug Conjugates: Possibilities and Challenges*. *Avicenna journal of medical biotechnology*, 2019. **11**(1): p. 3-23.
245. Vrettos, E.I., G. Mező, and A.G. Tzakos, *On the design principles of peptide-drug conjugates for targeted drug delivery to the malignant tumor site*. *Beilstein journal of organic chemistry*, 2018. **14**: p. 930-954.
246. Li, J. and D.J. Mooney, *Designing hydrogels for controlled drug delivery*. *Nature reviews. Materials*, 2016. **1**(12): p. 16071.
247. Zhang, Y., Y. Huang, and S. Li, *Polymeric micelles: nanocarriers for cancer-targeted drug delivery*. *AAPS PharmSciTech*, 2014. **15**(4): p. 862-871.
248. Mori, T., et al., *TNF α promotes osteosarcoma progression by maintaining tumor cells in an undifferentiated state*. *Oncogene*, 2014. **33**(33): p. 4236-4241.
249. Gordon, V.D., et al., *Measuring the mechanical stress induced by an expanding multicellular tumor system: a case study*. *Experimental Cell Research*, 2003. **289**(1): p. 58-66.
250. Greenstein, G., *Local Drug Delivery in the Treatment of Periodontal Diseases: Assessing the Clinical Significance of the Results*. *Journal of Periodontology*, 2006. **77**(4): p. 565-578.
251. Todd, P.A. and S.P. Clissold, *Naproxen*. *Drugs*, 1990. **40**(1): p. 91-137.
252. Robinson, D.R., *Regulation of prostaglandin synthesis by antiinflammatory drugs*. *J Rheumatol Suppl*, 1997. **47**: p. 32-9.
253. Dvornik, D.M., *Tissue selective inhibition of prostaglandin biosynthesis by etodolac*. *J Rheumatol Suppl*, 1997. **47**: p. 40-7.
254. Zhao, Y., et al., *Novel naproxen-peptide-conjugated amphiphilic dendrimer self-assembly micelles for targeting drug delivery to osteosarcoma cells*. *RSC Advances*, 2016. **6**(65): p. 60327-60335.
255. Watson, D.J., et al., *Lower Risk of Thromboembolic Cardiovascular Events With Naproxen Among Patients With Rheumatoid Arthritis*. *Archives of Internal Medicine*, 2002. **162**(10): p. 1105-1110.
256. Huynh, T., et al., *Remodeling of an acellular collagen graft into a physiologically responsive neovessel*. *Nat Biotechnol*, 1999. **17**(11): p. 1083-6.
257. Davidenko, N., et al., *Biomimetic collagen scaffolds with anisotropic pore architecture*. *Acta Biomater*, 2012. **8**(2): p. 667-76.
258. Xing, Q., et al., *Increasing mechanical strength of gelatin hydrogels by divalent metal ion removal*. *Scientific reports*, 2014. **4**: p. 4706-4706.
259. Segura, T., et al., *Crosslinked hyaluronic acid hydrogels: a strategy to functionalize and pattern*. *Biomaterials*, 2005. **26**(4): p. 359-371.
260. Hirakura, T., et al., *Hybrid hyaluronan hydrogel encapsulating nanogel as a protein nanocarrier: New system for sustained delivery of protein with a chaperone-like function*. *Journal of Controlled Release*, 2010. **142**(3): p. 483-489.
261. Tang, J., et al., *Super tough magnetic hydrogels for remotely triggered shape morphing*. *Journal of Materials Chemistry B*, 2018. **6**(18): p. 2713-2722.

262. Lim, K.S., et al., *Visible Light Cross-Linking of Gelatin Hydrogels Offers an Enhanced Cell Microenvironment with Improved Light Penetration Depth*. *Macromol Biosci*, 2019. **19**(6): p. e1900098.
263. Eroglu, I., et al., *Gel network comprising UV crosslinked PLGA-b-PEG-MA nanoparticles for ibuprofen topical delivery*. *Pharm Dev Technol*, 2019. **24**(9): p. 1144-1154.
264. Liu, J., et al., *Glucose-sensitive delivery of metronidazole by using a photo-crosslinked chitosan hydrogel film to inhibit Porphyromonas gingivalis proliferation*. *Int J Biol Macromol*, 2019. **122**: p. 19-28.
265. Tronci, G., S.J. Russell, and D.J. Wood, *Photo-active collagen systems with controlled triple helix architecture*. *J Mater Chem B*, 2013. **1**(30): p. 3705-3715.
266. Cheng, H., et al., *Activable Cell-Penetrating Peptide Conjugated Prodrug for Tumor Targeted Drug Delivery*. *ACS Applied Materials & Interfaces*, 2015. **7**(29): p. 16061-16069.
267. Marslin, G., et al., *Delivery as nanoparticles reduces imatinib mesylate-induced cardiotoxicity and improves anticancer activity*. *International journal of nanomedicine*, 2015. **10**: p. 3163-3170.
268. Sun, Y., et al., *RGD Peptide-Based Target Drug Delivery of Doxorubicin Nanomedicine*. *Drug Development Research*, 2017. **78**(6): p. 283-291.
269. Sartorio, A., A. Conti, and M. Monzani, *New markers of bone and collagen turnover in children and adults with growth hormone deficiency*. *Postgraduate Medical Journal*, 1993. **69**(817): p. 846.
270. Zigrino, P., et al., *Fibroblast-Derived MMP-14 Regulates Collagen Homeostasis in Adult Skin*. *The Journal of investigative dermatology*, 2016. **136**(8): p. 1575-1583.
271. Holmbeck, K., et al., *MT1-MMP-deficient mice develop dwarfism, osteopenia, arthritis, and connective tissue disease due to inadequate collagen turnover*. *Cell*, 1999. **99**(1): p. 81-92.
272. Holmbeck, K., et al., *The metalloproteinase MT1-MMP is required for normal development and maintenance of osteocyte processes in bone*. *Journal of Cell Science*, 2005. **118**(1): p. 147.
273. Bubnis, W.A. and C.M. Ofner, 3rd, *The determination of epsilon-amino groups in soluble and poorly soluble proteinaceous materials by a spectrophotometric method using trinitrobenzenesulfonic acid*. *Anal Biochem*, 1992. **207**(1): p. 129-33.
274. Friedman, M. and C.W. Sigel, *A Kinetic Study of the Ninhydrin Reaction**. *Biochemistry*, 1966. **5**(2): p. 478-485.
275. Liang, H., et al., *Monomer-Induced Customization of UV-Cured Atelocollagen Hydrogel Networks*. *Front Chem*, 2018. **6**: p. 626.
276. Fernandes, E., et al., *Spectroscopic Studies as a Toolbox for Biophysical and Chemical Characterization of Lipid-Based Nanotherapeutics*. *Frontiers in chemistry*, 2018. **6**: p. 323-323.
277. Kale, R. and A. Bajaj, *Ultraviolet spectrophotometric method for determination of gelatin crosslinking in the presence of amino groups*. *J Young Pharm*, 2010. **2**(1): p. 90-4.
278. Tronci, G., et al., *Protease-sensitive atelocollagen hydrogels promote healing in a diabetic wound model*. *Journal of Materials Chemistry B*, 2016. **4**(Royal Society of Chemistry): p. 7249-7258.
279. Goyal, N., et al., *Synthesis and characterization of pH responsive D-glucosamine based molecular gelators*. *Beilstein journal of organic chemistry*, 2014. **10**: p. 3111-3121.

280. Mehmood, Y., et al., *Application of UV spectrophotometric method for easy and rapid estimation of sulfasalazine in pharmaceutical formulation (suspension)*. *Pharmaceutical Methods*, 2017. **8**: p. 174-177.
281. Zhang, J.-z., et al., *Photo cross-linked biodegradable hydrogels for enhanced vancomycin loading and sustained release*. *Chinese Journal of Polymer Science*, 2013. **31**(12): p. 1697-1705.
282. Williams, C.G., et al., *Variable cytocompatibility of six cell lines with photoinitiators used for polymerizing hydrogels and cell encapsulation*. *Biomaterials*, 2005. **26**(11): p. 1211-1218.
283. Fedorovich, N.E., et al., *The effect of photopolymerization on stem cells embedded in hydrogels*. *Biomaterials*, 2009. **30**(3): p. 344-353.
284. Rickman, J., et al., *Rotation-assisted wet-spinning of UV-cured gelatin fibres and nonwovens*. *Journal of Materials Science*, 2019. **54**(14): p. 10529-10547.
285. El-Sayed, A.S.A., et al., *Aspergillus nidulans thermostable arginine deiminase-Dextran conjugates with enhanced molecular stability, proteolytic resistance, pharmacokinetic properties and anticancer activity*. *Enzyme Microb Technol*, 2019. **131**: p. 109432.
286. Masutani, E.M., et al., *Increasing Thermal Stability of Gelatin by UV-Induced Cross-Linking with Glucose*. *International Journal of Biomaterials*, 2014. **2014**: p. 979636.
287. Paletta, J.T., et al., *Synthesis and Reduction Kinetics of Sterically Shielded Pyrrolidine Nitroxides*. *Organic Letters*, 2012. **14**(20): p. 5322-5325.
288. Kirilyuk, I.A., et al., *Synthesis of the tetraethyl substituted pH-sensitive nitroxides of imidazole series with enhanced stability towards reduction*. *Organic & Biomolecular Chemistry*, 2004. **2**(7): p. 1025-1030.
289. Naganuma, J., Y. Yamazaki, and H. Gotoh, *Evaluation method of steric shielding effect around nitroxide radical reaction center based on molecular volume within a virtual ball*. *Structural Chemistry*, 2019. **30**(6): p. 2085-2092.
290. Lin, Z., et al., *Novel thermo-sensitive hydrogel system with paclitaxel nanocrystals: High drug-loading, sustained drug release and extended local retention guaranteeing better efficacy and lower toxicity*. *Journal of Controlled Release*, 2014. **174**: p. 161-170.
291. Missirlis, D., et al., *Doxorubicin encapsulation and diffusional release from stable, polymeric, hydrogel nanoparticles*. *European Journal of Pharmaceutical Sciences*, 2006. **29**(2): p. 120-129.
292. Kundu, J., et al., *Silk fibroin/poly(vinyl alcohol) photocrosslinked hydrogels for delivery of macromolecular drugs*. *Acta Biomaterialia*, 2012. **8**(5): p. 1720-1729.
293. Chen, P., et al., *Intra-articular delivery of sinomenium encapsulated by chitosan microspheres and photo-crosslinked GelMA hydrogel ameliorates osteoarthritis by effectively regulating autophagy*. *Biomaterials*, 2016. **81**: p. 1-13.
294. Cao, L., et al., *Bone regeneration using photocrosslinked hydrogel incorporating rhBMP-2 loaded 2-N, 6-O-sulfated chitosan nanoparticles*. *Biomaterials*, 2014. **35**(9): p. 2730-2742.
295. Pan, C., et al., *CD10 Is a Key Enzyme Involved in the Activation of Tumor-activated Peptide Prodrug CPI-0004Na and Novel Analogues: Implications for the Design of Novel Peptide Prodrugs for the Therapy of CD10⁺ Tumors*. *Cancer Research*, 2003. **63**(17): p. 5526.
296. Fujimori, E., *Ultraviolet light-induced change in collagen macromolecules*. *Biopolymers*, 1965. **3**(2): p. 115-119.
297. Weadock, K.S., et al., *Physical crosslinking of collagen fibers: Comparison of ultraviolet irradiation and dehydrothermal treatment*. *Journal of Biomedical Materials Research*, 1995. **29**(11): p. 1373-1379.

298. Lew, D.-H., P.H.-T. Liu, and D.P. Orgill, *Optimization of UV cross-linking density for durable and nontoxic collagen GAG dermal substitute*. Journal of biomedical materials research. Part B, Applied biomaterials, 2007. **82**(1): p. 51-56.
299. Burke, M. and L. Augenstein, *A comparison of the effects of ultraviolet and ionizing radiations on trypsin activity and on its constituent amino acids*. The Biochemical journal, 1969. **114**(3): p. 535-545.
300. Setlow, J.K., *Chapter V - The Effects of Ultraviolet Radiation and Photoreactivation* *Research sponsored by the U. S. Atomic Energy Commission under contract with the Union Carbide Corporation*, in *Comprehensive Biochemistry*, M. Florkin and E.H. Stotz, Editors. 1967, Elsevier. p. 157-209.
301. Ceylan Tuncaboylu, D., *Photo-crosslinked mechanically strong PCL4-PDMAEM hydrogels*. Reactive and Functional Polymers, 2018. **126**: p. 44-51.
302. Yuan, M., et al., *Thermosensitive and photocrosslinkable hydroxypropyl chitin-based hydrogels for biomedical applications*. Carbohydr Polym, 2018. **192**: p. 10-18.
303. Dorati, R., et al., *Gentamicin-Loaded Thermosetting Hydrogel and Moldable Composite Scaffold: Formulation Study and Biologic Evaluation*. J Pharm Sci, 2017. **106**(6): p. 1596-1607.
304. Palmese, L.L., et al., *Hybrid hydrogels for biomedical applications*. Current Opinion in Chemical Engineering, 2019. **24**: p. 143-157.
305. Qu, Y., et al., *A biodegradable thermo-responsive hybrid hydrogel: therapeutic applications in preventing the post-operative recurrence of breast cancer*. NPG Asia Materials, 2015. **7**(8): p. e207-e207.
306. Achet, D. and X.W. He, *Determination of the renaturation level in gelatin films*. Polymer, 1995. **36**(4): p. 787-791.
307. Bigi, A., S. Panzavolta, and K. Rubini, *Relationship between triple-helix content and mechanical properties of gelatin films*. Biomaterials, 2004. **25**(25): p. 5675-5680.
308. Bigi, A., et al., *Mechanical and thermal properties of gelatin films at different degrees of glutaraldehyde crosslinking*. Biomaterials, 2001. **22**(8): p. 763-768.
309. Robins, S.P. and A.J. Bailey, *The chemistry of the collagen cross-links. The mechanism of stabilization of the reducible intermediate cross-links*. The Biochemical journal, 1975. **149**(2): p. 381-385.
310. Stewart, S.A., et al., *Implantable Polymeric Drug Delivery Devices: Classification, Manufacture, Materials, and Clinical Applications*. Polymers, 2018. **10**(12): p. 1379.
311. Larrañeta, E., et al., *Microneedle arrays as transdermal and intradermal drug delivery systems: Materials science, manufacture and commercial development*. Materials Science and Engineering: R: Reports, 2016. **104**: p. 1-32.
312. Ji, Q., et al., *Hydrosoluble collagen based biodegradable hybrid hydrogel for biomedical scaffold*. Journal of Biomaterials Science, Polymer Edition, 2020: p. 1-21.
313. Picci, P., *Osteosarcoma (Osteogenic sarcoma)*. Orphanet Journal of Rare Diseases, 2007. **2**(1): p. 6.
314. Norouzi, M., B. Nazari, and D.W. Miller, *Injectable hydrogel-based drug delivery systems for local cancer therapy*. Drug Discovery Today, 2016. **21**(11): p. 1835-1849.
315. Tanya, P., R.S. Tiberiu, and Z. Meital, *Injectable hydrogel-based scaffolds for tissue engineering applications*. Reviews in Chemical Engineering, 2017. **33**(1): p. 91-107.
316. Panagopoulos, P.K. and G.I. Lambrou, *Bone erosions in rheumatoid arthritis: recent developments in pathogenesis and therapeutic implications*. Journal of musculoskeletal & neuronal interactions, 2018. **18**(3): p. 304-319.
317. Yan, Q., et al., *EDC/NHS activation mechanism of polymethacrylic acid: anhydride versus NHS-ester*. RSC Advances, 2015. **5**(86): p. 69939-69947.

318. Ofner, C.M., 3rd and W.A. Bubnis, *Chemical and swelling evaluations of amino group crosslinking in gelatin and modified gelatin matrices*. Pharm Res, 1996. **13**(12): p. 1821-7.
319. Brayton, C.F., *Dimethyl sulfoxide (DMSO): a review*. Cornell Vet, 1986. **76**(1): p. 61-90.
320. Williams, A.C. and B.W. Barry, *Penetration enhancers*. Adv Drug Deliv Rev, 2004. **56**(5): p. 603-18.
321. Kligman, A.M., *TOPICAL PHARMACOLOGY AND TOXICOLOGY OF DIMETHYL SULFOXIDE. 1*. Jama, 1965. **193**: p. 796-804.
322. Haagdorens, M., et al., *In Vitro Cultivation of Limbal Epithelial Stem Cells on Surface-Modified Crosslinked Collagen Scaffolds*. Stem Cells International, 2019. **2019**: p. 7867613.
323. Loebel, C., et al., *Precise tailoring of tyramine-based hyaluronan hydrogel properties using DM-TMM conjugation*. Carbohydrate Polymers, 2015. **115**: p. 325-333.
324. Lai, J.-Y., *Biocompatibility of chemically cross-linked gelatin hydrogels for ophthalmic use*. Journal of Materials Science: Materials in Medicine, 2010. **21**(6): p. 1899-1911.
325. Han, Y. and S. Lv, *Synthesis of chemically crosslinked pullulan/gelatin-based extracellular matrix-mimetic gels*. International Journal of Biological Macromolecules, 2019. **122**: p. 1262-1270.
326. Ratanavaraporn, J., et al., *Effects of acid type on physical and biological properties of collagen scaffolds*. Journal of Biomaterials Science, Polymer Edition, 2008. **19**(7): p. 945-952.
327. Salchert, K., et al., *In Vitro Reconstitution of Fibrillar Collagen Type I Assemblies at Reactive Polymer Surfaces*. Biomacromolecules, 2004. **5**(4): p. 1340-1350.
328. Yunoki, S. and T. Matsuda, *Simultaneous Processing of Fibril Formation and Cross-Linking Improves Mechanical Properties of Collagen*. Biomacromolecules, 2008. **9**(3): p. 879-885.
329. Abou Neel, E.A., et al., *Collagen — Emerging collagen based therapies hit the patient*. Advanced Drug Delivery Reviews, 2013. **65**(4): p. 429-456.
330. Mohanty, B. and H.B. Bohidar, *Microscopic structure of gelatin coacervates*. International Journal of Biological Macromolecules, 2005. **36**(1): p. 39-46.
331. Ugarte-Berzal, E., et al., *Inhibition of MMP-9-dependent Degradation of Gelatin, but Not Other MMP-9 Substrates, by the MMP-9 Hemopexin Domain Blades 1 and 4*. J Biol Chem, 2016. **291**(22): p. 11751-60.
332. Yamaguchi, T., R. Sato, and Y. Sawae, *Propagation of Fatigue Cracks in Friction of Brittle Hydrogels*. Gels (Basel, Switzerland), 2018. **4**(2): p. 53.
333. Marani, D., et al., *Influence of hydroxyl content of binders on rheological properties of cerium–gadolinium oxide (CGO) screen printing inks*. Journal of the European Ceramic Society, 2015. **35**.
334. Kocen, R., et al., *Viscoelastic behaviour of hydrogel-based composites for tissue engineering under mechanical load*. Biomedical Materials, 2017. **12**(2): p. 025004.
335. Garmon, T., M. Wittling, and S. Nie, *MMP14 Regulates Cranial Neural Crest Epithelial-to-Mesenchymal Transition and Migration*. Dev Dyn, 2018. **247**(9): p. 1083-1092.
336. Stawowczyk, M., et al., *Matrix Metalloproteinase 14 promotes lung cancer by cleavage of Heparin-Binding EGF-like Growth Factor*. Neoplasia, 2017. **19**(2): p. 55-64.
337. Ohuchi, E., et al., *Membrane type 1 matrix metalloproteinase digests interstitial collagens and other extracellular matrix macromolecules*. J Biol Chem, 1997. **272**(4): p. 2446-51.

338. Gifford, V. and Y. Itoh, *MT1-MMP-dependent cell migration: proteolytic and non-proteolytic mechanisms*. *Biochem Soc Trans*, 2019. **47**(3): p. 811-826.
339. Albrechtsen, R., et al., *ADAM12 redistributes and activates MMP-14, resulting in gelatin degradation, reduced apoptosis and increased tumor growth*. *Journal of Cell Science*, 2013. **126**(20): p. 4707.
340. Sinthusamran, S., S. Benjakul, and H. Kishimura, *Molecular characteristics and properties of gelatin from skin of seabass with different sizes*. *Int J Biol Macromol*, 2015. **73**: p. 146-53.
341. Cantor, C.R. and P.R. Schimmel, *Biophysical Chemistry Part III: The Behavior of Biological Macromolecules*. FEBS LETTERS, 1981.
342. Broberger, C., et al., *Differential effects of intrastriatally infused fully and endcapped phosphorothioate antisense oligonucleotides on morphology, histochemistry and prodynorphin expression in rat brain*. *Brain Res Mol Brain Res*, 2000. **75**(1): p. 25-45.
343. Kridel, S.J., et al., *A unique substrate binding mode discriminates membrane type-1 matrix metalloproteinase from other matrix metalloproteinases*. *J Biol Chem*, 2002. **277**(26): p. 23788-93.
344. Xu, B., et al., *Guanidinium Group Remains Protonated in a Strongly Basic Arginine Solution*. *Chemphyschem*, 2017. **18**(12): p. 1503-1506.
345. Fitch, C.A., et al., *Arginine: Its pKa value revisited*. *Protein science : a publication of the Protein Society*, 2015. **24**(5): p. 752-761.
346. Armstrong, C.T., et al., *Arginine side chain interactions and the role of arginine as a gating charge carrier in voltage sensitive ion channels*. *Scientific Reports*, 2016. **6**(1): p. 21759.
347. Yu, B., et al., *A designed supramolecular cross-linking hydrogel for the direct, convenient, and efficient administration of hydrophobic drugs*. *International journal of pharmaceutics*, 2020. **578**: p. 119075.
348. Lee, K.Y., et al., *Controlling Mechanical and Swelling Properties of Alginate Hydrogels Independently by Cross-Linker Type and Cross-Linking Density*. *Macromolecules*, 2000. **33**(11): p. 4291-4294.
349. Verberk, J.D.M., et al., *Contribution of Prior, Multiple-, and Repetitive Surgeries to the Risk of Surgical Site Infections in the Netherlands*. *Infect Control Hosp Epidemiol*, 2017. **38**(11): p. 1298-1305.
350. Maxwell, H., *Knee arthroscopy*. 2020: Bupa Healthcare Website.
351. Qin, S., et al., *Immunolocalization of membrane-type 1 MMP in human rheumatoid synovium tissues*. *Int J Clin Exp Pathol*, 2015. **8**(8): p. 9286-92.
352. Boncel, S. and K. Walczak, *Novel Acyclic Amide-Conjugated Nucleosides and Their Analogues*. *Nucleosides, Nucleotides & Nucleic Acids*, 2009. **28**(2): p. 103-117.
353. Gao, C., et al., *Bone biomaterials and interactions with stem cells*. *Bone Research*, 2017. **5**(1): p. 17059.
354. Ferreira, A.M., et al., *Collagen for bone tissue regeneration*. *Acta Biomaterialia*, 2012. **8**(9): p. 3191-3200.
355. Lei, B., et al., *Hybrid polymer biomaterials for bone tissue regeneration*. *Frontiers of Medicine*, 2019. **13**(2): p. 189-201.
356. Vanden Eynde, J.J., et al., *Breakthroughs in Medicinal Chemistry: New Targets and Mechanisms, New Drugs, New Hopes-6*. *Molecules (Basel, Switzerland)*, 2019. **25**(1): p. 119.
357. Zhang, X., et al., *Matrix metalloproteinases-2/9-sensitive peptide-conjugated polymer micelles for site-specific release of drugs and enhancing tumor accumulation: preparation and in vitro and in vivo evaluation*. *International journal of nanomedicine*, 2016. **11**: p. 1643-1661.

358. Bashir, S., et al., *pH responsive N-succinyl chitosan/Poly (acrylamide-co-acrylic acid) hydrogels and in vitro release of 5-fluorouracil*. PloS one, 2017. **12**(7): p. e0179250-e0179250.
359. Kocak, G., C. Tuncer, and V. Bütün, *pH-Responsive polymers*. Polymer Chemistry, 2017. **8**(1): p. 144-176.
360. Lin, A., et al., *Off-target toxicity is a common mechanism of action of cancer drugs undergoing clinical trials*. Science Translational Medicine, 2019. **11**(509): p. eaaw8412.
361. Chidambaram, M., R. Manavalan, and K. Kathiresan, *Nanotherapeutics to overcome conventional cancer chemotherapy limitations*. J Pharm Pharm Sci, 2011. **14**(1): p. 67-77.
362. Kamaly, N., et al., *Degradable Controlled-Release Polymers and Polymeric Nanoparticles: Mechanisms of Controlling Drug Release*. Chemical reviews, 2016. **116**(4): p. 2602-2663.
363. Tiwari, G., et al., *Drug delivery systems: An updated review*. International journal of pharmaceutical investigation, 2012. **2**(1): p. 2-11.
364. Chau, Y., et al., *Investigation of targeting mechanism of new dextran-peptide-methotrexate conjugates using biodistribution study in matrix-metalloproteinase-overexpressing tumor xenograft model*. J Pharm Sci, 2006. **95**(3): p. 542-51.
365. Albright, C.F., et al., *Matrix metalloproteinase-activated doxorubicin prodrugs inhibit HT1080 xenograft growth better than doxorubicin with less toxicity*. Mol Cancer Ther, 2005. **4**(5): p. 751-60.
366. Rizwan, M., et al., *pH Sensitive Hydrogels in Drug Delivery: Brief History, Properties, Swelling, and Release Mechanism, Material Selection and Applications*. Polymers, 2017. **9**(4): p. 137.
367. Fullerton, G.D. and I.L. Cameron, *Chapter One - Water Compartments in Cells*, in *Methods in Enzymology*, D. Häussinger and H. Sies, Editors. 2007, Academic Press. p. 1-28.
368. Mu, Q., T. Hu, and J. Yu, *Molecular insight into the steric shielding effect of PEG on the conjugated staphylokinase: biochemical characterization and molecular dynamics simulation*. PloS one, 2013. **8**(7): p. e68559-e68559.